

Review

New features in the redox coordination chemistry of metal nitrosyls $\{M-NO^+; M-NO^\bullet; M-NO^-(HNO)\}^\star$

Federico Roncaroli, Mariela Videla, Leonardo D. Slep, José A. Olabe*

Department of Inorganic, Analytical and Physical Chemistry, and INQUIMAE, CONICET, Facultad de Ciencias Exactas y Naturales,
Universidad de Buenos Aires, Pabellón 2, Ciudad Universitaria, C1428EHA Buenos Aires, Argentina

Received 20 November 2006; accepted 13 April 2007

Available online 19 April 2007

Contents

1. Introduction	1904
2. Structure and spectroscopy in the redox interconvertible forms of $\{MNO\}^n$	1905
2.1. $n=6$	1906
2.2. $n=7$	1908
2.3. $n=8$	1909
3. Formation and dissociation reactions of NO^+ , NO^\bullet , and NO^-/HNO complexes	1910
3.1. $M^II NO^+ - M^III NO^+$	1911
3.2. $M^II NO^\bullet - M^III NO^\bullet$	1911
3.3. $M^II NO^-/HNO - M^III NO^-/HNO$	1913
3.4. $Fe^II(Por)(NO)$ and $Fe^III(Por)(NO)$ (Por = porphyrins and hemoproteins)	1914
3.5. $Fe^II(Por)NO^-/HNO - Fe^III(Por)NO^-/HNO$	1914
4. Electrophilic reactivity of bound nitrosonium (NO^+)	1915
4.1. The mechanism of the reactions of $M(CN)_5NO^{2-}$ ($M = Fe, Ru, Os$) and $Ru(bpy)(tpm)NO^{3+}$ ions with OH^- : a generalization for $ML_5(NO^+)$ systems	1915
4.2. NO_2^- as a nucleophile: reactions with nitrosyl ferri-hemes	1919
4.3. The reactions of $Fe(CN)_5NO^{2-}$ with nitrogen hydrides. A case study for hydrazine, N_2H_4 , and substituted derivatives	1921
4.4. The reactions of different $ML_5(NO^+)$ complexes with cysteine	1922
5. Nucleophilic reactivity of bound NO^\bullet : the reactions with O_2	1923
6. Reactivity of bound NO^-/HNO complexes: protonation, metal-dissociation and reactions toward electrophiles or nucleophiles	1925
7. Conclusions and outlook	1925
Acknowledgments	1926
References	1926

Abbreviations: AcN, acetonitrile; bpy, 2,2'-bipyridine; bpz, 2,2'-bipyrazine; bpb, 1,2-bis(pyridine-2-carboxamido)benzene(2-); CN, coordination number; Cy, cyclohexyl; cyclam, 1,4,8,11-tetraazacyclotetradecane; cyclam-ac, 1,4,8,11-tetraazacyclotetradecane-1-acetic acid(1-); cyt^{III} , ferricytochrome c; dpk, 2,2'-dipyridyl ketone; dmsO, dimethylsulphoxide; EDTA, ethylenediaminetetraacetate; en, ethylenediamine; HAO, hydroxylamine oxidoreductase; Hb, hemoglobin; HbO_2 , oxy-hemoglobin; HOMO, highest occupied molecular orbital; L^{Pr} , 1-isopropyl-4,7-(4-*tert*-butyl-2-mercaptobenzyl)-1,4,7-triazacyclononane(2-); NO^+ , nitrosonium; HNO , nitroxyl; NO^- , nitroxyl anion; L^{Py} , *N*-(2-methylpyridyl)1,4,8,11-tetraazacyclotetradecane; LUMO, lowest unoccupied molecular orbital; Mb, myoglobin; MbO_2 , oxymyoglobin; metHb, methemoglobin; 1-Melm, 1-methylimidazole; metMb, metmyoglobin; Me_3TACN , *N,N',N''*-trimethyl-1,4,7-triazacyclononane; NHE, normal hydrogen electrode; nic, nicotinic acid; NIR, nitrite reductase; NOR, nitric oxide reductase; NOS, NO synthase; NTA, nitrilotriacetate; OEP, octaethylporphyrinato(2-); $PaPy_3$, *N,N*-bis(2-pyridylmethyl)amine-*N*-ethyl-2-pyridine-2-carboxamide(1-); ph, phenyl; phpy, 2-phenylpyridine(1-); Por , generalized porphyrine ligand; Por^{8+} , 5,10,15,20-tetrakis-(4'-*tert*-butyl-2',6'-bis(4-*tert*-butylpyridine)phenyl)porphyrinato; Por^{8-} , 5⁴,10⁴,15⁴,20⁴-tetra-*tert*-butyl-5²,5⁶,15²,15⁶-tetrakis[2,2-bis(carboxylato)ethyl]-5,10,15,20-tetraphenylporphyrin; py, pyridine; pyN_4 , 2,6- $C_5H_3N[CMc(CH_2NH_2)_2]_2$; 'pyS₄', 2,6-bis(2-mercaptophenylthiomethyl)pyridine(2-); 'py^{bu}S₄', 2,6-bis(2-mercapto-3,5-di-*tert*-butylphenylthio)dimethylpyridine(2-); $py^{Si}S_4$, 2,6-bis(3-triphenylsilyl-2-sulfanylphenylthiomethyl)-pyridine(2-); pz, pyrazine; sGC, soluble guanylyl cyclase; SNP, sodium nitroprusside or sodium pentacyanonitrosylferrate(II); TMPs, *meso*-tetrakis(2,4,6-trimethyl-3-sulfonatophenyl)porphyrinato(6-); $TMPyP$, *meso*-tetrakis(*N*-methyl-4-pyridyl)porphyrinato(2+); $TpivPP$, $\alpha,\alpha,\alpha,\alpha$ -tetrakis(*o*-pivalamidophenyl)-porphyrinato(2-); tpm, tris(1-pyrazolyl)methane; TPP, tetraphenylporphyrinato(2-); TPPS, tetra(4-sulfonatophenyl)porphyrinato(6-); trpy, 2,2':6',2''-terpyridine; TTP, tetratolylporphyrinato(2-)

* Based on a keynote lecture presented at the 37th International Conference on Coordination Chemistry, 13–18 August 2006, Cape Town, South Africa.

* Corresponding author. Tel.: +54 11 45763358; fax: +54 11 45763341.

E-mail address: olabe@qi.fcen.uba.ar (J.A. Olabe).

Abstract

We describe new developments in the coordination chemistry of bound nitrosyl, considering its three formal redox states: NO^+ , NO^\bullet and NO^-/HNO . We emphasize on the correlation between well disclosed structural and spectroscopic aspects and different reactivity properties associated with the total electron content, according to the $\{\text{MNO}\}^n$ description ($n=6, 7, 8$ for the above mentioned nitrosyls, respectively). The selected systems contain mainly six-coordinated nitrosyl-complexes with different ML_x fragments ($\text{M}=\text{Fe}, \text{Ru}, \text{Os}$; $\text{L}=\text{cyanides}, \text{polypyridines}, \text{amines}, \text{EDTA}, \text{porphyrins}, \text{etc.}$). We focus heavily on the pentacyanonitrosylferrate systems, though with an eye toward a generalized description. For the NO^+ -complexes ($n=6$), the electrophilic reactivity toward selected nucleophiles: OH^- , N_2H_4 , NO_2^- and cysteine is analyzed. We provide a mechanistic analysis, including DFT calculations for describing the reactants, transition states, intermediates and products. The crucial role of the redox potential associated to the $\text{NO}^+/\text{NO}^\bullet$ couples, $E_{\text{NO}^+/\text{NO}^\bullet}$, in determining the electrophilic addition reactivities is highlighted. We employ a similar approach for studying the nucleophilic reactivity of NO^\bullet -complexes ($n=7$) toward O_2 , a reaction that has great biological significance. Finally, some recent results covering structural, spectroscopic and reactivity aspects of NO^- and HNO -complexes ($n=8$) are reviewed. © 2007 Elsevier B.V. All rights reserved.

Keywords: Nitric oxide; Nitrosonium; Nitroxyl; Electrophilic reactivity; Nucleophilic reactivity

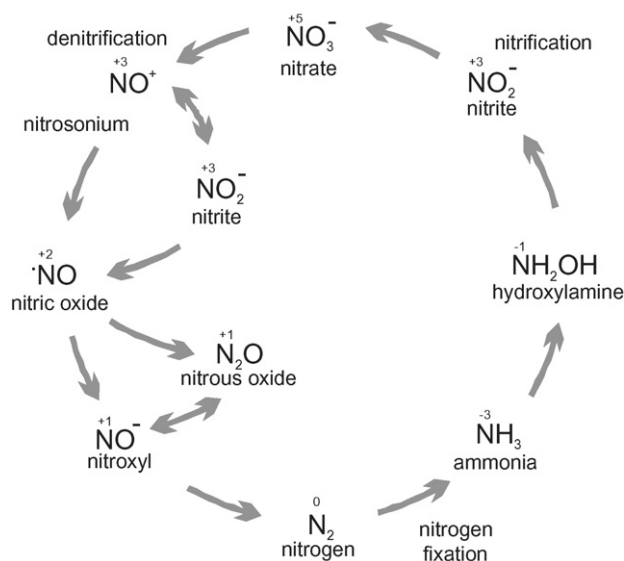
1. Introduction

Up to the 1970s, the chemistry of nitrogen monoxide (NO_X) and other reactive nitrogen oxide species, NO_X , was largely focused on their known toxicity as constituents of air pollution [1]. It is now well established that NO plays fundamental roles in biochemical processes, including blood pressure control, neurotransmission and immune response, in tissue damage and carcinogenesis [2]. NO has a ubiquitous place in the coordination chemistry of small nitrogen-containing molecules present in the redox cycles in Nature, Scheme 1 [3]. Denitrification processes generate N_2 and N_2O during the conversions of NO_2^- to NH_3 in plants, bacteria and fungi. These redox reactions are catalyzed by a variety of metalloenzymes, which also operate in the reverse nitrification processes (e.g., $\text{NH}_3 \rightarrow \text{NO}_2^-$) [4].

In vivo generation of NO in mammals is achieved by oxidation of L-arginine, mediated by the NO synthase enzyme (NOS) [5]. The principal targets for NO under bioregulatory conditions are metal centers, primarily iron proteins [6]. NO binds to the ferro-heme protein soluble guanylyl cyclase (sGC), with further

reactivity leading to vasodilation and other physiologically relevant processes [7], and may inhibit the action of heme enzymes as cytochrome P450 [8a], cytochrome oxidase [8b], nitrile hydratase [8c–e], catalase [8f] and of a non-heme ferric uptake regulator protein (Fur) [8g]. A main sink for NO in biofluids occurs through the very fast reactions with oxyMb and oxyHb, giving NO_3^- [9]. Also biorelevant is the use of the so-called “NO-donor” drugs: *N*-hydroxyurea, hydroxylamine (NH_2OH), sodium nitroprusside (SNP, $\text{Na}_2[\text{Fe}(\text{CN})_5\text{NO}]$), organic nitrates and nitrites (viz., glyceryl trinitrate, GTN), etc., which must be metabolized in the body through oxidative or reductive processes up to NO generation in order to be rendered physiologically active [10].

Not only the paramagnetic NO^\bullet species, but also the diamagnetic, one-electron oxidized NO^+ (nitrosonium), and the one-electron reduced species (either NO^- , the nitroxyl anion, or its protonated form HNO, nitroxyl) have been considered to be involved in the reactions with diverse substrates [11]. The three species, in which the identity of the diatomic moiety is maintained, may bind to metal ions, with the potential onset of reversible interconversions, as will be analyzed along this review. For the nitrite reductases (NIR) [4], the initial coordination of NO_2^- to the Fe(II) center leads rapidly to $\text{Fe}^{\text{II}}\text{NO}^+$. NO is successively released upon one-electron reduction, in cd_1NIR [12a]. Alternatively, a full six-electron reduction of NO_2^- to NH_3 is afforded by the assimilatory NIR siroheme enzymes [12b], as well as by ccNIR [12c]. The action of ccNIR has been modeled by considering the participation of one-electron intermediates, including HNO [4,12c]. The chemistry of bound $\text{NO}-\text{NO}^-/\text{HNO}$ is also relevant to the NO reductases (NOR), yielding N_2O [4,13], and to the hydroxylamine oxidoreductase enzyme (HAO) that transforms NH_2OH into NO_2^- [14]. Little direct evidence exists for the formation of NO^-/HNO in biological systems, although HNO has been proposed as the immediate precursor of NO through the activity of NOS, and has been reported as a major product during turnover of NOS in the absence of biopterin [15]. HNO has also been linked to vasodilation [16] and cytotoxicity [17], and has a physiological activity distinct from that of NO, including the inhibition of aldehyde dehydrogenase [18]. Crucial differences between the mechanistic actions of NO and HNO have been proposed [19]. For all the above reasons, there is a growing interest in



Scheme 1.

the emerging coordination chemistry of HNO, which has been recently reviewed [20].

We focus on recent achievements dealing with structure-reactivity correlations for the three diatomic species, $\text{NO}^{+/-}$, pointing to the role of metals in controlling the reactivity of the bound species. In Sections 2 and 3 we summarize central issues on basic NO coordination chemistry: bonding, spectroscopy and stability (formation and dissociation reactions), extending the information provided by past reviews [21]. In a similar way, Sections 4 and 5 describe the reactivity aspects, with a sharp distinction between the electrophilic and nucleophilic reactions of bound NO^{+} and NO^{\bullet} , respectively [22,23]. The less explored issue of bound NO^{-}/HNO reactivity is addressed in Section 6. The selection of metallonitrosyls is based on recent achievements and/or specific biochemical relevance, with emphasis on iron and group eight analogs.

2. Structure and spectroscopy in the redox interconvertible forms of $\{\text{MNO}\}^n$

Transition metal nitrosyl-complexes span variable geometries, coordination numbers (CN) and electronic properties due to the differences in electronic configurations of the metal centers and *covalent* MNO interactions. The nitrosyl-containing species are described as $\{\text{MNO}\}^n$ (regardless of the coligands), where n stands for the number of electrons in the metal d and π_{NO}^* orbitals [21a]. This description allows for a comprehensive account of several geometries (mainly CN 4, 5, 6) with different electron contents, n . We concentrate in compounds with CN 6, comprising values of $n=6, 7, 8$, with occasional reference to structurally or kinetically relevant five-coordinated species. By using a simplified, *limiting approach*, we describe them as containing bound NO^{+} , NO^{\bullet} or NO^{-} , respectively [21]. Eventual protonation of the MNO moieties will be considered.

In 1981, a comprehensive X-ray structural survey [21b] revealed, for the hexa-coordinated nitrosyl complexes, 36 cases with $n=6$ (tentative formal oxidation states are indicated: NO^{+} , with $\text{M}=\text{Cr}^0, \text{Mo}^0, \text{W}^0, \text{Mn}^{\text{I}}, \text{Re}^{\text{I}}, \text{Fe}^{\text{II}}, \text{Ru}^{\text{II}}, \text{Os}^{\text{II}}, \text{Ir}^{\text{III}}$), four complexes with $n=7$ (NO^{\bullet} , remarkably all with Fe^{II}) and five complexes with $n=8$ (NO^{-} , only for $\text{M}=\text{Co}^{\text{III}}$ and Rh^{III}). In the recent years, many other crystalline structures have been solved for $n=6$ [24] and a more limited number for $n=7$ [24a–c,25]. The additional crystalline structures for $n=8$ revealed the presence of HNO, not of NO^{-} [26]. Noteworthy, there are still no examples for all the three solid structures containing identically six-coordinated $\text{ML}_x(\text{NO}^m)$ ($m=+1, 0, -1$). We show in Fig. 1 the X-ray geometries of three pseudooctahedral complexes containing NO^{+} , NO^{\bullet} and HNO, with a similar coligand environment, although with different metals, Fe^{II} and Ru^{II} .

Despite the above comment, the $\{\text{MNO}\}^n$ complexes may be interconverted ($n=6, 7, 8$) either in aqueous or (more usually) in nonaqueous solutions by chemical means or by using cyclic voltammetry (CV). They usually display one-electron reversible waves in a remarkably broad potential range ($E_{1/2(\text{NO}^{+}/\text{NO}^{\bullet})}$, from ca. 0.6 to -0.4 V versus NHE, in aqueous solutions), depending on the metal and the coligands. Shifted values have been measured by changing the solvent, as in acetonitrile (AcN)

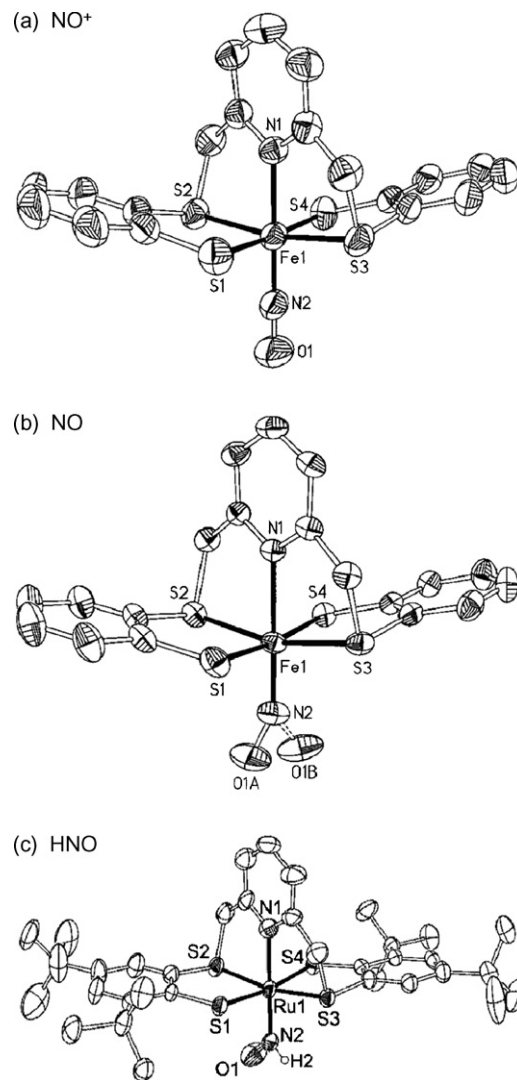


Fig. 1. Molecular structures of iron- and ruthenium-nitrosyl complexes containing the three redox forms of nitrosyl and a pentadentate ligand (four equatorial sulfur bonds and a *N*-pyridinic bond *trans* to NO, see Table 1). (a) $[\text{Fe}(\text{NO})(\text{pyS}_4')]\text{PF}_6$; (b) $[\text{Fe}(\text{NO}^{\bullet})(\text{pyS}_4')]\cdot 2\text{CH}_2\text{Cl}_2$ (the disordered O atoms of the nitrosyl ligand are indicated as O1A and O1B). (c) $[\text{Ru}(\text{HNO})(\text{py}^{\text{bu}}\text{S}_4')]\cdot 2\text{CH}_2\text{Cl}_2\cdot \text{MeOH}$. In (b) and (c), the C-bound H atoms and solvate molecules have been omitted [24a,26a].

solutions, in a range of 0.96–0.0 V. Additional one-electron waves may occur at more negative potentials ($E_{1/2(\text{NO}^{\bullet}/\text{NO}^{-})}$, range 0.3 to -0.5 V, in AcN) [24–28]. The latter waves are frequently irreversible at room temperature, suggesting ligand labilization in the $\{\text{MNO}\}^8$ moieties. By sweeping to even more negative potentials, a third irreversible multielectronic wave may be observed, leading to NH_2OH and/or NH_3 [29]. Fig. 2 shows a display of CV waves corresponding to reversible redox behavior in the $[\text{Fe}(\text{cyclam-ac})\text{NO}]^{2+/+/-0}$ series, measured in AcN [24c]. Both single-electron redox processes comprise mainly NO-based orbitals [28].

Detailed and reliable characterizations of nitrosyl complexes in solution require the use of state-of-the art spectroscopies: IR, EPR, NMR, UV–vis, resonance Raman, Mössbauer, magnetic circular dichroism (MCD), etc., and modern theoretical

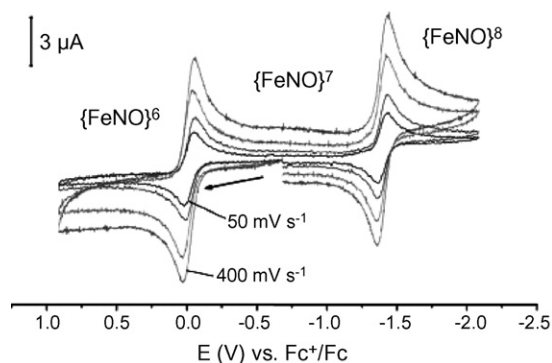


Fig. 2. Cyclic voltammogram of [Fe(cyclam-ac)(NO)](PF₆) in acetonitrile at 20 °C (0.10 M [N(*n*-Bu)₄](PF₆) supporting electrolyte; glassy carbon working electrode; scan rates 50, 100, 200 and 400 mV s⁻¹ [24c].

calculations [24–26,30]. This is essential for describing the true electron density inside the {MNO}^{*n*} moieties, beyond the simplified approach comprising limiting oxidation states for M and NO.

The bonding in mononitrosyl complexes can be readily understood from a molecular orbital (MO) treatment [31]. Fig. 3 shows the ordering of orbitals, implying donor–acceptor σ–π interactions between M and NO. Fig. 3a corresponds to the *n* = 6 situation and Fig. 3b to *n* = 7 (it can be used also for *n* = 8). We present first the experimental background related to the bonding picture, and we discuss this information later for the complexes with different *n* values.

Table 1 contains structural (distances d_{M–N}, d_{N–O}, and ∠MNO) and spectroscopic information (total spin state *S* and infrared nitrosyl-stretching frequencies, ν_{NO}) for a representative though not exhaustive amount of compounds with available solid state structures.

The indicators in Table 1 reflect the detailed electronic structures in the {MNO}^{*n*} moieties. The comparisons must be done with caution when the metal and coligands vary simultaneously for a given {MNO}^{*n*} moiety, or alternatively when the counterions or the solvent are changed. The values of ν_{NO} are particularly sensitive to the electron content *n*. Fig. 4 shows the IR spectra corresponding to redox conversions obtained upon successive one-electron oxidations of Ru('py^{bu}S₄')(HNO) (*n* = 8) with [Cp₂Fe]PF₆ in THF solution, giving the NO• and NO⁺ complexes [26a].

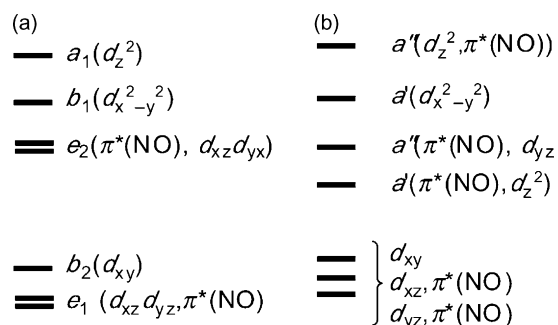


Fig. 3. Arrangement of molecular orbitals in six-coordinate {MNO}^{*n*} complexes, with M–N–O in: (a) a linear situation, *n* = 6, and (b) angular situation, *n* = 7 and 8.

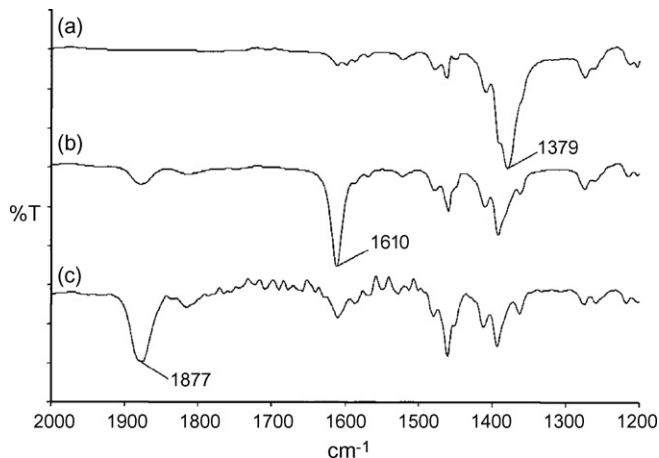
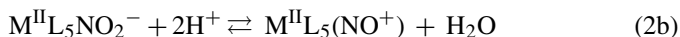
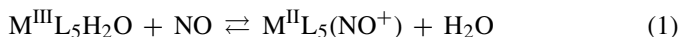


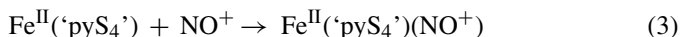
Fig. 4. Monitoring the oxidation of [Ru('py^{bu}S₄')(HNO)] in solution by IR spectroscopy: (a) complex in THF (ν_{NO}: 1379 cm⁻¹), (b) after addition of one equivalent of FcPF₆, indicating the formation of [Ru('py^{bu}S₄')(NO)]⁰ (ν_{NO}: 1610 cm⁻¹), and (c) after addition of a second equivalent of FcPF₆, or direct addition of one equivalent of HX, forming the NO⁺-complex (ν_{NO}: 1877 cm⁻¹; X = H₂PO₃⁻, Br⁻, CF₃SO₃⁻) [26a].

2.1. *n* = 6

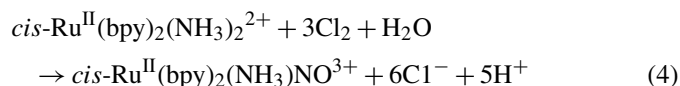
The {MNO}⁶ complexes can be prepared either by coordination of NO into the adequate M^{III} precursors, namely labile solvento- or coordinatively unsaturated complexes, Eq. (1), or alternatively by mixing NO₂⁻ with the corresponding M^{II} analogs [24]. The latter reactions may be carried out in aqueous solutions by direct mixing of the aqua-complexes with NO₂⁻ in sufficiently acid medium, Eqs. (2a) and (2b), or through a previous isolation of the nitro-complex and subsequent proton-assisted dehydration generating the NO⁺-complexes, Eq. (2b):



Alternatively, in CH₂Cl₂, NOBF₄ may react with a five-coordinated metal site, Eq. (3) [24a]:



Chemical oxidation of bound nitrogen hydrides is also viable, Eq. (4) [32]:



All these complexes contain diamagnetic (*S* = 0) and nearly linear MNO moieties, *independently of the L coligands involved*. From Fig. 3a we may derive the electronic configuration, (e₁)⁴(b₂)²(e₂)⁰. In this arrangement (or in another with fewer metal d electrons), the population of the strongly bonding (e₁) and nearly non-bonding metal centered (b₂) MO's, and the vacancy at the antibonding e₂ MO (both e₁ and e₂ are mixtures of metal d and π_{NO}^{*} orbitals) explain the multiple bond order along the linear MNO moiety. The σ–π interactions within the MNO moiety are influenced by the nature and charge of the metal,

Table 1

Selected list of nitrosyl complexes, $[\text{ML}_5(\text{NO})^m]^n$ containing different L coligands and redox states for NO ($m = +1, 0, -1$)

	Compound	<i>S</i>	ν_{NO} (cm^{-1})	$d_{\text{M-N}}$ (Å)	$d_{\text{N-O}}$ (Å)	$\angle\text{MNO}$ (°)	Reference
<i>n</i> = 6							
1	$[\text{Fe}(\text{'pyS}_4\text{'})\text{NO}]\text{PF}_6$	0	1893	1.634(3)	1.141(3)	179.5(3)	[24a]
2	$[\text{Fe}(\text{PaPy}_3)\text{NO}](\text{ClO}_4)_2$	0	1919	1.677(2)	1.139(3)	173.1(2)	[24b]
3	$[\text{Fe}(\text{cyclam-ac})\text{NO}](\text{PF}_6)_2$	0	1904	1.663(4)	1.132(5)	175.5(3)	[24c]
4	$[\text{Fe}(\text{TpivPP})(\text{NO}_2)\text{NO}]$	0	1893	1.668(2)	1.132(3)	180.0	[24d]
5	$\text{Na}_2[\text{Fe}(\text{CN})_5\text{NO}]\cdot 2\text{H}_2\text{O}$	0	1945	1.6656(7)	1.1331(10)	176.03(7)	[24e]
6	$\text{Na}_2[\text{Ru}(\text{CN})_5\text{NO}]\cdot 2\text{H}_2\text{O}$	0	1926	1.776(5)	1.127(6)	173.9(5)	[24f]
7	$[\text{Ru}(\text{bpy})(\text{tpm})\text{NO}](\text{ClO}_4)_3$	0	1959	1.774	1.093	179.1	[24g]
8	$[\text{Ru}(\eta^2\text{-phpy})(\text{trpy})\text{NO}](\text{PF}_6)_2$	0	1858	1.826(4)	1.139(5)	167.1(4)	[24h]
9	$[\text{Ru}(\text{NH}_3)_5\text{NO}]\text{Cl}_3$	0	1903	1.770(9)	1.172(14)	172.8(9)	[24i]
10	<i>trans</i> - $[\text{Ru}(\text{NH}_3)_4(\text{nic})\text{NO}]_2(\text{SiF}_6)_3$	0	1940	1.71(2)	1.17(2)	177(1)	[24j]
11	<i>trans</i> - $[\text{RuCl}(\text{cyclam})\text{NO}](\text{ClO}_4)_2$	0	1875	1.747(4)	1.128(5)	178.0(4)	[24k]
12	<i>trans</i> - $[\text{RuCl}(\text{py})_4\text{NO}](\text{ClO}_4)_2$	0	1910	1.766(8)	1.123(1)	172.9(8)	[24l]
13	<i>trans</i> - $[\text{Ru}(\text{OH})(\text{py})_4\text{NO}](\text{ClO}_4)_2$	0	1868	1.756(3)	1.145(4)	172.8(3)	[24m]
14	$[\text{Ru}(\text{dpk})(\text{trpy})\text{NO}](\text{ClO}_4)_3$	0	1949	1.764(7)	1.126(6)	173.1(12)	[24n]
15	$[\text{Ru}(\text{bpb})(\text{Cl})\text{NO}](\text{ClO}_4)_3$	0	1867	1.7534(14)	1.1444(19)	172.37(14)	[24n]
16	$[\text{Ru}(\text{HEDTA})\text{NO}]$	0	1890	1.756(4)	1.156(5)	172.3(4)	[24o]
17	$\text{K}_2[\text{RuCl}_5\text{NO}]$	0	1843	1.738(2)	1.131(3)	176.7(5)	[24p]
18	$\text{Na}_2[\text{Os}(\text{CN})_5\text{NO}]\cdot 2\text{H}_2\text{O}$	0	1897	1.774(8)	1.14(1)	175.5(7)	[24q]
19	$(\text{PPh}_4)_2[\text{OsCl}_5\text{NO}]$	0	1802	1.830(5)	1.147(4)	178.5(8)	[24r]
20	$\text{K}[\text{IrCl}_5\text{NO}]$	0	1952	1.760(11)	1.124(17)	174.3(11)	[24s]
<i>n</i> = 7							
7	$[\text{Fe}(\text{'pyS}_4\text{'})\text{NO}]$	1/2	1648	1.712(3)	1.211(7)	143.8(5)	[24a]
8	$[\text{Fe}(\text{PaPy}_3)\text{NO}](\text{ClO}_4)$	1/2	1615	1.7515(16)	1.190(2)	141.29(15)	[24b]
9	$[\text{Fe}(\text{cyclam-ac})\text{NO}](\text{PF}_6)$	1/2	1615	1.722(4)	1.166(6)	148.7(4)	[24c]
10	$[\text{Fe}(\text{pyN}_4)\text{NO}]\text{Br}_2$	1/2	1620	1.737(6)	1.175(8)	139.4(5)	[25a]
11	$\text{K}(222)[\text{Fe}(\text{TpivPP})(\text{NO}_2)\text{NO}]$	1/2	1668	1.840(6)	1.134(8)	137.4(6)	[25b]
12	$[\text{Fe}(\text{TPP})(\text{l-Melm})\text{NO}]$	1/2	1625	1.743(4)	1.121(8)	142.1(6)	[25c]
13	<i>trans</i> - $[\text{FeCl}(\text{cyclam})\text{NO}]\text{ClO}_4$	1/2	1611	1.820(4)	–	144.0(6)	[25d]
14	$[\text{Fe}(\text{L}^{\text{Pr}})\text{NO}]$	3/2	1682	1.749(2)	1.182(3)	147.0(2)	[25e]
15	$[\text{Fe}(\text{Me}_3\text{TACN})(\text{N}_3)_2\text{NO}]$	3/2	1690	1.738(5)	1.142(7)	155.5(10)	[25f]
<i>n</i> = 8							
16	$[\text{CoCl}(\text{en})_2\text{NO}](\text{ClO}_4)$	0	1611	1.820(11)	1.043(17)	124.4(11)	[62c]
17	$[\text{Rh}(\text{NCMe})_3(\text{PPh}_3)_2\text{NO}](\text{PF}_6)_2$	0		2.026(8)	1.159(10)	118.4(6)	[62e]
18	$[\text{Ru}(\text{py}^{\text{bu}}\text{S}_4\text{'})](\text{HNO})]$	0	1358	1.875(7)	1.242(9)	130.0(6)	[26a]
19	$[\text{OsCl}_2(\text{CO})(\text{PPh}_3)_2](\text{HNO})]$	0	1410	1.915(6)	1.193(7)	136.9(6)	[26b]
20	$[\text{IrHCl}_2(\text{PPh}_3)_2](\text{HNO})]$	0	1493	1.879(7)	1.235(11)	129.8(7)	[26c]

The superscript *n* corresponds to the total number of ($d + \pi_{\text{NO}}^*$) electrons = 6, 7, 8, according to the Enemark–Feltham formalism. Total spin-state (*S*), nitrosyl stretching frequencies (ν_{NO}) and relevant distances and angles have been detailed.

and by the donor–acceptor abilities of the coligands. A high metal charge favors the σ -binding strength for any ligand, and disfavors the π -back donation. From the ligand side, σ - and/or π -donor as well as π -acceptor abilities must be considered. We may extract some useful comparisons from Table 1. The values of ν_{NO} cover a relatively broad range, 1800–1950 cm^{-1} for the selected Fe^{II} , Ru^{II} , Os^{II} and Ir^{III} complexes. By comparing the values of ν_{NO} for the three $\text{M}(\text{CN})_5\text{NO}^{2-}$ complexes ($\text{M} = \text{Fe}^{\text{II}}$, Ru^{II} , Os^{II}), it can be seen that ν_{NO} decreases when going from Fe^{II} to Os^{II} , in agreement with the increasing back-donation to NO^+ (cf. also the trends for $\text{MCl}_5\text{NO}^{2-}$, $\text{M} = \text{Ru}$, Os). Particularly low values of ν_{NO} may be found for strongly back bonding situations, as for $\text{K}_3[\text{Mn}^{\text{I}}(\text{CN})_5\text{NO}]$, 1700 cm^{-1} [33]. In general, increasing the ν_{NO} values reflects a stronger “nitrosonium” character, assuming the establishment of a pure NO^+ ligand as a limiting case affording a triple N–O bond order [28]. The situation for $\text{K}[\text{Ir}^{\text{III}}\text{Cl}_5\text{NO}]$ in propionitrile, with $\nu_{\text{NO}} = 1952 \text{ cm}^{-1}$, reflects an approach to this idealized descrip-

tion, with a poor back-donation probably associated with the high charge in the metal [34]. Interestingly, the highest value ever measured for a *solid* nitrosonium complex has been found in $\text{K}[\text{Ir}^{\text{III}}\text{Cl}_5\text{NO}]$, with ν_{NO} at 2006 cm^{-1} [35]. The nature of the counterions or of the solvent medium may influence the ν_{NO} values because of the specific donor-acceptor interactions afforded by some ligands such as chlorides, amines and cyanides [36].

The M^{II} -complexes containing highly electron-acceptor ligands (viz., polypyridines, azoimines, AcN) display values of $\nu_{\text{NO}} > 1900 \text{ cm}^{-1}$, while the σ/π donor ligands like OH^- or Cl^- tend to decrease ν_{NO} . For $[\text{Ru}^{\text{II}}(\eta^2\text{-phpy})(\text{trpy})\text{NO}](\text{PF}_6)_2$ (containing a strong σ -donor coligand, phpy) and for $[\text{Os}^{\text{II}}\text{Cl}_5\text{NO}]^{2-}$ (with a strong π -donor metal), the relative decrease in ν_{NO} and increase in $d_{\text{M-N}}$ can be ascribed to the build-up of very electron rich MNO moieties. In the first case, a significant deviation of $\angle\text{RuNO}$ from linearity has also been observed, resembling the situation found for some iron- and ruthenium-nitrosyl por-

phyrins containing aryl- and alkyl-coligands in *trans* position [37].

Theoretical calculations have been valuable in describing the detailed orbital compositions of the HOMO and LUMO, supporting the assignment of electronic transitions [38]. The pioneering work with SNP [39] allowed to calculate a metal-centered HOMO, with a ca. 30% $\pi^*(\text{NO})$ contribution in the e_1 MO (Fig. 3a). A similar composition has been found for $\text{Fe}(\text{cyclam-ac})\text{NO}^{2+}$ [24c], and for some non-heme analogs of nitrile hydratase, an enzyme with a $\text{Fe}(\text{III})$ center exhibiting reversible coordination of NO [40]. In some cases, the nature of the HOMO depends on the coligands, as for *trans*- $\text{Ru}(\text{NH}_3)_4(\text{L})\text{NO}^{3+/2+}$ complexes. With $\text{L} = \text{NH}_3, \text{H}_2\text{O}, \text{Cl}^-$ and OH^- , the HOMO is still metal centered, but the π interaction with NO^+ may lower enough the energy of the metal orbitals, leading to filled frontier orbitals that are mostly located on the coligands, as for $\text{L} = \text{py}$ and pz [41]. A similar behavior has been calculated for $\text{Ru}(\text{bpy})(\text{tpm})\text{NO}^{3+}$, with the HOMO strongly localized on the bpy ligand, and only a marginal contribution from metal orbitals [24g]. In contrast with the above descriptions for the HOMO, the LUMO becomes predominantly $\pi^*(\text{NO})$ in all of the nitrosyl complexes calculated so far, although with significant metal d participation.

In general, the synthetic efforts to prepare new complexes with specially designed coligands L have shown no innovative geometric or spectroscopic features to the above description [42]. Searching for a detailed electronic distribution, some EPR-silent metalloporphyrins were originally described as $\text{Fe}^{\text{III}}\text{NO}^\bullet$, with low-spin Fe^{III} ($S = 1/2$) antiferromagnetically coupled to NO^\bullet ($S = 1/2$), as suggested by Mossbauer spectroscopy [24d]. However, the latter measurements cannot strictly distinguish between purely diamagnetic $\text{Fe}^{\text{II}}\text{NO}^+$ and antiferromagnetically coupled $\text{Fe}^{\text{III}}\text{NO}^\bullet$, as recently discussed for the heme-containing protein nitrophorin [43]. There is some consensus supporting $\text{Fe}^{\text{II}}\text{NO}^+$ as a dominant contribution in the delocalized $\{\text{FeNO}\}^6$ moieties for the nitrosyl “ferri-hemes”, as with classical complexes [21,22]. This could be also the case with nitrophorins, consistently with the high values of ν_{NO} , ca. 1900 cm^{-1} . It has been proposed that the ruffling of the nonplanar hemes could favor the alternative $\text{Fe}^{\text{III}}\text{NO}^\bullet$ limiting structure, in order to account for the facile release of NO, which is at odds with the high strength of the Fe–N bond in the $\text{Fe}^{\text{II}}\text{NO}^+$ distribution [43].

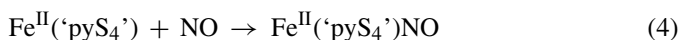
The $\{\text{MNO}\}^6$ moieties are generally very stable toward oxidation, as a consequence of the strong stabilization of the HOMO. An unusual case of reversible electrochemical oxidation was reported for $[\text{Ru}^{\text{II}}\text{Cl}_5\text{NO}]^{2-}$ in *n*-butyronitrile, at -40°C [34]. For the oxidized complex, RuCl_5NO^- , $n = 5$ and $\nu_{\text{NO}} = 1922\text{ cm}^{-1}$. It has been described as $\text{Ru}^{\text{III}}\text{NO}^+$ from EPR, IR spectra and DFT calculations, revealing a metal-centered oxidation of the $\text{Ru}^{\text{II}}\text{NO}^+$ complex and a linear RuNO arrangement.

The complexes with high values of ν_{NO} behave as oxidants, related to the build-up of positive charge at the MNO moiety. Therefore, the redox potentials for nitrosyl reduction, $E_{1/2}(\text{NO}^+/\text{NO}^\bullet)$, may be related to the values of ν_{NO} . Fairly linear correlations between these parameters have been found for different series of RuL_xNO complexes [28,24h,42a,c]. However, significant deviations from linearity are found when the metals

and/or coligands are changed [27]. In general, it can be seen that $E_{1/2}(\text{NO}^+/\text{NO}^\bullet)$ and ν_{NO} decrease when the metal becomes more electron-rich, i.e., with the stronger σ/π -donor or weaker π -acceptor abilities of L.

2.2. $n = 7$

Most of the preparations involve direct mixing of NO with solutions of the appropriate precursor, Eq. (4), which becomes related to Eq. (3) [24a]:



Similarly, the isolation of $[\text{Fe}^{\text{II}}(\text{pyN}_4)\text{NO}]\text{Br}_2$ involved a previous direct mixing of $[\text{Fe}(\text{pyN}_4)\text{Br}]\text{Br}$ with NO in methanol [25a]. The $[\text{Fe}^{\text{II}}(\text{TpivPP})(\text{NO}_2)\text{NO}]^-$ complex was obtained by the reaction of $[\text{Fe}(\text{TpivPP})]$ with NO_2^- and NO, in $\text{C}_6\text{H}_5\text{Cl}$ [25b]. Analogous processes have been carried out in aqueous solutions, by bubbling NO into $\text{Fe}^{\text{II}}(\text{CN})_5\text{H}_2\text{O}^{3-}$, previously generated in situ through aquation of $\text{Fe}^{\text{II}}(\text{CN})_5\text{NH}_3^{3-}$ [44]. Stoichiometric amounts of reactant NO should be employed, in order to prevent the formation of dinitrosyls in excess NO conditions (see below).

Table 1 includes some examples of new compounds reported in the recent years. All the complexes are bent, with $\angle\text{MNO}$ ca. $140\text{--}150^\circ$. By comparing with $n = 6$ complexes, a general decrease of ν_{NO} is observed, with values in the range $1600\text{--}1700\text{ cm}^{-1}$ for the M^{II} complexes. When the same metal/coligand environment is considered, the elongation of $d_{\text{M-N}}$ and $d_{\text{N-O}}$ can be clearly observed. Fig. 3 describes the MO situation. If an additional electron is added to the $\{\text{MNO}\}^6$ moiety (Fig. 3a), the new configuration $(e_1)^4(b_2)^2(e_2)^1$ implies a partial occupation of the totally antibonding π -type MNO-orbital. The consequent removal of the degeneracy of the e type orbitals leads to a new orbital distribution (Fig. 3b), with weaker M–N and N–O bonds, and bending of $\angle\text{MNO}$ according to Walsh's rules [21c].

By using EPR spectroscopy, complexes with ground states $S = 1/2$ or $3/2$ have been identified. The first situation is generally found in relatively strong ligand field systems. The unpaired electron resides in the a' single occupied molecular orbital (SOMO), which has metal d_z^2 and $\pi^*(\text{NO})$ components [21c]. For the six-coordinate porphyrin derivative $\text{Fe}(\text{TpivPP})(\text{NO}_2)\text{NO}^-$ and for $\text{Fe}(\text{OEP})\text{NO}$, both with $S = 1/2$, the unpaired electron has been assigned to a SOMO with a highly predominant d_z^2 character, suggesting a nearly pure $\{\text{Fe}^{\text{I}}\text{NO}^+\}$ distribution [45]. The EPR spectra of some nitrosyl metalloproteins (MbNO and HbNO) have been interpreted on similar grounds [46]. Recent evidence from MCD, Mossbauer and IR spectroscopies, and from DFT calculations [47], support the above assignment for $\text{Fe}(\text{TPP})\text{NO}$, although with a more mixed electronic distribution, ca. 50% in Fe and NO. On the other hand, the six-coordinate $\text{Fe}(\text{TPP})(1\text{-MeIm})\text{NO}$ shows a nitrosyl-centered SOMO (ca. 20% in Fe), and can be best described as $\text{Fe}^{\text{II}}\text{NO}^\bullet$. Fig. 5 shows the EPR spectrum of the $\text{Ru}(\text{bpy})(\text{tpm})\text{NO}^{2+}$ cation [24g]. Remarkably similar EPR spectra have been measured with other metal NO^\bullet -complexes with very different L coligands [48] (viz., $\text{M}^{\text{II}}(\text{CN})_5\text{NO}^{3-}$ ($\text{M} = \text{Fe}$,

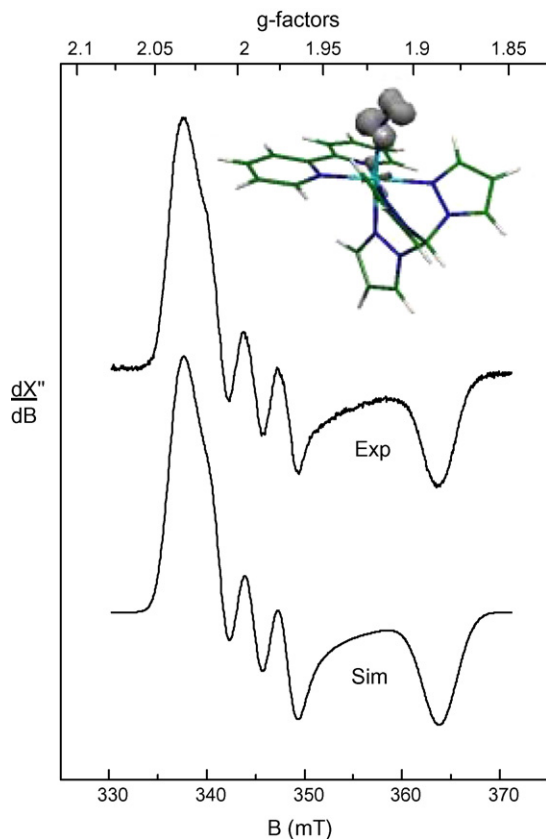


Fig. 5. Top right: DFT-calculated spin density of $[\text{Ru}(\text{bpy})(\text{tpm})\text{NO}^\bullet]^{2+}$ in a vacuum (B3LYP level, LanLDz basis set). Middle: EPR spectrum of the electrogenerated cation in $\text{MeCN}/0.1 \text{ M Bu}_4\text{NPF}_6$ at 110 K. Bottom: computer simulated spectrum. See parameters in Ref. [24g].

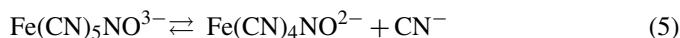
Ru, Os) [49], $\text{Ru}^{\text{II}}(\text{NH}_3)_4(\text{H}_2\text{O})\text{NO}^{2+}$ [50], $\text{Ir}^{\text{III}}\text{Cl}_5\text{NO}^{2-}$ [34], etc.). The spin electron density is located ca. 65% at the NO moiety (with two thirds at N), showing a sizeable metal contribution of ca. 35%.

Non-heme ferrous centers in some metalloproteins react reversibly with NO forming nitrosyl species with $S=3/2$ [51]. X-ray, resonance Raman, MCD, Mossbauer spectroscopies, and DFT calculations support a best description as $\text{Fe}^{\text{III}}\text{NO}^-$ (high spin ferric, $S=5/2$, antiferromagnetically coupled to NO^- , $S=1$). Similar structures have been proposed for the classical complexes $\text{Fe}(\text{L}^{\text{Pr}})\text{NO}$ [25e], $\text{Fe}(\text{EDTA})\text{NO}$ [25f], $\text{Fe}(\text{Me}_3\text{TACN})(\text{N}_3)_2\text{NO}$ [25f], and for the “brown-ring” compound, $\text{Fe}(\text{H}_2\text{O})_5\text{NO}^{2+}$ [52]. Interestingly, $\text{Fe}(\text{L}^{\text{Pr}})\text{NO}$ displays spin equilibrium between the valence tautomers $S=1/2$ and $3/2$ in the solid state.

Reasonable assignments of the complex pattern of electronic UV–vis absorption bands [24g,53], strongly dependent on the nature of the metal and coligands L, have been reported through DFT-calculations, which also allow to estimate the mixed compositions of the HOMO and LUMO. The electronic absorption bands are significantly shifted with respect to those observed in the corresponding $\{\text{MNO}\}^6$ systems [24a,g].

An important structural fact for $n=7$ complexes is the elongation of the M–L bond in the *trans*-ligand to NO, which sometimes may lead to dissociation of L [54]. This has a

great bioinorganic relevance, because the action of NO as an essential cellular signaling agent involves its coordination to the ferro-heme center in sGC, with subsequent release of the proximal histidine ligand [7,55]. This effect has been quantitatively demonstrated for $\text{Fe}^{\text{II}}(\text{CN})_5\text{NO}^{3-}$, the one-electron reduced product of SNP [56]. The subsequent labilization of cyanide is described by Eq. (5), with $K_5=6.75 \times 10^{-5} \text{ M}$:



The pH influences the equilibrium concentrations of $\text{Fe}(\text{CN})_5\text{NO}^{3-}$ and $\text{Fe}(\text{CN})_4\text{NO}^{2-}$, with the latter one increasing in acid medium, due to HCN formation. The anions can be distinguished through the UV–vis, IR and EPR spectra [57]. The relatively high value of $\nu_{\text{NO}} = 1755 \text{ cm}^{-1}$ for $\text{Fe}(\text{CN})_4\text{NO}^{2-}$ suggests a significant contribution of $\text{Fe}^{\text{I}}\text{NO}^+$ to the electronic distribution, in contrast with $\text{Fe}(\text{CN})_5\text{NO}^{3-}$, $\nu_{\text{NO}} = 1608 \text{ cm}^{-1}$ (dominant $\text{Fe}^{\text{II}}\text{NO}^\bullet$). Related situations comprising the dissociation of *trans*-chloride ligands have been observed for $\text{Ru}^{\text{II}}\text{Cl}(\text{cyclam})\text{NO}^+$ [24k], for several $\text{Ru}^{\text{II}}(\text{NH}_3)_4(\text{L})\text{NO}^{2+}$ [58], and for $\text{Os}^{\text{II}}\text{Cl}_5\text{NO}^{3-}$ [24r]. The *trans*-labilizations may be thought as arising in repulsion effects of the unpaired electron in the SOMO (with significant d_z^2 character) with the donor *trans*-ligands. Interestingly, the complexes *cis*- $\text{Os}^{\text{II}}(\text{bpy})_2\text{ClNO}^+$ [24r], *cis*- $\text{Ru}(\text{L}^{\text{Py}})\text{NO}^{2+}$ [59], and $\text{Ru}^{\text{II}}(\text{bpy})(\text{tpm})\text{NO}^{2+}$ [24g] behave as robust species, probably because the *trans*-position is occupied by the chelating ligand. Nevertheless, the DFT calculations indicate some relative elongation of the *trans*-Ru–N bond for the last two complexes.

Given that the $\text{M}^{\text{II}}\text{NO}^\bullet$ moieties are more electron rich than the $\text{M}^{\text{II}}\text{NO}^+$ ones, the possibility of protonation should be considered. The blue species arising upon reduction of SNP was initially proposed to be $\text{Fe}^{\text{II}}(\text{CN})_5(\text{NOH})^{2-}$ [49a]. This needs to be modified, on the basis of the conclusive evidence favoring $\text{Fe}(\text{CN})_4\text{NO}^{2-}$, for which a stable solid salt has been isolated [57a]. DFT calculations [60] afford a stable species for $\text{Fe}(\text{CN})_4\text{NO}^{2-}$, although not for $\text{Fe}^{\text{II}}(\text{CN})_5(\text{NOH})^{2-}$. Instead, cyanide-protonation has been predicted, in agreement with experimental evidence on the formation of $\text{Fe}^{\text{II}}(\text{CN})_4(\text{CNH})\text{L}^{n-}$ complexes at pHs <3 [61]. No other examples of protonation on bound NO have been reported.

2.3. $n=8$

Complexes containing bound NO^- have been much studied, with a predominance of five-coordinated species [21b]. A main preparative route for six-coordinated complexes [62] involved the reaction of monodentate ligands (NCS^- , Cl^- , Br^- , etc.) with five-coordinated linear nitrosyl moieties. Reaction (6) describes a representative example for a Co-complex. The perchlorate salt of the product was the first compound of this type studied by X-ray methods (Table 1) [62c]:

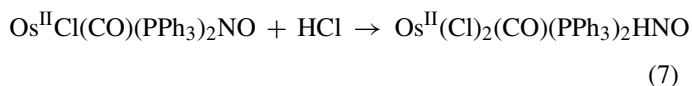


The structures of several cobalt nitrosyl porphyrins containing strongly bent MNO moieties have been obtained [63], and a formal $\text{Co}^{\text{III}}\text{NO}^-$ distribution has been assigned. All of them

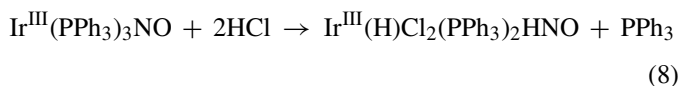
are five-coordinate square-pyramidal systems, probably because of the great *trans*-effect displayed by NO[−] [54]. The reduced form of aquacobalamin (vitamin B_{12r}, Cbl^{II}) binds NO under physiological conditions yielding a diamagnetic six-coordinate product with a weakly bound *a*-dimethylbenzimidazole and a bent nitrosyl coordinated to cobalt at the β -site of the corrin ring. It has also been described as Co^{III}NO[−], on the basis of UV–vis, ¹H, ³¹P and ¹⁵N NMR data [64].

The occurrence of bound NO[−] may be inferred for other Ni^{II}, Co^{III} and Ir^{III} nitrosyl complexes in aqueous or nonaqueous solutions, but there is no spectroscopic evidence on the detailed electronic structure [65]. For Fe(cyclam-ac)NO⁰, electrochemical, Mossbauer and IR measurements including ¹⁵N and ¹⁸O labelling, as well as DFT calculations, support the presence of NO[−] in acetonitrile [24c]. Indeed, there is strong evidence for the formation of a complex with *n* = 8, although the lack of structural or ¹H and ¹⁵N NMR information precludes a clear discrimination between NO[−] and HNO.

Three crystalline structures have been reported for six-coordinated HNO-complexes (Table 1). The first one was published in 1979 [26b], on the basis of a previous preparation described by Eq. (7) [66]. It involves the addition of HCl, or in other words, the formal protonation of bound NO[−] to HNO:



A similar procedure was used for an Ir unsaturated complex, Eq. (8) [66], with further structure elucidation [26c]:



Finally, the first structure for a Ru^{II}HNO complex (Fig. 1) involved a solid isolated after the two-electron reduction of a Ru^{II}NO⁺ complex with NaBH₄ in methanol [26a], Eq. (9):



Additional M–HNO-complexes were more recently well characterized in nonaqueous solution [67]. Among them, the first porphyrin-derivative, Ru^{II}(TTP)(1-MeIm)HNO was obtained similarly as in reaction (9) [68a]. The Re^I(CO)₃(PPh₃)₂HNO complex was prepared by two-electron oxidation of the hydroxylamine precursor with Pb(Ac)₄ [68b]. A new alternative synthetic route for the latter Re^I complex proceeds by direct insertion of NO⁺ into the metal-hydride bond in Re^I(H)(CO)₂(PPh₃)₂ [68c]. Finally, *cis-trans*-Re^ICl(CO)₂(PR₃)₂HNO (R = Ph, Cy) have been obtained through similar protonation reactions as in Eqs. (7) and (8) [68d].

With the exception of Fe(cyclam-ac)NO⁰ [24c], the absence of Fe^{II} complexes (and the general insolubility in water) are remarkable drawbacks in the above picture. The first hemoprotein nitroxyl derivative, Mb^{II}HNO, has been prepared in aqueous solution by chemical (Cr^{II}) [69a] or electrochemical [69b] reduction of Mb^{II}NO, and has been characterized by using different spectroscopies. The ¹H NMR spectrum in D₂O shows a signal at 14.8 ppm which transforms into a doublet by using ¹⁵N

(*J*_{NH} = 72 Hz). This evidence, together with ν_{NO} at 1385 cm^{−1} obtained by resonance Raman spectroscopy provides a strong support to the identity of the HNO ligand in Mb^{II}HNO, complemented by XANES and XAFS spectroscopies [69c] and by a study of the ¹H NMR structure at the heme pocket [69d]. A structural, electronic and vibrational characterization of Fe–HNO porphyrinates by DFT methodologies has been achieved, giving consistency to the apparently abnormal, high $\nu_{\text{Fe–N}}$ value observed with Mb^{II}HNO compared to $\nu_{\text{Fe–N}}$ in the related redox partners, which do not correlate with the expected loosening of the Fe–HNO bond [69e].

An apparently stable product with an intense absorption at ca. 440 nm has been generated through the electrochemical two-electron reduction of SNP in aqueous solution [70a]. It was proposed to be Fe^{II}(CN)₄(NC)NO^{4−}, but the evidence is poor. Work is going on to better characterize the reduced species [70b]. An alternative assignment as the elusive Fe^{II}(CN)₅HNO^{3−} ion could be considered, based on theoretical predictions, which provide consistent values for ν_{NO} and for the relevant Fe–N and N–O distances and MNO angle [60]. Recently, a distinctive intense band at 505 nm has been reported upon the two-electron electrochemical reduction of Ru^{II}(dpk)(trpy)NO³⁺ (*n* = 6) in AcN [24n]. It has been related to the presence of bound NO[−], although a more detailed characterization would be desirable.

All the NO[−]/HNO complexes display common structural and spectroscopic features in the solid state and in solution. They are all diamagnetic (*d*⁶ low-spin metal, singlet NO[−]), with an MNO angle near to 120°, reflecting a more pronounced bending than for *n* = 7 systems, as seen in Table 1. The combined ¹H/¹⁵N NMR evidence has been crucial for the conclusive identification of the HNO ligand in solution for most of the above reported complexes. The ν_{NO} values appear at ca. 1300–1400 cm^{−1} for the M^{II}HNO complexes [26,68], but values ≥ 1500 cm^{−1} have been observed with the Co^{III}NO[−] complexes [62]. Overall, they reflect a diminished bond order for NO[−]/HNO in comparison with NO[•]- and NO⁺-complexes, consistent with a full population of the *a'* antibonding MO (Fig. 3b).

The reasons for the preferential occurrence of bound NO[−] or HNO constitute an open issue. M^{III} complexes apparently favor the NO[−] situation. The low π -donor ability of M^{III} may explain the comparative high ν_{NO} values as well as the more facile deprotonation of HNO, in contrast with the M^{II} systems.

3. Formation and dissociation reactions of NO⁺, NO[•], and NO[−]/HNO complexes

In order to get an insight into the redox reactivity of nitrosyl ligands, we need to know about the stability of the corresponding complexes, as described by Eq. (10), and, if possible, to obtain kinetic and mechanistic information on the direct and reverse reactions, namely the formation and dissociation rate constants, *k*_{on} and *k*_{off} [21]:

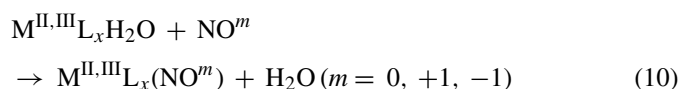


Table 2

Dissociation rate constants, $k_d = k_{\text{off}}$, and activation parameters for different $\text{Fe}^{\text{II}}(\text{CN})_5\text{X}^{n-}$ complexes^a

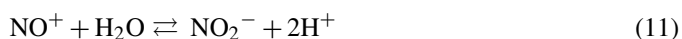
Ligand	k_d (s^{-1})	ΔH_d^\ddagger (kJ mol^{-1})	ΔS_d^\ddagger ($\text{J K}^{-1} \text{mol}^{-1}$)	ΔV_d^\ddagger ($\text{cm}^3 \text{mol}^{-1}$)	Reference
NO^+	Not detected	–	–	–	
CO^b	$<10^{-8}$	–	–	–	[78b]
CN^-^c	4×10^{-7}	–	–	–	[78c]
NO^\bullet	1.6×10^{-5}	106.4	20	7.1	[44]
dmsO	7.5×10^{-5}	110.0	46	–	[78d]
pz	4.2×10^{-4}	110.5	59	13.0	[80]
py	1.1×10^{-3}	103.8	46	–	[80]
NH_3	1.8×10^{-2}	102	68	16.4	[78e]

^a $T = 25.0^\circ\text{C}$; $I = 0.1 \text{ M}$.^b Estimated number, measured by using pz as a scavenger.^c Extrapolated from data reported at higher temperatures.

In Eq. (10), we focus our analysis on six-coordinate systems usually containing one labile water site and other more robust coordination sites ($x = 5$ means either five identical monodentate L's = aqua, cyano, ammine, etc., or a mixed system eventually containing mono- and polidentate ligands, like polypyridines, EDTA, cyclam, porphyrins, etc.). We will consider separately the chemistry of M^{II} and M^{III} complexes for each $\text{NO}^+/\text{NO}/\text{NO}^-$ situation.

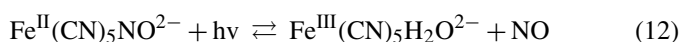
3.1. $\text{M}^{\text{II}}\text{NO}^+ - \text{M}^{\text{III}}\text{NO}^+$

The formation rate constants, k_{on} , cannot be measured in aqueous solutions for NO^+ , because its lifetime is very short, being readily hydrolyzed to NO_2^- , Eq. (11) [71]:



There are no reports for k_{off} values related to the release of NO^+ from classical $\text{M}^{\text{II}}\text{NO}^+$ complexes (cf. SNP [72], $\text{Ru}^{\text{II}}(\text{NH}_3)_4(\text{L})\text{NO}^{n+}$ [73], etc.). Assuming a dissociative mechanism, the multiple bond character in the $\text{M}^{\text{II}}\text{NO}^+$ moiety explains the extremely high thermal inertness of NO^+ . Consequently, NO^+ may be placed at the top of the so-called “spectrochemical series”, behaving as a stronger ligand than CO or CN^- , see Table 2.

In contrast to the thermally robust $\text{Fe}^{\text{II}}\text{NO}^+$ systems, photochemical activation readily occurs through irradiation into the appropriate electronic absorption bands [74]. As a prototypical case, reaction (12) describes the light-induced reactivity of SNP [74b,c]:



The event implies an intramolecular electron transfer process with metal oxidation and NO^+ reduction. From Fig. 2a, both the depopulation of the HOMO and population of the predominantly $\pi^*(\text{FeNO})$ orbital upon excitation weaken the Fe–N bond. The formation of $\text{Fe}^{\text{III}}\text{NO}$ in the excited state allows for the facile release of NO, which has also been observed for the Ru- and Os-analogs of SNP with a decreasing quantum yield [74b]. Similar photoinduced reactions have been detected for other complexes with $n = 6$ [74d–f].

As a strongly electron acceptor ligand, NO^+ induces electronic changes in the *trans*-position, as demonstrated for

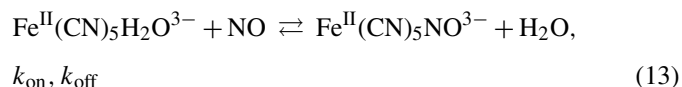
trans- $\text{Ru}^{\text{II}}(\text{NH}_3)_4(\text{H}_2\text{O})\text{NO}^{3+}$ [75]. The water ligand becomes acidic ($\text{p}K_a = 3.1$, of the same order as in $\text{Ru}^{\text{III}}(\text{NH}_3)_5\text{H}_2\text{O}^{3+}$, 4.4), and more inert toward substitution with other ligands. In this *trans*-influence, the integrity of the six-coordinated species is maintained.

Finally, we have not found any reported complex with a $\text{Fe}^{\text{III}}\text{NO}^+$ structure ($n = 5$). As said above, the $\text{Fe}^{\text{II}}\text{NO}^+$ complexes are very stable toward oxidation (see above for the unusual $\text{Ru}^{\text{III}}\text{NO}^+$ complex).

3.2. $\text{M}^{\text{II}}\text{NO}^\bullet - \text{M}^{\text{III}}\text{NO}^\bullet$

Little kinetic work has been carried out with NO^\bullet as a ligand in classical complexes. Careful removal of impurities in the gas stream and absence of NO_2^- and/or NO_2 in solution must be ensured [22c]. Clean substitution processes occur with reduced metal centers. Thus, NO binds reversibly to high spin $\text{Fe}^{\text{II}}\text{L}_x\text{H}_2\text{O}$ complexes (L = EDTA, NTA and derivatives), which are potential catalysts for NO removal from gas streams. By using fast techniques, k_{on} values were found in the range 10^6 to $10^8 \text{ M}^{-1} \text{ s}^{-1}$, at 25°C [76], whereas k_{off} values vary between 10^{-1} and 10^3 s^{-1} , depending on L. Similarly, for $\text{Fe}(\text{H}_2\text{O})_5\text{NO}^{2+}$, $k_{\text{on}} = 1.41 \times 10^6 \text{ M}^{-1} \text{ s}^{-1}$ and $k_{\text{off}} = 3.2 \times 10^3 \text{ s}^{-1}$ [52]. In all cases the electronic structure of the nitrosylated products ($S = 3/2$) has been described as $\text{Fe}^{\text{III}}\text{NO}^-$ (see above). Water exchange measurements and activation parameters sustain a dissociative-interchange mechanism [77].

The $\text{Fe}^{\text{II}}(\text{CN})_5\text{NO}^{3-}$ ion may be considered a typical model for d^6 , low-spin $\text{M}^{\text{II}}\text{NO}^\bullet$ systems [44]. Fig. 6 shows the spectral changes for the reaction of NO with aquated $\text{Fe}^{\text{II}}(\text{CN})_5\text{NH}_3^{3-}$, Eq. (13):



The inset of Fig. 6 shows that the initially attained absorption at 350 nm corresponding to $\text{Fe}^{\text{II}}(\text{CN})_5\text{NO}^{3-}$ decays subsequently in excess of NO, suggesting decomposition (see below). Independently of this complication, the faster traces reflect a well-behaved pseudo-first order process. The values of k_{obs} depend linearly on the concentration of NO, and a value of $k_{\text{on}} = 250 \text{ M}^{-1} \text{ s}^{-1}$ can be derived. This value is similar to oth-

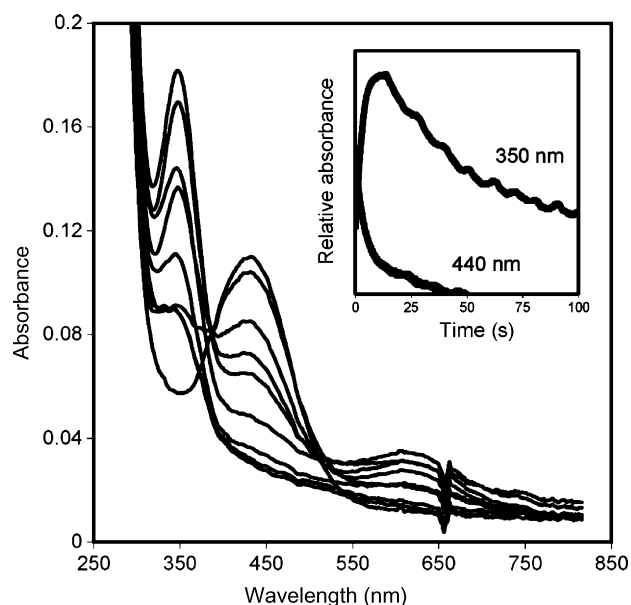
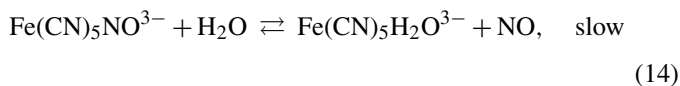


Fig. 6. Successive spectra in the reaction of 5×10^{-5} M $[\text{Fe}(\text{CN})_5\text{H}_2\text{O}]^{3-}$ with 1.8×10^{-3} M NO, pH 10, $T = 25.4^\circ\text{C}$, $I = 0.1$ M. Decay of the aqua-ion at 440 nm and build-up of $[\text{Fe}(\text{CN})_5\text{NO}]^{3-}$ at 350 nm. Absorptions at ca. 600 nm reflect the presence of $[\text{Fe}(\text{CN})_4\text{NO}]^{2-}$. Inset: time dependence of fast reactant decay and product formation. The further decay at 350 nm reflects product decomposition (see text) [44].

ers measured for the coordination of several ligands (CO, NH_3 , py, etc.) into $\text{Fe}(\text{CN})_5\text{H}_2\text{O}^{3-}$ [61,78a], reflecting a dissociative mechanism in which the release of water is rate-limiting, as supported by the positive activation enthalpies, entropies and volumes. It can be concluded that NO behaves like other Lewis-base ligands, at least with the Fe(II) metal centers, without a particular influence of the single unpaired electron on the mechanism of the formation reaction. A similar conclusion has been drawn by studying the reaction of NO with the five-coordinate $\text{M}^{\text{II}}\text{H}(\text{Cl})(\text{CO})\text{L}_2$ complexes ($\text{M} = \text{Ru}, \text{Os}$; $\text{L} = \text{P}^i\text{Pr}_3$) in benzene and in equimolar conditions, giving $\text{MH}(\text{Cl})(\text{CO})(\text{NO})\text{L}_2$ [79].

Fig. 7 shows the spectral changes upon dissociation of NO from $\text{Fe}(\text{CN})_5\text{NO}^{3-}$ (reverse of Eq. (13)). According to an accepted mechanistic description for the dissociation of X from $\text{Fe}^{\text{II}}(\text{CN})_5\text{X}^{3-}$ complexes [78,80], Eqs. (14) and (14') describe the rate-determining decay of the reactant and the formation of the final product under conditions of an excess of cyanide, which acts as a fast scavenger of the aqua-complex:



The value of $k_{\text{off}} (k_{14}) = 1.6 \times 10^{-5} \text{ s}^{-1}$ (25.0°C , pH 10) [44], obtained under saturation conditions, is included in Table 2 together with a list of related k_{-x} values obtained for other $\text{Fe}^{\text{II}}(\text{CN})_5\text{X}^{n-}$ complexes [78,80].

The trend is consistent with the magnitude of the σ – π interactions in the Fe^{II} –X bond. It can be concluded that NO^\bullet is a moderate-to-strong ligand, weaker than carbonyl or cyanide, and

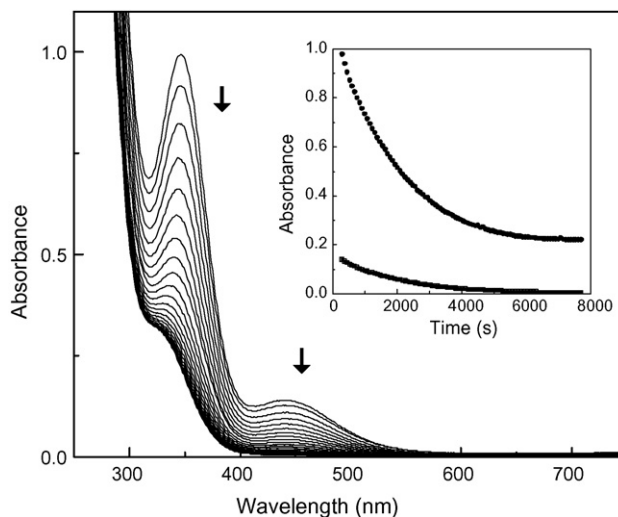
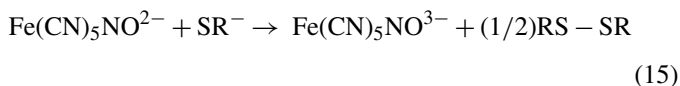


Fig. 7. Spectral changes during the dissociation of NO from 3×10^{-4} $[\text{Fe}(\text{CN})_5\text{NO}]^{3-}$, in the presence of free cyanide. pH 10.2, $T = 50.4^\circ\text{C}$, $I = 0.1$ M. Inset: time dependence for the decay at 347 and 440 nm [44].

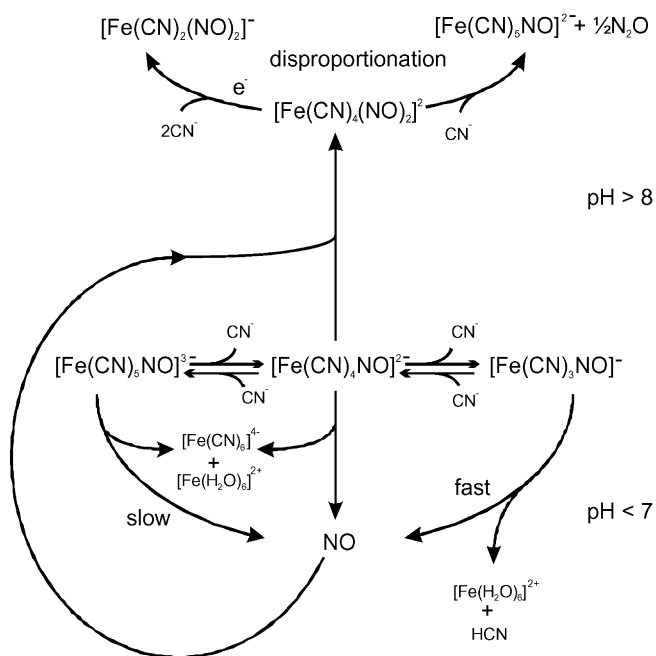
certainly than the NO^+ ligand (lower π -acceptor ability of NO^\bullet , despite a significant σ -contribution). Reliable dissociation rate data for $\text{ML}_5\text{NO}^\bullet$ -systems are scarce. For several members of the $\text{Ru}^{\text{II}}(\text{NH}_3)_4(\text{L})\text{NO}^{2+}$ series, values of $k_{\text{off}} (k_{-\text{NO}})$ have been estimated by CV, upon reduction of the corresponding NO^+ -complexes [73]. The values appear as strikingly high (range 1 – 10^{-4} s^{-1}), compared to the quoted one for $\text{Fe}(\text{CN})_5\text{NO}^{3-}$. Indeed, the electron-donor coligands aid in NO-labilization. More experimental work is needed, particularly to assess the influence of metal and coligands, as well as the interplay of *trans*-L and NO^\bullet -labilization.

The value of k_{off} for $\text{Fe}(\text{CN})_5\text{NO}^{3-}$ appears as too low for explaining the rapid vasorelaxation activity of SNP solutions after injection in the bodily fluids, assuming that a fast conversion to $\text{Fe}(\text{CN})_5\text{NO}^{3-}$ is operative under the action of biological reductants such as cysteine, Eq. (15), with a further NO-release to the medium [81,82]:



A comprehensive study of the spontaneous thermal decomposition of equilibrated $\text{Fe}(\text{CN})_5\text{NO}^{3-}$ and $\text{Fe}(\text{CN})_4\text{NO}^{2-}$ (cf. Eq. (5)) is summarized in Scheme 2 [83].

The pH conditions are crucial for analyzing the results. At pH 7, $\text{Fe}(\text{CN})_4\text{NO}^{2-}$ becomes the predominant species, see Eq. (5), and also decays with a low value of k_{off} , ca. 10^{-5} s^{-1} . A faster decomposition of $\text{Fe}(\text{CN})_4\text{NO}^{2-}$ occurs in the minute time scale at pHs 4–5, with successive cyanide- and NO-release and the generation of Prussian blue-type precipitates (Scheme 2, below). Thus, the currently accepted idea that $\text{Fe}(\text{CN})_4\text{NO}^{2-}$ is the necessary precursor for a fast NO-release under physiological conditions cannot be attributed merely to a pH effect, but is probably related to the exposure of the cyano-ligands to donor interactions with specific acceptor protein sites, thus promoting decomposition [81]. At pHs 6–8, slow NO^\bullet -release is followed by the formation of

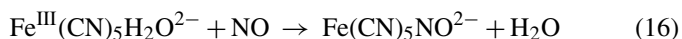


Scheme 2.

an EPR-inactive intermediate (**I**), with a characteristic UV–vis spectrum and $\nu_{\text{NO}} = 1695 \text{ cm}^{-1}$, formed through the reaction of NO with another $[\text{Fe}(\text{CN})_4\text{NO}]^{2-}$ molecule (see Scheme 2). (**I**) is a precursor of NO-disproportionation into $\text{Fe}(\text{CN})_5\text{NO}^{2-}$ and N_2O , displaying a rigorous 1:0.5 molar stoichiometry. The overall evidence suggests that (**I**) is a dinitrosyl species, *trans*- $\text{Fe}(\text{CN})_4(\text{NO})_2^{2-}$. Preliminary DFT calculations support the above formulation, consistent with a recent proposal for an iron-porphyrin, $\text{Fe}(\text{Por})(\text{NO})_2$ [84]. The formation of *trans*- $\text{Fe}(\text{CN})_4(\text{NO})_2^{2-}$ is supported by independent kinetic data on the reaction of $\text{Fe}(\text{CN})_4\text{NO}^{2-}$ with excess NO, leading to a second order rate law with $k = 4.3 \times 10^4 \text{ M}^{-1} \text{ s}^{-1}$. A related dinitrosyl compound, $\text{Fe}(\text{NO})_2(\text{'pyS}_4\text{'})$ has also been obtained by mixing $\text{Fe}(\text{'pyS}_4\text{'})$ with an excess of NO [24a]. The synthetic, structural and reactivity aspects of dinitrosyl compounds are quite relevant to the chemistry of NO-reductases [4,13].

Also remarkable in Scheme 2 is the appearance of a final decomposition product associated with a new EPR signal, indicative of the presence of the so-called “ $g = 2.03$ ” dinitrosyls, which are biologically relevant and labile species, active toward vasodilation [85]. Their general formula is $\text{Fe}(\text{L})_2(\text{NO})_2$, in a pseudo-tetrahedral arrangement, with L = thiolates, imidazolates, etc. as coligands [86]. In the reported reaction conditions of Scheme 2, the L ligand should be necessarily cyanide.

We consider now the reactions of low-spin M^{III} complexes with NO. Recent studies with iron cyano-complexes [87] may be represented by Eq. (16):

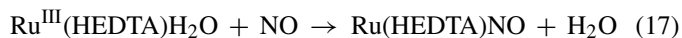


There is an electron transfer in reaction (16), namely a *reductive nitrosylation*, as far as the nitroprusside product can be described as a $\text{Fe}^{\text{II}}\text{NO}^+$ species. The rate constant, $k_{\text{on}} = 0.252 \text{ M}^{-1} \text{ s}^{-1}$ (25.5 °C, pH 3, $I = 0.1 \text{ M}$) is several orders of magnitude higher

than the values currently found for the coordination of different X ligands into $\text{Fe}^{\text{III}}(\text{CN})_5\text{H}_2\text{O}^{2-}$, which are assumed to react through dissociative-interchange mechanisms [78a]. The k_{on} value, together with activation parameters, $\Delta H^\ddagger = 52 \text{ kJ mol}^{-1}$, $\Delta S^\ddagger = -82 \text{ J K}^{-1} \text{ mol}^{-1}$, $\Delta V^\ddagger = -13.9 \text{ cm}^3 \text{ mol}^{-1}$, suggest a rate determining step involving electron transfer with formation of Fe^{II} -intermediates, for which direct evidence has been provided. Reaction (16) was erroneously reported as of “outer-sphere” type [87]. An associative mechanism involving an heptacoordinated transition state has been suggested [22a], related to the one previously discussed for the coordination of NO into $[\text{Ru}^{\text{III}}(\text{NH}_3)_5\text{L}]^{n+}$ complexes ($\text{L} = \text{NH}_3, \text{H}_2\text{O}, \text{Cl}^-$) [88]. Alternatively, an inner-sphere pathway involving initial association of NO with bound cyanides in the precursor complex, leading to the formation of NO^+ , reduced $\text{Fe}(\text{II})$ and further chemistry would also be feasible, avoiding the proposal of an intermediate with CN 7 [44].

Reaction (16) is irreversible, as evidenced by the zero intercept in the plot of k_{obs} (s^{-1}) against $[\text{NO}]$. Remarkably, the reactants are the effective products in the *photochemical activation* of SNP, Eq. (12).

A similar interplay between a negligible thermal $\text{Fe}^{\text{II}}\text{NO}^+$ dissociation and a rapid photochemical NO-release has been reported for $\text{Fe}(\text{PaPy}_3)\text{NO}^{2+}$, an $n = 6$ complex, see Table 1 [24b]. For the $\text{Ru}^{\text{III}}(\text{HEDTA})(\text{H}_2\text{O})$ complex [89], very high coordination rates have been found, with k_{on} exceeding $10^8 \text{ M}^{-1} \text{ s}^{-1}$ at physiological temperature, Eq. (17):



The diamagnetic product has been described as $\text{Ru}^{\text{II}}\text{NO}^+$, and the reaction type appears as similar to Eq. (16). An associative interchange mechanism has been proposed. The unusual high value of k_{on} has been ascribed to the extreme lability of the coordinated water molecule, which interacts with the pendant carboxylate group creating an “open” area for site of attack of the incoming NO. This $\text{Ru}(\text{III})$ complex has been used as an effective scavenger of NO in different disease states including sepsis, allograft rejection and cancer, as well as in kinetic studies of reversible reactions of NO with metal complexes, for which a fast trapping of released NO is needed [90].

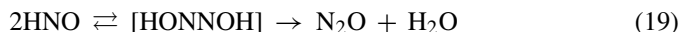
Finally, classical complexes with $\text{M}^{\text{III}}\text{NO}^\bullet$ electronic structure have not been identified in the ground state, for which the alternative $\text{M}^{\text{II}}\text{NO}^+$ formulation has been always assigned. On the other hand, excited state $\text{M}^{\text{III}}\text{NO}^\bullet$ complexes release NO in the nanosecond time-scale [74b].

3.3. $\text{M}^{\text{II}}\text{NO}^-/\text{HNO}-\text{M}^{\text{III}}\text{NO}^-/\text{HNO}$

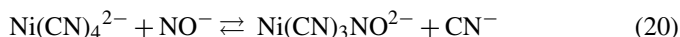
No reports exist in the literature on the coordination rates of NO^-/HNO into Fe^{II} or Fe^{III} in classical coordination compounds. HNO may be generated in aqueous solution by using Angeli’s salt, $\text{Na}_2\text{N}_2\text{O}_3$, which reacts according to Eq. (18), in a pH-independent way in the range 4–8 [20a]:



The k_{on} values for HNO are difficult to study because of the high rate of competitive HNO-coupling, Eq. (19), with $k_{19} = 8 \times 10^6 \text{ M}^{-1} \text{ s}^{-1}$ [91]:



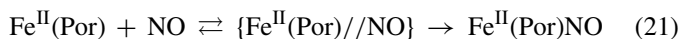
Thus, at least for low-spin systems, reactions of HNO with the inert Fe(II) or Fe(III) aqua-complexes (cf. $\text{Fe}^{\text{II,III}}(\text{CN})_5\text{H}_2\text{O}^{3,2-}$, see above) are unable to compete with self-dimerization. Coordination may be achieved with high spin, labile metal ions. The reaction of $\text{Ni}(\text{CN})_4^{2-}$ with $\text{N}_2\text{O}_3^{2-}$ leads to a deep violet color at $\text{pH} > 9$, and has been described by Eq. (20) [65a]:



Reaction (20) implies the displacement of CN^- by NO^- , providing evidence for free NO^-/HNO in aqueous solution. The electronic distribution in the tetrahedral $\text{Ni}(\text{CN})_3\text{NO}^{2-}$ ion remains uncertain. From the value of $\nu_{\text{NO}} = 1780 \text{ cm}^{-1}$, a $\{\text{Ni}^0\text{NO}^+\}^{10}$ distribution has been suggested [65a].

3.4. $\text{Fe}^{\text{II}}(\text{Por})(\text{NO})$ and $\text{Fe}^{\text{III}}(\text{Por})(\text{NO})$ (Por = porphyrins and hemoproteins)

These reactions have been comprehensively reviewed [22]. With high spin $\text{Fe}^{\text{II}}(\text{Por})$ compounds (Por = water-soluble TPPS and TMPS, Hb, Mb, sGC), very fast NO-coordination ensues, with $k_{\text{on}} = \text{ca. } 10^7\text{--}10^9 \text{ M}^{-1} \text{ s}^{-1}$. On the basis of the low values of the activation enthalpies and entropies, the mechanisms have been discussed in terms of the diffusion-limited formation of an encounter complex, prior to NO bond formation according to Eq. (21):

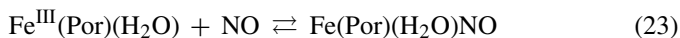
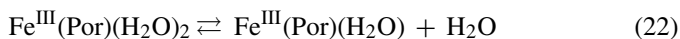


The reactant is probably a five-coordinate heme complex, and the formation of a Fe–NO bond would not require the displacement of another ligand; thus, it is not limited by the rate of ligand labilization. These very fast reactions are relevant to the activation of sGC or to the inhibition of cytochrome oxidase [22].

Also important are the reverse NO-dissociation reactions of $[\text{Fe}^{\text{II}}(\text{Por})\text{NO}]$, which cover a broad range of k_{off} values, from 10^{-2} to 10^{-5} s^{-1} , depending on the conditions and the nature of substituents in the heme-ligands [22,92].

Studies on the reversible reactions of $\text{Fe}^{\text{III}}(\text{Por})$ with NO involved systematic measurements to determine k_{on} and k_{off} [22]. The $\text{Fe}^{\text{III}}(\text{Por})(\text{H}_2\text{O})_2$ species are considered to be spin-admixed with $S = 3/2$ and $5/2$ [93]. The k_{on} values are mostly around $10^5 \text{ M}^{-1} \text{ s}^{-1}$ [22], with higher values for catalase ($3 \times 10^7 \text{ M}^{-1} \text{ s}^{-1}$) [94] and a noticeably lower one for cyt^{III} , $7.2 \times 10^2 \text{ M}^{-1} \text{ s}^{-1}$ [94], which is attributed to occupation of the axial coordination sites by an imidazole nitrogen and by a methionine sulfur of the protein. Large and positive activation entropies and volumes determine a substitution mechanism dominated by dissociation of the aqua-ligand according to Eq. (22), followed by the very fast reaction of the unsaturated intermediate with NO, Eq. (23). The latter process implies a considerable charge transfer to give a linear, diamagnetic FeNO

moiety, which may be formally represented as $\text{Fe}^{\text{II}}\text{NO}^+$. Therefore, the mechanism of the “off” reaction (reverse of reaction (23)) also reflects the intrinsic entropy and volume changes associated with the spin and solvent reorganizations:



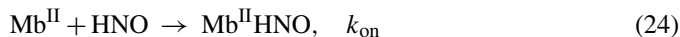
In principle, reactions (22) and (23) imply a simple Lewis-base substitution reaction, with little (if any) influence of the free radical nature of NO^\bullet on the kinetics and mechanism of the NO-heme interactions. A recent study with $\text{Fe}^{\text{III}}(\text{TMPS})$ at pHs 4–5 [95a] allowed to confirm the results and mechanistic interpretations for the $\text{Fe}^{\text{III}}(\text{Por})$ nitrosylations [22]. However, working at $\text{pH} \geq 8$ (the pK_a is 6.9), k_{on} decreased by two orders of magnitude with respect to the values at pHs 4–5. Based on the changes in the activation parameters (entropies and volumes) from positive to negative values with increasing pHs, a change in mechanism from dissociative (when H_2O is the coligand) to associative (with OH^- as the coligand) has been suggested. At high pHs, the mechanism would imply a fast association of NO with the presumably five-coordinated $\text{Fe}^{\text{III}}(\text{TMPS})(\text{OH})$ complex, with a subsequent rate-limiting electronic redistribution forming the spin-changed product, $\text{Fe}^{\text{II}}(\text{TMPS})(\text{NO}^+)(\text{OH})$. This behavior has been reproduced for a water soluble octa-anionic $\text{Fe}^{\text{III}}(\text{Por}^{8-})$ complex ($\text{pK}_a = 9.26$) [95b]. Preliminary measurements with other $\text{Fe}^{\text{III}}(\text{Por})$ compounds anticipate that this is a general feature of NO coordination in these systems. It has been reported that the k_{off} values also decrease at the high pHs, reflecting the spin changes associated with a larger demand for reorganization of d electrons upon reformation of $\text{Fe}^{\text{III}}(\text{Por})(\text{OH})$ from $\text{Fe}^{\text{II}}(\text{Por})(\text{NO}^+)(\text{OH})$ (i.e., $S = 0 \rightarrow S = 5/2$) in comparison to that occurring for $\text{Fe}^{\text{II}}(\text{Por})(\text{NO}^+)(\text{H}_2\text{O})$ ($S = 0 \rightarrow S = 5/2, 3/2$). Evidently, these new results suggest that, in addition to the lability of water, other factors such as the overall charge of the porphyrin ligand, spin state, number and nature of the axial ligands and solvent interactions ought to be considered in the mechanistic analysis of these important and biorelevant processes.

The reversibility of reactions (22) and (23) indicates that heme-compounds are able to afford spontaneously the back conversion of NO^+ into NO^\bullet , in contrast with the results found for classical low-spin Fe^{III} complexes. Although these reverse processes are usually described as NO-dissociations, it becomes evident that k_{off} involves a strong electronic redistribution coupled to the ligand interchange. The same can be said on the direct k_{on} reaction, which although considered a nitrosyl formation reaction, may be alternatively described as a *reductive nitrosylation* process (see below).

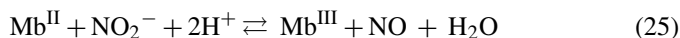
3.5. $\text{Fe}^{\text{II}}(\text{Por})\text{NO}^-/\text{HNO}-\text{Fe}^{\text{III}}(\text{Por})\text{NO}^-/\text{HNO}$

A significant kinetic result on the coordination of HNO into ferro-heme systems has been obtained through reaction (24), by reacting deoxyMb (Mb^{II}) with free HNO produced from the

decomposition of Angeli's salt (cf. Eq. (18)) [96]:

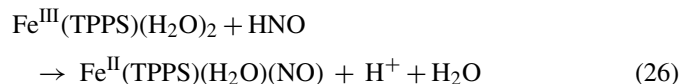


The reaction of Angeli's salt with Mb^{II} is a matter of some controversy, because a complex mixture of products is generated, including the transient formation of metMb (Mb^{III}), ultimately giving $\text{Mb}^{\text{II}}\text{NO}$, a reaction that had been previously observed [97]. It has been shown that the formation of Mb^{III} ensues according to reaction (25), implying a competing reactivity of Mb^{II} with the NO_2^- byproduct formed in reaction (18):



$\text{Mb}^{\text{II}}\text{HNO}$ has been quantified by ^1H NMR and UV–vis spectroscopies in the mixtures also containing $\text{Mb}^{\text{II}}\text{NO}$ [69a,96]. The maximum yield was ca. 80%, and this was obtained by raising the pH in order to inhibit reaction (25). Kinetic simulations considering the overall set of reactions give a lower limit to the bimolecular rate of trapping as $k_{\text{on}} = 1.4 \times 10^4 \text{ M}^{-1} \text{ s}^{-1}$. Reaction (24) showed to be irreversible, with unmeasurable k_{off} values, revealing that $\text{Mb}^{\text{II}}\text{HNO}$ is very inert toward dissociation.

For MetMb, MetHb and other ferric hemoproteins, the reactions with HNO, generated according to Eq. (18), led to reductive nitrosylation with formation of the corresponding $\text{Fe}^{\text{II}}\text{NO}$ products [98]. More recently, this trapping reaction has been also carried out with a model porphyrin, $\text{Fe}^{\text{III}}(\text{TPPS})$, Eq. (26) [99]. A similar reaction has been observed with a Mn^{III} -porphyrin [100]:



4. Electrophilic reactivity of bound nitrosonium (NO^+)

As NO^+ behaves as a very strong electrophile, NO_2^- or HNO_2 are rapidly formed as dominant products in aqueous solution, with extremely low concentrations of free NO^+ [22c]. However, NO^+ may be stabilized by coordination to metal ions. In this way, NO_2^- solutions can readily generate metal- NO^+ complexes by coordination and proton assisted dehydration, Eqs. (1) and (2).

In addition to the different manifestations of the electron-acceptor ability of the NO^+ ligand, related to the high values of ν_{NO} , facile NO -centered reductions, and photoinduced activity rendering free NO , we describe now the main thermal reactivity mode for bound NO^+ , the addition of a nucleophile B, as described by reaction (27):



The thermodynamics and kinetics of reaction (27) depend on the nature of the metal M, the coligands L, and of the nucleophile B (with its deprotonated B^- active form). Reactions of OH^- , NH_3 and other nitrogen hydrides such as amines, hydrazine (N_2H_4), hydroxylamine (NH_2OH), hydrazoic acid (HN_3), etc., sulfur containing species as SH^- , thiolates (SR^-), SO_3^{2-} , and finally a

variety of organic molecules have a very long and distinguished history, and have been comprehensively reviewed [23].

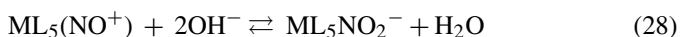
Reaction (27) is an equilibrium process for the formation and back-dissociation of the $\{\text{ML}_5\text{N}(\text{O})\text{B}\}$ adduct. B^- has a free electron pair that interacts with the positive charge in the delocalized LUMO of the MNO moiety, mainly located at the N-atom. The adduct may dissociate back to the reactants or react subsequently, either losing a proton (as in the reaction with OH^- , see below), or through redox processes involving reduction of NO^+ and oxidation of B^- . The latter is the case for the reactions with nitrogen hydrides leading to gas evolution: N_2 , N_2O or mixtures of them, constituting one possible origin of denitrification processes in soils [4,101]. Also, nitrosothiolate adducts, $\{\text{FeL}_5\text{NOSR}\}$, or the dissociated NOSR's, have been proposed as nitrosyl carriers in the biological fluids, precursors of NO generation [11,81,82].

The stoichiometries of many addition reactions on $\text{ML}_5(\text{NO}^+)$ complexes were well established over the 1970s, though with limited evidence on the characterization of the adducts. The electrophilicity of the different NO^+ -complexes used to be considered in terms of the magnitude of the equilibrium constant for reaction (27). Predictive estimations of the electrophilic reactivity were also done by considering the values of ν_{NO} . In this way, complexes with ν_{NO} above 1860–1890 cm^{-1} were found to show some reactivity with at least one nucleophile. This picture has been useful, but fails in making a quantitative prediction of reactivity for different $\text{ML}_5(\text{NO}^+)$ systems [23].

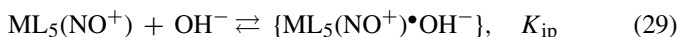
In this section we describe recent advances on the following issues: (i) *Rate constants* for the elementary steps comprising the adduct formations have been estimated, based on a detailed discussion of the underlying mechanisms. This includes a proper description of the adduct-intermediates using experimental and/or theoretical methods. (ii) A generalized approach has been proposed for understanding and predicting reactivity, in terms of the redox potentials, $E_{\text{NO}^+/\text{NO}}$, of the different $\text{ML}_5(\text{NO}^+)$ complexes, rather than the ν_{NO} values. We elaborate on the possibility of including the heme-nitrosyls together with classical coordination complexes under a common mechanistic framework. (iii) The advances in the chemistry of the nitrogen hydrides and thiolates, with the inclusion of NO_2^- or HNO_2 as biologically relevant nucleophiles. (iv) The influence of subtle changes in the structure of the nucleophile on the stoichiometry and mechanisms for a given nitrosyl complex (SNP) has been studied (viz., for N_2H_4 and substituted derivatives).

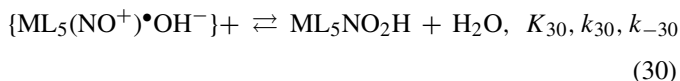
4.1. The mechanism of the reactions of $\text{M}(\text{CN})_5\text{NO}^{2-}$ ($\text{M} = \text{Fe}, \text{Ru}, \text{Os}$) and $\text{Ru}(\text{bpy})(\text{tpm})\text{NO}^{3+}$ ions with OH^- : a generalization for $\text{ML}_x(\text{NO}^+)$ systems

The reactions of OH^- with $\text{ML}_5(\text{NO}^+)$ systems can be described by the following global stoichiometry, Eq. (28):



In the mechanistic analysis we consider a set of successive reactions [24q]:





These reactions have been usually studied spectrophotometrically, measuring the increase in the concentration of the product with time. A pseudo-first order behavior has been found, with pH-dependent k_{obs} rate constants. The experimental rate law is of the form: $k_{\text{obs}} = a[\text{OH}^-] + b/[\text{OH}^-]$. By considering reactions (29)–(31), the following rate law can be deduced, with $k_{\text{OH}} = K_{\text{ip}}k_{30}$ and $K_{\text{eq}} = K_{\text{ip}}K_{30}K_{31}$ [24q]:

$$k_{\text{obs}} = k_{\text{OH}} \{[\text{OH}^-] + 1/K_{\text{eq}} [\text{OH}^-]\} \quad (32)$$

The values of K_{ip} can be calculated by knowing the charges and radii of the reactants, and in this way we can get values for k_{30} , which is the unimolecular rate constant for the conversion of the outer-sphere complex into the inner-sphere addition intermediate, Eq. (30). Usually, we employ the second order rate constants, k_{OH} , for comparing the nucleophilic reactivities of different complexes toward OH^- , assuming that they reflect the trends in the values of k_{30} , with a minor influence of K_{ip} . Finally, reaction (31) comprises a fast deprotonation step.

Kinetic studies with $\text{Fe}(\text{CN})_5\text{NO}_2^-$ have been performed [102], followed by extensions to the Ru- [24f] and Os-analogs [24q]. The values of k_{OH} for the reactions of Fe- and Ru- nitrosyl-complexes are very similar, 0.55 and $0.95 \text{ M}^{-1} \text{ s}^{-1}$, respectively, at 25.0°C . Ruthenium displays a stronger back bonding to NO^+ , and we should expect a smaller nucleophilic rate constant compared to iron. Apparently, this is compensated by the greater polarizability of the ruthenium-nitrosyl fragment. For the osmium complex, $k_{\text{OH}} = 1.37 \times 10^{-4} \text{ M}^{-1} \text{ s}^{-1}$. The sharp decrease in k_{OH} has been ascribed to the stronger comparative π -donor ability of the Os-pentacyano fragment [24q].

The recently prepared complex $[\text{Ru}(\text{bpy})(\text{tpm})\text{NO}](\text{PF}_6)_3$ showed a very high ν_{NO} , 1959 cm^{-1} , and was useful for exploring the electrophilic reactivity [24g]. Fig. 8 shows the successive spectra obtained for the $\text{RuNO}^+ \rightarrow \text{RuNO}_2^-$ conversion.

The inset in Fig. 8 shows the exponential increase of absorbance corresponding to the build-up of the nitro-complex, see Eqs. (29)–(31). Fig. 9 shows a plot of k_{obs} versus $[\text{OH}^-]$, which has the form described by Eq. (32).

The value of $k_{\text{OH}} = 3.1 \times 10^6 \text{ M}^{-1} \text{ s}^{-1}$ is close to the highest value ever measured for nitrosyl complexes, $5.60 \times 10^6 \text{ M}^{-1} \text{ s}^{-1}$, for *cis*- $\text{Ru}(\text{AcN})(\text{bpy})_2\text{NO}^{3+}$ [27]. Note that Fig. 9 displays a linear dependence on the concentration of OH^- , only for sufficiently high pHs. For low pH values, a leveling off of k_{obs} is observed. As shown by Eq. (32), this is a consequence of the influence of the second term inside the parenthesis. In these low pH conditions, the addition reaction is evidently very slow, although the value of k_{30} may be evaluated accurately from the fit. The independence of k_{obs} values on the pH for some related reactions has been considered as being associated with the action of water, not of OH^- , as the true nucleophile (see below) [42a–c].

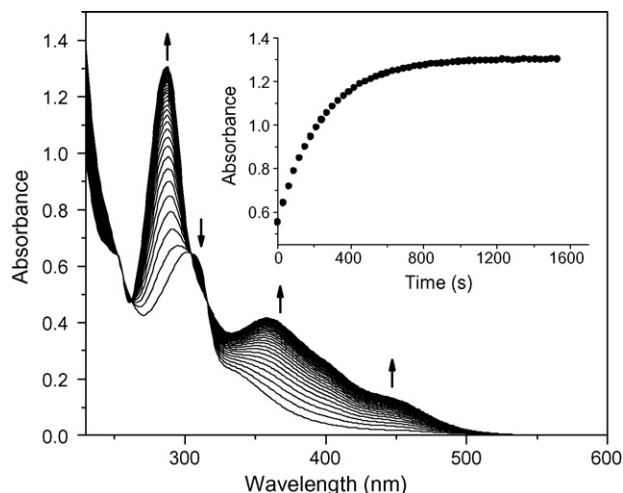


Fig. 8. Successive spectra for the reaction of $5.4 \times 10^{-5} [\text{Ru}(\text{bpy})(\text{tpm})\text{NO}]^{3+}$ with OH^- , $I = 1 \text{ M}$, $T = 25^\circ\text{C}$, $[\text{OH}^-] = 2.2 \times 10^{-9} \text{ M}$. Inset: absorption increase with time at 288 nm [24g].

The proposal of $\text{Ru}(\text{bpy})(\text{tpm})\text{NO}_2\text{H}^{2+}$ as an intermediate in reactions (29)–(31) is consistent with the rigorous stoichiometry found for many $\text{ML}_5(\text{NO}^+)$ systems. In general, the highly reactive NO_2H intermediates have not been directly identified. Fig. 10 shows the optimized DFT geometries calculated along the reaction coordinate, with $\text{ML}_5 = \text{Fe}(\text{CN})_5^{3-}$, including the transition state [27].

We may associate the addition process with a geometric change from linear to bent (N -hybridization changes from sp to sp^2), or alternatively with an addition of the electron pair of OH^- to the LUMO, involving a formal conversion from $n = 6$ to 8 in the $\{\text{MNO}\}^n$ moiety. The geometrical and IR parameters calculated through the DFT procedure are in agreement with the proposed scheme [27].

Looking for a generalized description of the OH^- -addition process, the reactivities of a great number of $\text{ML}_5(\text{NO}^+)$ complexes have been measured [27]. All of them lead to the corresponding nitro-complexes, with the same overall stoichiometry. The different nitro-complexes may show a variable stability toward the dissociation of NO_2^- , Eq. (33), but the latter

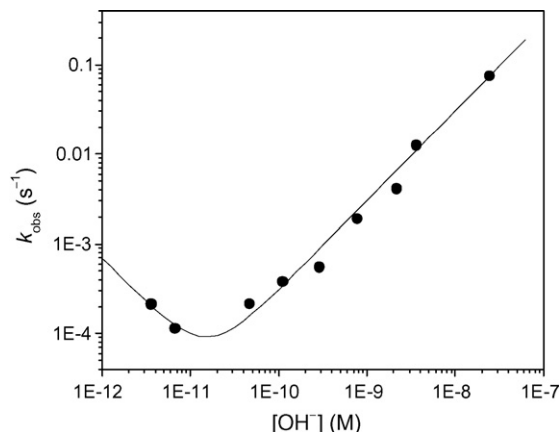


Fig. 9. Dependence of k_{obs} on $[\text{OH}^-]$ for the reaction of $(2.5\text{--}5.5) \times 10^{-5} \text{ M}$ $[\text{Ru}(\text{bpy})(\text{tpm})\text{NO}]^{3+}$ with OH^- . $T = 25^\circ\text{C}$, $I = 1 \text{ M}$ [24g].

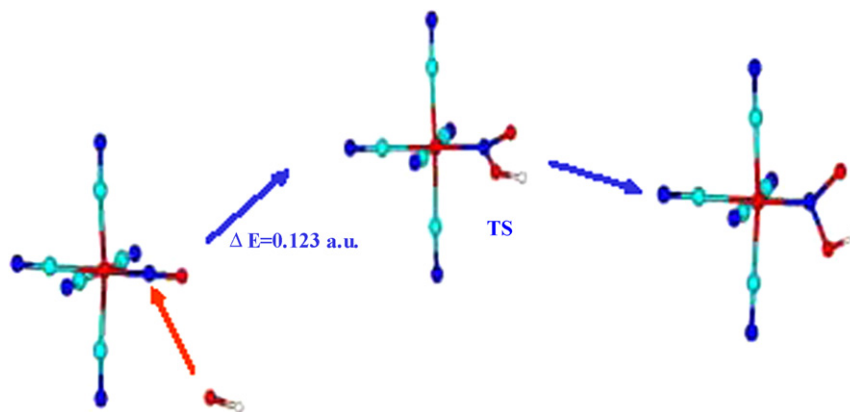


Fig. 10. Optimized geometries for the initial steps of the reaction of $[\text{Fe}(\text{CN})_5\text{NO}]^{2-}$ with OH^- , giving the transition state and the HNO_2 intermediate [27].

processes show to be sufficiently slow compared to the previous reactions (29)–(31):

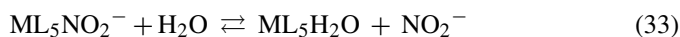


Fig. 11 shows a plot of $\ln k_{\text{OH}}$ against the corresponding $E_{\text{NO}^+/\text{NO}}$ values for different $\text{ML}_5(\text{NO}^+)$ complexes, and Table 3 includes some selected examples, providing values of relevant parameters such as ν_{NO} , k_{OH} and K_{eq} .

The plot implies a Marcus-type linear free energy relationship (LFER), which currently holds when a group of

reactions are governed by a common mechanism [103]. Marcus extended his original model for weakly-coupled outer-sphere electron transfer reactions to the interpretation of inner-sphere mechanisms [104], i.e., comprising some associative character, which is the actual situation found in the nucleophilic additions. The plot has a slope fairly close to the theoretical prediction, 19.4 V^{-1} , and spans a range of rate constant values of ca. 10 orders of magnitude, as well as a difference of ca. 1.2 V for the values of the extreme redox potentials. Obviously, the position of each complex in the plot is a consequence of the different coligands involved, which determine the value of the net positive charge in the acceptor MNO moieties. A correlation of k_{30} with these DFT-calculated charges, as well as with the LUMO energies, has been also found [27].

Fig. 11 constitutes a valuable predictive tool for quantifying the relative electrophilic reactivities of different metal nitrosyls (by the way, using a kinetic indicator!). Noticeably, a parallel line stands for a series of $\text{trans-Ru}(\text{L})(\text{py})_4\text{NO}^{3+}$ complexes, which react slower than expected, probably because of steric restrictions. The recent value of k_{30} for $\text{Ru}(\text{bpy})(\text{tpm})\text{NO}^{3+}$ [24g] fits very well in the plot displayed in Fig. 11, in the upper right side, and the same can be said for $\text{Ru}(\text{EDTA})\text{NO}^-$ [24o]. We can confidently assume that all the complexes described in Fig. 11 react through the same mechanism. Even for the highly reactive nitrosyl complexes promoting a full conversion of MNO^+ into MNO_2^- at low pHs (range 0–3), the above treatment strongly suggests that OH^- is always the relevant nucleophile. Highly electrophilic complexes like IrCl_5NO^- [34] and $\text{Ru}(\text{trpy})(\text{L})\text{NO}^{2+}$ (L = azoimines) [42b] must be maintained in strongly acid media in order to avoid the conversion into the nitro-complexes.

Following the pioneering studies on the reductive nitrosylation reactions of hemoproteins [105a], the electrophilic reactivity of nitrosyl ferri-hemes in aqueous solution has been comprehensively reviewed [105b,c]. This reaction type involves the reduction of the oxidizing metal center by NO, with generation of $\text{NO}^+/\text{NO}_2^-$ products. The participation of nucleophiles is shown in a generalized way in Eq. (34):

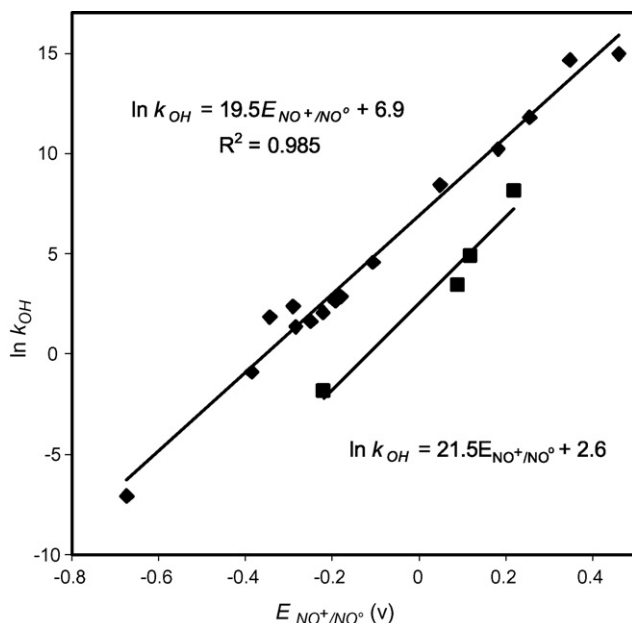
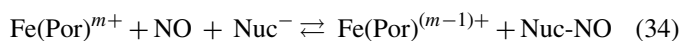


Fig. 11. LFER plot of $\ln k_{\text{OH}}$ (addition rate constant) against $E_{\text{NO}^+/\text{NO}}$ (vs. Ag/AgCl 3 M KCl) for the reactions of a series of ML_5NO^n complexes with OH^- . Main plot, from left to right, in order of increasing potentials: $[\text{Os}(\text{CN})_5\text{NO}]^{2-}$; $\text{trans-}[\text{Ru}(\text{his})(\text{NH}_3)_4\text{NO}]^{3+}$; $[\text{Ru}(\text{CN})_5\text{NO}]^{2-}$; $[\text{Ru}(\text{EDTA})\text{NO}]$; $[\text{Fe}(\text{CN})_5\text{NO}]^{2-}$; $\text{trans-}[\text{Ru}(4\text{-Mepy})(\text{NH}_3)_4\text{NO}]^{3+}$; $\text{trans-}[\text{Ru}(\text{NH}_3)_4\text{NO}(\text{py})]^{3+}$; $\text{trans-}[\text{Ru}(\text{Clpy})(\text{NH}_3)_4\text{NO}]^{3+}$; $\text{trans-}[\text{Ru}(\text{NH}_3)_4\text{NO}(\text{nic})]^{3+}$; $\text{trans-}[\text{Ru}(\text{NH}_3)_4\text{NO}(\text{pz})]^{3+}$; $\text{cis-}[\text{Ru}(\text{bpy})_2\text{ClNO}]^{2+}$; $[\text{Ru}(\text{bpy})(\text{trpy})\text{NO}]^{3+}$; $\text{cis-}[\text{Ru}(\text{bpy})_2\text{ClNO}]^{2+}$; $\text{cis-}[\text{Ru}(\text{AcN})(\text{bpy})_2\text{NO}]^{3+}$; $[\text{Ru}(\text{bpy})(\text{tpm})\text{NO}]^{3+}$. Secondary plot: $\text{trans-}[\text{Ru}(\text{OH})\text{NO}(\text{py})_4]^{2+}$; $\text{trans-}[\text{RuClNO}(\text{py})_4]^{2+}$; $\text{trans-}[\text{Ru}(\text{NCS})\text{NO}(\text{py})_4]^{2+}$; $\text{trans-}[\text{NCRu}(\text{py})_4\text{CNRu}(\text{py})_4\text{NO}]^{3+}$ [24g,24o,27].

Table 3

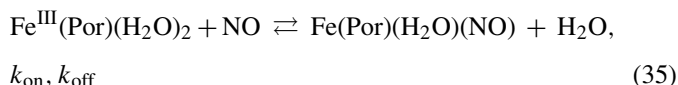
Kinetic results for the OH[−]-addition reactions on different NO-complexes

	k_{OH}^{a} (M ^{−1} s ^{−1})	k_{30}^{b} (s ^{−1})	ΔH^\ddagger (kJ mol ^{−1})	ΔS^\ddagger (J K ^{−1} mol ^{−1})	$E_{\text{NO}^+/\text{NO}}^{\text{c}}$ (V)	$\nu_{\text{NO}}^{\text{d}}$ (cm ^{−1})	K^{e} (M ^{−2})	Reference
[Ru(bpy)(tpm)NO] ³⁺	3.1×10^6	1.4×10^6	94	193	0.31	1959	4.4×10^{21}	[24g]
[Ru(bpy)(trpy)NO] ³⁺	3.2×10^5	1.3×10^5	89	159	0.25	1946	2.1×10^{23}	[27]
<i>cis</i> -[Ru(bpy) ₂ (Cl)NO] ²⁺	8.5×10^3	4.6×10^3	100	164	0.05	1933	1.6×10^{15}	[27]
<i>trans</i> -[Ru(NH ₃) ₄ (pz)NO] ³⁺	1.8×10^2	9.6×10^1	76	54	−0.11	1942	6.0×10^8	[27]
[Ru(EDTA)NO] [−]	4.35	ca. 3×10^1	60	−31	−0.34	1890	10^3	[24o]
[Ru(CN) ₅ NO] ^{2−}	0.95	6.4	57	−54	−0.35	1926	4.4×10^6	[27]

Activation parameters, redox potentials, nitrosyl stretching frequencies, and equilibrium constants.

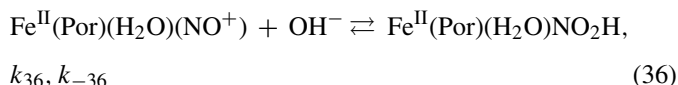
^a Fitted from the experimental rate law, Eq. (32).^b Ummolecular rate constant for the conversion of the outer-sphere- into the inner-sphere OH[−]-addition complex, Eq. (30). Estimated as $k_{\text{OH}}/K_{\text{ip}}$; see Ref. [27] for details on the estimation of K_{ip} .^c V vs. Ag/AgCl, 3 M KCl (0.21 V vs. NHE).^d Measured in aqueous solution or with KBr pellets, see the references.^e Corresponds to Eq. (28).

It is usual to describe the complete process occurring for reductive nitrosylation in terms of a set of successive reactions, as described in Scheme 3 and Eqs. (35)–(39):

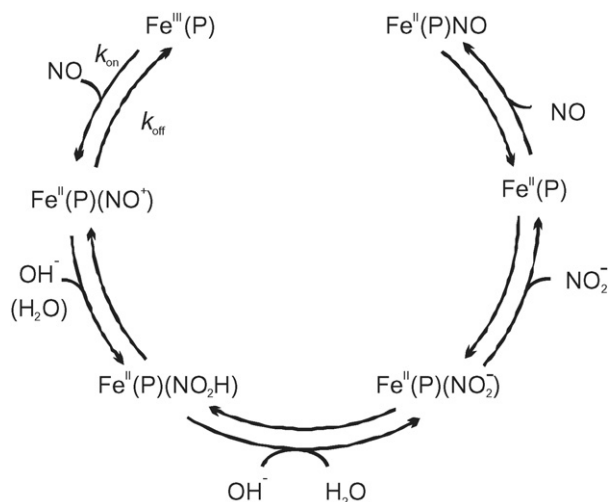


Reaction (35) comprises the reversible coordination of NO on the high spin ferri-heme moieties, with the rate-constants usually identified as k_{on} , k_{off} . The product can be described as low-spin Fe^{II}NO⁺. In this way, the forward reaction is the *true reductive nitrosylation step*, with concomitant metal reduction and oxidation of NO to NO⁺.

In the second step of Scheme 3, Eq (36), it is assumed that OH[−] adds reversibly to the Fe^{II}NO⁺ moiety generating the highly reactive and elusive Fe^{II}(NO₂H) intermediate:

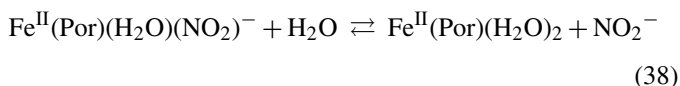
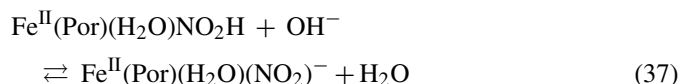


The current description for the heme-complexes omits the introduction of the ion-pair formation constant, Eq. (29). Thus, reaction (36) may be considered as equivalent to 29 + 30, and

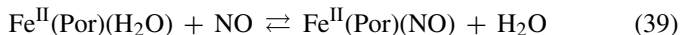


Scheme 3.

$k_{\text{OH}} = k_{36}$. We describe separately the rapid deprotonation step, Eq. (37), and the dissociation of NO₂[−], Eq. (38):



In the final step, the excess NO conditions favor a very fast reaction leading to the stable, moderately inert Fe^{II}(P)NO complex, Eq. (39):



The kinetic studies have been performed by following spectrophotometrically the first order decay of the stable Fe(Por)(H₂O)NO intermediates, formed in reaction (35), evolving to the Fe^{II}(Por)NO final products, Eq. (39). With these k_{obs} values, and by measuring the equilibrium constants for reaction (35), the rate constants for the reductive nitrosylation process, k_{red} , s^{−1}, can be estimated. It has been pointed out that k_{red} may represent the sum of several terms dependent on the medium. In general, k_{red} may be obtained from k_{obs} values by knowing K_{NO} and [NO].

Evidently, if we want to have a close look to the nucleophilic addition step, the picture of reactions (35)–(39) appears as more complex than the previously discussed scheme with classical complexes, Eqs. (29)–(31). In the latter systems, we started with well defined nitrosonium complexes, while in the present situation we deal with a formation reaction, Eq. (35), whose equilibrium constant must be determined in the reaction conditions. This can be done successfully, but sometimes a pH dependence of the K_{35} values has been found. Reaction (36) is formally the same as reaction (29 + 30), and reaction (37) may be also reasonably considered as a fast deprotonation step, as in Eq. (31). Finally, two limiting situations may arise depending on the relative rates of reactions (37) and (38) and the nucleophilic addition step, Eq. (36). It can be assumed that reactions (37) and (38) are *fast* ligand interchange processes, compared to reaction (36), or just the opposite situation [22].

A first order dependence on the concentration of OH^- has been found in the reductive nitrosylation reactions of cyt^{III} , metHb and metMb [105a]. From the slopes of the plots of k_{obs} against $[\text{OH}^-]$ values of $k_{\text{OH}} = \text{ca. } 10^2\text{--}10^3 \text{ M}^{-1} \text{ s}^{-1}$ have been calculated. They indicate a moderate-to-high electrophilic reactivity of the hemoproteins, which compares qualitatively with the classical complexes located at the upper right part of Fig. 11. A more quantitative prediction is precluded because of the above mentioned uncertainties in the mechanistic treatment and the lack of accurate values for the redox potentials of the hemoproteins, $E_{\text{NO}^+/\text{NO}}$ [105].

The metMb compound revealed a pH-independent path for reductive nitrosylation at pHs <6, in addition to the specific base-catalyzed path (i.e., $k_{\text{red}} = k_1 + k_{\text{OH}} [\text{OH}^-]$). The k_1 path was attributed to H_2O as the actual nucleophile, probably acting in a generalized base-catalyzed process. Alternatively, a non zero intercept could arise from the reversibility of the nucleophilic addition step in Eq. (36), in a situation similar to the one depicted in Fig. 8 for $\text{Ru}(\text{bpy})(\text{tpm})\text{NO}^{3+}$.

The existence of a generalized base-catalyzed path was demonstrated in a set of experiments with different buffer concentrations [106]. For acetate, it was found that $k_{\text{red}} = k_0 + k_{\text{B}} [\text{B}]$. The interpretation of k_0 should be related to the buffer-independent path associated with the OH^- -addition. The value of k_{B} was $2.4 \times 10^{-3} \text{ M}^{-1} \text{ s}^{-1}$; this is a very low value, compared to the above quoted k_{OH} for the specific base-catalyzed process. However, it becomes measurable because of the low rate of OH^- -addition in the low-pH conditions.

The work on the reductive nitrosylation reactions has been extended more recently to several porphyrin compounds: $\text{Fe}^{\text{III}}(\text{TPPS})$, $\text{Fe}^{\text{III}}(\text{TMPyP})$ [106], and two octacationic and octaanionic species, $\text{Fe}^{\text{III}}(\text{Por}^{8+})$ and $\text{Fe}^{\text{III}}(\text{Por}^{8-})$ [95b,107]. Only pH-independent k_{red} values have been reported, spanning a range of 10^{-4} to 10^{-2} s^{-1} . If we tentatively assume that these rate constants do in fact reflect the action of OH^- as a nucleophile (see above), values of k_{OH} can be roughly estimated to

be in the range 10^3 to $10^8 \text{ M}^{-1} \text{ s}^{-1}$. Moreover, the trends in k_{red} (and k_{OH}) are: $\text{Por}^{8+} > \text{TMPyP}^{4+} > \text{TPPS}^{4-} > \text{Por}^{8-}$ (Table 3). The increase of k_{OH} with the overall charge on the porphyrins is consistent with the greater electrophilicities at the $\{\text{FeNO}\}$ moieties. Besides, the measurements involving $\text{Fe}^{\text{III}}(\text{Por}^{8+})$ made at pH 8 (well above $\text{pK}_{\text{a}} = 5$ for $\text{Fe}^{\text{III}}(\text{Por}^{8+})(\text{H}_2\text{O})_2$), reveal a decrease in k_{red} of about an order of magnitude with respect to the values measured at pHs 2–4. This is consistent with the presence of the *trans*- OH^- ligand, which makes the $\{\text{FeNO}\}$ moiety more electron rich.

4.2. NO_2^- as a nucleophile: reactions with nitrosyl ferri-hemes

In the context of the reductive nitrosylation studies with the ferri-hemes, recent pioneering results allow to include NO_2^- as a potential nucleophile adding to the electrophilic $\{\text{FeNO}\}$ moieties [106]. NO_2^- is a ubiquitous impurity in NO-solutions because it is the product of NO autoxidation [108]. Its role in biochemistry is being revisited, by considering it as a possible vascular storage pool of NO mediated by the reduction of NO_2^- with Hb [109]. When solutions of diverse $\text{Fe}^{\text{III}}(\text{Por})$ complexes (Por = TPPS, TMPyP, as well as metHb and metMb) were made to react with NO in the presence of varying amounts of added NO_2^- at moderately acidic pHs (4–5), greater rates of reductive nitrosylation were obtained. A linear dependence of k_{obs} values on the concentration of NO_2^- was found, namely: $k_{\text{obs}} = (k_{\text{red}} + k_{\text{nitrite}} [\text{NO}_2^-] \times f(\text{NO}))$, with $f(\text{NO})$ accounting for the role of NO in Eq. (35). From the slope, values of k_{nitrite} can be calculated. Table 4 shows these values for a series of NO-porphyrins, including those for the “spontaneous” (i.e., without added NO_2^-) reductive nitrosylations, k_{red} . Table 4 also displays the more recent results for the NO_2^- -additions to the highly charged anionic and cationic $\text{Fe}^{\text{III}}(\text{Por})$ compounds, measured at different pHs, showing a similar behavior [107].

Table 4

Addition rate constants for OH^- and NO_2^- as nucleophiles, calculated from the reductive nitrosylation rates, for differently charged iron nitrosyl porphyrins and hemoproteins

Porphyrin ^a	pK_{a} ^b	$k_{\text{red}}^{\text{c}}$ (s^{-1})	k_{OH}^{d} ($\text{M}^{-1} \text{ s}^{-1}$)	$k_{\text{NO}_2^-}^{\text{e}}$ ($\text{M}^{-1} \text{ s}^{-1}$)	Reference
P^{8+}	5.0	$4 \times 10^{-2} \text{ f}$	$4.0 \times 10^8 \text{ g}$	242	[107]
TMPyP^{2+}	5.5	$9.8 \times 10^{-3} \text{ h}$	$3.3 \times 10^7 \text{ g}$	83	[106c]
TPPS^{6-}	7.0	$2.8 \times 10^{-4} \text{ i}$	$2.8 \times 10^5 \text{ g}$	3.1	[106a,c]
P^{8-}	9.2	$2.8 \times 10^{-4} \text{ j}$	$2.8 \times 10^3 \text{ g}$	2.1	[107]
cit^{III}	—	—	$1.5 \times 10^3 \text{ k}$	1.6	[105a,106b]
Hb^{III}	—	—	$3.2 \times 10^3 \text{ k}$	0.14	[105a,106b]
Mb^{III}	8.99	—	$3.2 \times 10^3 \text{ k}$	0.011	[105a,106b]

^a See the abbreviations list.

^b pK_{a} value of the corresponding di-aqua complex.

^c Corresponds to the pseudo-first order reductive nitrosylation rates.

^d Nucleophilic second-order rate constant for OH^- -addition.

^e Nucleophilic second-order rate constant for nitrite-addition, obtained from the linear plot of k_{red} vs. $[\text{NO}_2^-]$.

^f Measured at pH 4; same value at pH 2.

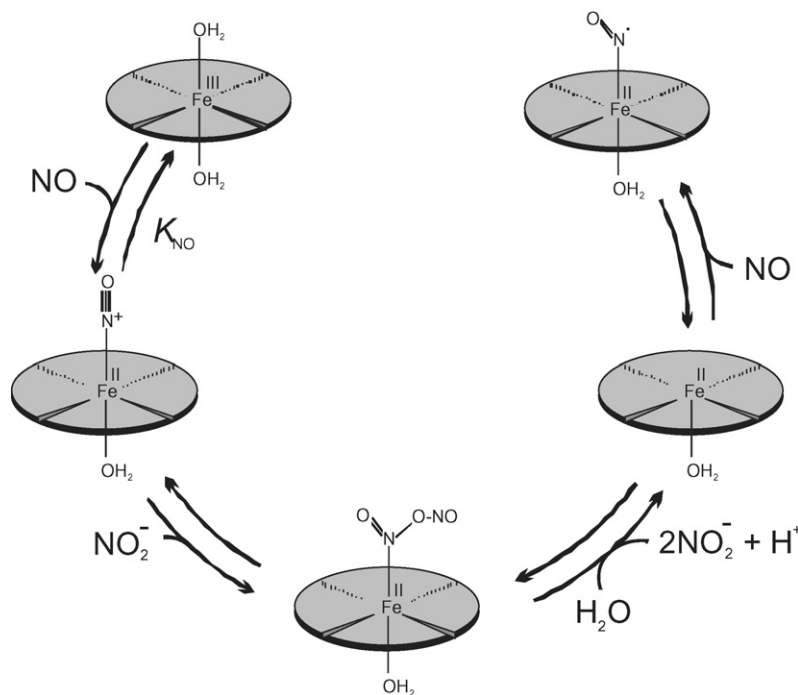
^g Roughly estimated as $k_{\text{OH}} = k_{\text{red}}/[\text{OH}^-]$, by assuming first order in $[\text{OH}^-]$.

^h Measured at pH 4.5.

ⁱ measured at pH 5.

^j Measured at pH 7.

^k Obtained from the linear plot of k_{red} vs. $[\text{OH}^-]$.



Scheme 4.

Overall, the values of k_{nitrite} are in the range 1.1×10^{-2} to $2.4 \times 10^2 \text{ M}^{-1} \text{ s}^{-1}$. They show a similar trend as found for the “spontaneous” processes occurring through OH^- -additions, in the sense that the rate constants increase with the positive charge on the porphyrins. However, the nucleophilic ability of NO_2^- turns out to be significantly lower than for OH^- , by several orders of magnitude. On the other hand, k_{nitrite} shows to be greater than $k_{\text{buffer}} = 2.4 \times 10^{-3} \text{ M}^{-1} \text{ s}^{-1}$, in the acetate-catalyzed reductive nitrosylations. By studying the pH-dependence of the NO_2^- -additions, it has been found that both NO_2^- and HNO_2 contribute to the rates, with NO_2^- being faster by a factor of two [107].

In the mechanistic analysis (Scheme 4), N_2O_3 has been proposed as the bound adduct-intermediate. This should be released very fast and hydrolyzed to NO_2^- or HNO_2 , depending on pH. Finally, $\text{Fe}^{\text{II}}(\text{Por})$ would rapidly bind NO, as in the reactions described in Section 4.1.

An alternative outer-sphere process with NO_2^- being oxidized to NO_2 and concomitant $\text{Fe}^{\text{II}}\text{NO}^\bullet$ formation has been proposed; subsequently, NO_2 would react very fast with excess NO to form N_2O_3 , with further hydrolysis to nitrite [106]. A reason for choosing the latter mechanism consisted in the rough dependence of k_{nitrite} values with $E_{\text{NO}^+/\text{NO}}$ for the heme-nitrosyl complexes. The authors displayed a LFER plot [106c], similar to the one shown in Fig. 11 for the OH^- -additions, although with a much greater slope than predicted by the Marcus treatment, with the points in the fitted line showing a high dispersion (this probably reflects the uncertainties in the values of $E_{\text{NO}^+/\text{NO}}$). Besides, these LFER's cannot discriminate between both mechanisms, because they are valid either for inner- or outer-sphere processes, with similar slopes in the $\ln k_{\text{nuc}}$ versus $E_{\text{NO}^+/\text{NO}}$ plots (cf. Section 4.1) [104].

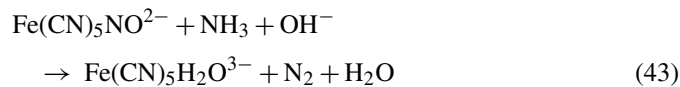
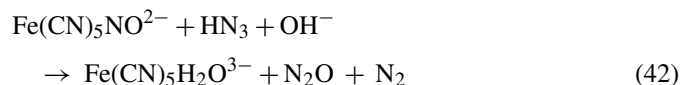
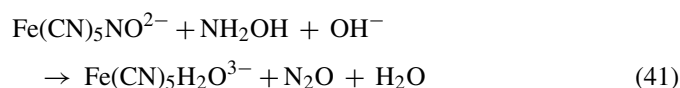
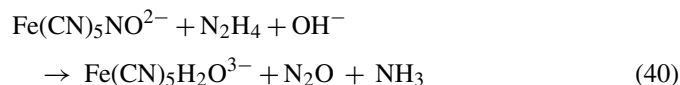
The trends for the NO_2^- -additions to the different nitrosyl-porphyrins have been discussed in terms of activation parameters, including the activation volumes [107]. By considering a general associative mechanism for NO_2^- addition into the $\{\text{Fe}^{\text{II}}\text{NO}^+\}$ moieties, Eq. (27), it has been found that the positively charged porphyrins, $\text{Fe}^{\text{II}}(\text{Por}^{8+})(\text{H}_2\text{O})\text{NO}^+$ react faster, affording positive activation entropies and volumes, than the $\text{Fe}^{\text{II}}(\text{Por}^{8-})(\text{H}_2\text{O})\text{NO}^+$ analogs, which react much slower, with negative values for the same parameters. The decrease has been traced to the bond formation process being accompanied by some charge neutralization, causing a decrease in electrostriction, thus partially offsetting the negative intrinsic entropy and volume contributions. Conversely, the values are positive for $\text{Fe}^{\text{II}}(\text{Por}^{8+})(\text{H}_2\text{O})\text{NO}^+$, indicating a major decrease in electrostriction during bond formation. Similar trends in the activation parameters have been previously found for the OH^- -additions to differently charged $\text{ML}_5(\text{NO}^+)$ complexes, cf. Table 3, [27]. A specific decrease in rates has been also detected for the nitrite-additions when working at pHs higher than the pK_a of the $\text{Fe}^{\text{III}}(\text{Por}^{8+})(\text{H}_2\text{O})_2$ complex, as already discussed above for the OH^- -additions [107]. Finally, the work on NO_2^- -catalyzed reductive nitrosylations has been complemented by the direct measurements of NO_2^- binding to $\text{Fe}^{\text{III}}(\text{Por}^{8+})(\text{H}_2\text{O})_2$ and $\text{Fe}^{\text{III}}(\text{Por}^{8+})(\text{OH}^-)(\text{H}_2\text{O})$, revealing a similar behavior as found for the binding of NO to these complexes (see above).

The above results and interpretation are more consistent with the inner-sphere route for the reductive nitrosylation process. This interpretation also supports the inclusion of NO_2^- as an additional nucleophile toward bound NO^+ , behaving as all others, as described in Eq. (27). Its nucleophilic ability appears as significantly lower than found for the thiolates, OH^- and the nitrogen hydrides (see below). In aqueous solutions, however,

NO_2^- additions can be put in evidence with an adequate selection of pH-conditions, although in an unavoidable competition with OH^- additions.

4.3. The reactions of $\text{Fe}(\text{CN})_5\text{NO}^{2-}$ with nitrogen hydrides. A case study for hydrazine, N_2H_4 , and substituted derivatives

Nitrogen hydrides are also able to promote nucleophilic additions according to Eq. (27). We describe the stoichiometries of the reactions for the more important nucleophiles with SNP [110–112]:

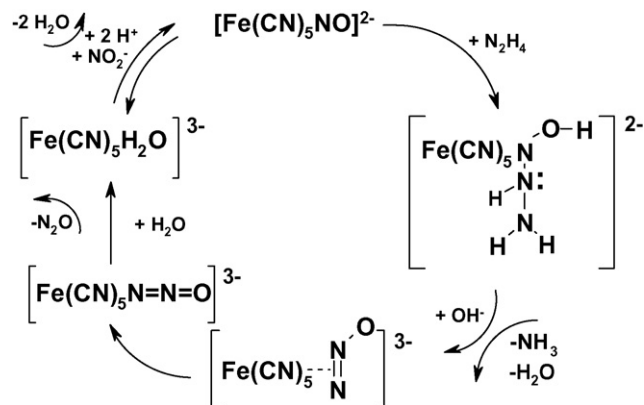


Gas evolution processes are operative after the initial addition step. N_2 , N_2O or equimolar mixtures may appear, depending on the nucleophile. Kinetic studies afford values of the rate constants for each of the corresponding addition steps, most of them having the same order of magnitude as the one found for OH^- [102]. The values for N_2H_4 [110], NH_2OH and HN_3 [111] are: 0.43, 4.6 and $0.2 \text{ M}^{-1} \text{ s}^{-1}$ at 25°C , respectively. A much lower value has been measured for NH_3 , ca. 10^{-4} to $10^{-5} \text{ M}^{-1} \text{ s}^{-1}$ (50°C) [112]. This is probably related to the high pH involved in the required deprotonation of NH_3 . Overall, these values allow the use of a common mechanistic framework, as described above for OH^- . Although only scarce spectrophotometric information has been obtained on the intermediates, DFT calculations have been useful, as detailed below [110,113]. No kinetic studies for complexes other than SNP have been performed, in contrast with the above described work for the OH^- -additions.

We describe the N_2H_4 -addition in more detail, Eq. (40). Scheme 5 describes this reaction with SNP, which becomes catalytic for NO_2^- reduction under specific conditions [110].

The first step involves the addition of deprotonated N_2H_4 to NO^+ , with subsequent proton migration and cleavage of the N–N bond in the bound N_2H_4 . After the loss of NH_3 the formation of a novel $\eta^2\text{-N}_2\text{O}$ isomer is postulated, which further isomerizes to the linear $\eta^1\text{-N}_2\text{O}$ form and then releases N_2O to the medium. In this way, the aqua-ion is able to bind NO_2^- again (as NO^+) and continue with the addition process in a catalytic way if more N_2H_4 is present. Fig. 12 shows the DFT calculations for the species affording stable minima in the potential energy surface.

A similar calculation for NH_2OH as a nucleophile is included in Fig. 12, describing the formation of $\text{N}_2\text{O} + \text{H}_2\text{O}$, Eq. (3). Note

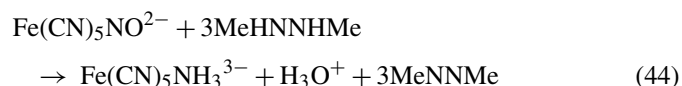


Scheme 5.

that in the latter case, only the $\eta^1\text{-N}_2\text{O}$ isomer is predicted, and this is not only consistent with minimizing reorganization barriers, but also with experimental results with labeled ^{18}O and ^{15}N , demonstrating that the oxygen and central nitrogen of N_2O come from NH_2OH [111].

A distinct feature has been found with N_2H_4 -additions to some Ru-complexes, viz. $\text{Ru}(\text{NH}_3)_5\text{NO}^{3+}$ [114]. N_3^- has been obtained as a product, instead of N_2O . The different behavior probably depends on the different adduct reorganization modes, that could be in turn dependent on the overall charge of the complex [110]. Recently, $[\text{Ru}(\text{py}^{\text{Si}}\text{S}_4)\text{NO}]\text{Br}\cdot\text{THF}$ has also been shown to react in MeOH/DMF similarly as SNP, producing N_2O and NH_3 , with NH_3 remaining finally bound to ruthenium [115]. These N_2H_4 -nitrosations are mechanistically connected with the reaction of HNO_2 with N_2H_4 , in which both types of products have been found [116].

In the reactions of some substituted derivatives of N_2H_4 adding to $\text{Fe}(\text{CN})_5\text{NO}^{2-}$, viz. NH_2NHMe and $\text{NH}_2\text{N}(\text{Me})_2$, alternative paths with a decreasing reactivity have been suggested as a consequence of the steric effects arising in the presence of methyl groups adjacent to the N-adding atom of the nucleophile [110]. The main stoichiometries are similar to the one described in Eq. (40), with N_2O and NH_2Me or $\text{NH}(\text{Me})_2$ replacing NH_3 . Furthermore, the variation of pH has revealed the occurrence of alternative nucleophilic addition paths, which we do not discuss in detail here. We do emphasize however on the very drastic mechanistic change found with MeHNNHMe , for which azomethane (MeNNMe) and NH_3 were found as products, Eq. (44), revealing a full six-electron reduction of SNP. The stoichiometry in reaction (44) supports a mechanistic route involving two-electron reduced intermediates comprising bound HNO^- and NH_2OH , in contrast with the two-electron reduction of NO^+ to N_2O when using N_2H_4 , NH_2NHMe and $\text{NH}_2\text{N}(\text{Me})_2$:



We refer to the original work [110] for a comprehensive discussion of this interesting set of reactions, where subtle changes in the structure of the nucleophile lead to drastic changes in the overall stoichiometries and addition mechanisms.

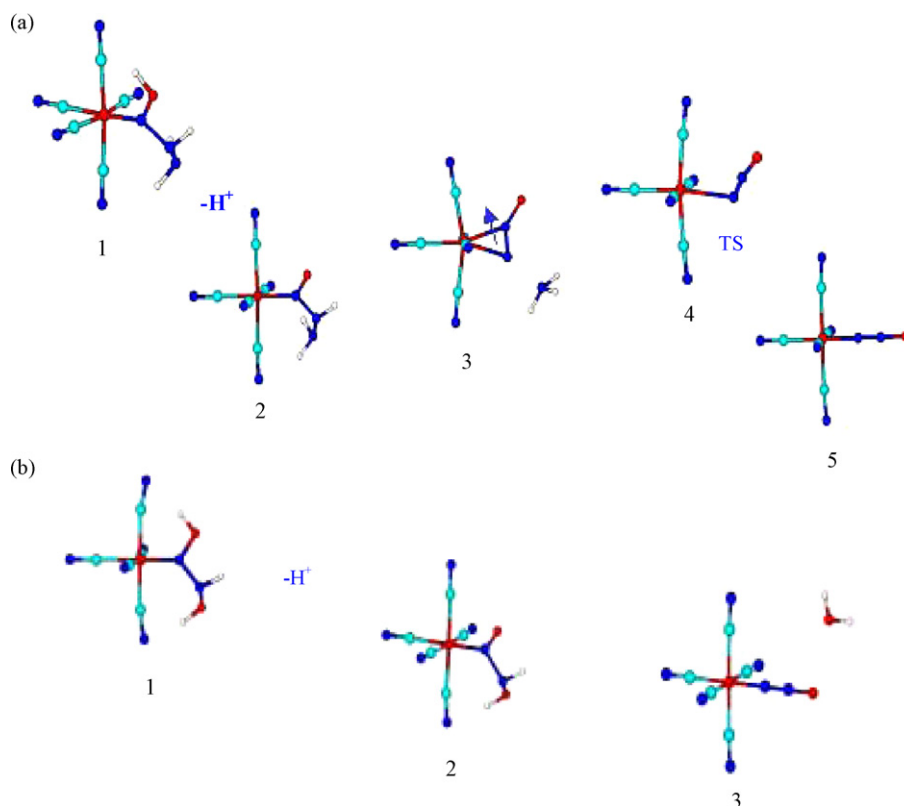


Fig. 12. (a) Schematic representation of the initial steps involved in the reaction of $\text{Fe}(\text{CN})_5\text{NO}^{2-}$ with N_2H_4 , rendering the N_2O -bound intermediates. The structures correspond to singular points in the potential hypersurface, calculated at a B3LYP/6-31G** level. Relative energies (γ -coordinate) are not drawn to scale. From left to right: (1) $[(\text{NC})_5\text{FeN}(\text{OH})\text{NHNH}_2]^{2-}$; (2) $[(\text{NC})_5\text{FeN}(\text{O})\text{NHNH}_2]^{3-}$; (3) $[(\text{NC})_5\text{Fe}-\eta^2-\text{N}_2\text{O}]^{3-}$; (4) TS structure; (5) $[(\text{NC})_5\text{Fe}-\eta^1-\text{N}_2\text{O}]^{3-}$. (b) The same for NH_2OH . From left to right: (1) $[(\text{NC})_5\text{FeN}(\text{OH})\text{NHOH}]^{2-}$; (2) $[(\text{NC})_5\text{FeN}(\text{O})\text{NHOH}]^{3-}$; (3) $[(\text{NC})_5\text{Fe}-\eta^1-\text{N}_2\text{O}]^{3-}$ [110].

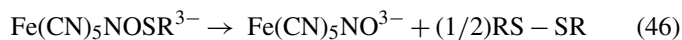
4.4. The reactions of different $\text{ML}_5(\text{NO}^+)$ complexes with cysteine

The reactions of $\text{ML}_5(\text{NO}^+)$ complexes with cysteine and related thiols (HSR) as nucleophiles have been explored by using the $\text{Fe}(\text{CN})_5\text{NO}^{2-}$ ion [117]. Typical red colors arise upon mixing, with further decay. The addition process requires thiol-deprotonation, and the electronic absorption maxima, all around 520 nm, with ϵ values of ca. $10^4 \text{ M}^{-1} \text{ cm}^{-1}$, are attributed to metal-to-ligand charge transfer transitions to the nitrosothiolate ligand, NOSR:



The infrared evidence aids in the identification of $\text{Fe}(\text{CN})_5\text{NOSR}^{3-}$, showing ν_{NO} at 1350 cm^{-1} (for NOSEt) [57d], revealing a double bond character in NO. The first crystalline structure in this family of metal-bound nitrosothiolates has been recently published for the surprisingly stable *trans*- $\text{K}[\text{IrCl}_4(\text{CH}_3\text{CN})\text{N}(\text{O})\text{SCH}_2\text{Ph}]$ complex [118]. The kinetic rate constants for both the direct and reverse fast processes in Eq. (45) have been measured for different thiolates by using stopped-flow and T-jump methods. The values for the direct addition rate constants, k_{SR} , are in the range 10^3 – $10^4 \text{ M}^{-1} \text{ s}^{-1}$. These values are significantly greater than the previously analyzed ones for OH^- and nitrogen hydrides, due to the more polarizable character of the sulfur-binding nucleophiles [119].

The subsequent processes related to the decay of the red adducts have been studied in detail for $\text{Fe}(\text{CN})_5\text{NO}^{2-}$ with cysteine and other thiolates [82]. The reactions are mechanistically complex, involving radical paths. The initial decomposition product associated with the decay of the red color involves an intramolecular redox reaction, producing the one-electron reduced, EPR active $\text{Fe}(\text{CN})_5\text{NO}^{3-}$, together with the cysteinyl radical, a precursor of cystine, Eq. (46):



Recently, a comprehensive study, similar as the one described for OH^- -additions, has been carried out for the reactions of a set of $\text{RuL}_5(\text{NO}^+)$ complexes with cysteine (L = polypyridines, NH_3 , EDTA, etc.) [120]. Although these reactions were much faster than those with OH^- , they could be successfully studied by lowering the pH, thus controlling the effective concentration of cysteinate. The reactions showed to be complex, and different processes could be identified for increasing time scales. The following reaction Scheme 6 has been proposed for the successive addition of *two* cysteinate ions, followed by a final intramolecular redox process that leads to the ruthenium aqua ion, N_2O and cystine.

For the Ru nitrosyl complexes, a two-electron reduction of NO^+ is involved. The mechanism is distinctive from the one-electron process observed with $\text{Fe}(\text{CN})_5\text{NO}^{2-}$, Eqs. (15) and (46). This has been tentatively attributed to the more oxidizing



Scheme 6.

capability of the ruthenium nitrosyls. Fig. 13 displays two LFER plots, similar as those presented in Fig. 11.

The upper trace relates to the faster processes associated with the addition of the first cysteinate; it can be seen that the points with the higher k values deviate from the straight line because of approaching the diffusion control limit. The other points, however, are aligned with a slope close to the theoretically predicted value, revealing a similar situation as the one discussed previously for OH^- . The lower trace can be associated with the addition of the second cysteinate, and provides a valuable evidence for the ongoing nucleophilic process. That the second addition is slower than the first one appears as consistent with the expected diminished electrophilic ability of the MNO system. The study of these thiolate-additions could be biologically relevant, and an extension to other complexes is desirable, in order to disclose which are the factors controlling the appearance of one- or two-electron reduction products of $ML_5(NO^+)$.

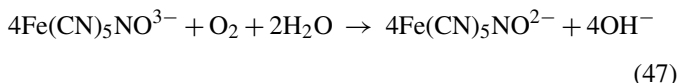
As a final conclusion, a picture emerges for considering the electrophilic reactivity of metal nitrosyls under a common framework described by Eq. (27), taking due account of the different metals, coligands or nucleophiles involved (as proved for OH^- and thiolates, and seemingly valid also for nitrogen hydrides or nitrite). The unified view can be established tentatively also for the heme-compounds, even although the adducts may decompose in different ways according to the nature of B and the $ML_5(NO^+)$ moieties. The key point relates to the precise mechanistic assignment for the second-order k_{nucl} values, in the

sense that they represent the true, elementary addition steps, as described by Eq. (30) or (36).

5. Nucleophilic reactivity of bound NO^\bullet : the reactions with O_2

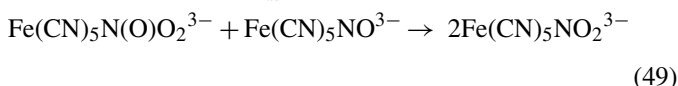
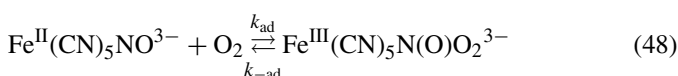
In the same way as electrophilic reactivity can be predicted for NO^+ -complexes, we may anticipate a nucleophilic reactivity for the more electron-rich NO -complexes. Although nitrosyl protonation reactions seem not to occur at the $\{MNO\}^7$ moieties, many complexes in this series have been proved to be oxygen-sensitive [24a–c,25]. Remarkably, only scarce data are available on the kinetics of these reactions [22]. A study on the autoxidation reaction of $Fe(CN)_5NO^{3-}$ in aqueous solution has been performed recently [121]. The latter ion can be obtained from the corresponding NO^+ -complex, SNP, by chemical reduction with dithionite. Fig. 14a shows the decay of $Fe(CN)_5NO^{3-}$ with successive additions of dissolved O_2 .

Through a titration experiment with O_2 and a quantitative estimation of product formation, the following stoichiometry has been established, Eq. (47):



In excess of dissolved O_2 , $Fe(CN)_5NO^{3-}$ decays exponentially in a stopped-flow timescale (inset Fig. 14a). Fig. 14b shows that the experimental pseudo-first order rate constant k_{obs} correlates linearly with $[O_2]$, leading to a global second-order rate law: $-(1/4)d[Fe(CN)_5NO^{3-}]/dt = k_{47}[Fe(CN)_5NO^{3-}][O_2]$, with $k_{47} = (3.5 \pm 0.2) \times 10^5 M^{-1} s^{-1}$ at 25 °C, pH 10. The activation parameters were: $\Delta H^\ddagger = 40 kJ mol^{-1}$, $\Delta S^\ddagger = 12 J K^{-1} mol^{-1}$. In all the experiments an excess of free CN^- had to be used to minimize *trans*-labilization of this ligand, Eq. (1). The rate constant was insensitive to changes in pH (9–11) and ionic strength (0.1–1 M). However, for pH < 10 and without extra cyanide, the oxidation rate *decreased* markedly.

The above results cannot be accommodated by an outer-sphere mechanism because of the endergonic character of the first one-electron transfer process involving the formation of $Fe^{II}(CN)_5NO^{2-}$ and superoxide, $O_2^{\cdot-}$. Alternative O_2 -coordination steps following the dissociation of NO or CN^- have also been discarded. Instead, an associative route through reactions (48) and (49) has been proposed for the initial mechanistic steps associated with reaction (47):



Reaction (48) involves the formation of a new covalent bond between bound NO and O_2 . The product has been described

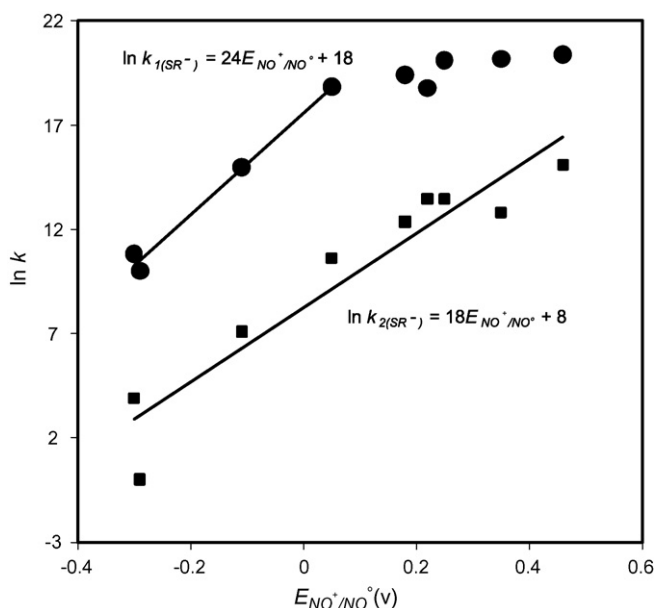


Fig. 13. LFER plot of $\ln k_{1(SR^-)}$ and $\ln k_{2(SR^-)}$ against E_{NO^+/NO^\bullet} (vs. Ag/AgCl 3 M KCl) for the addition reactions of cysteine into a series of $[RuL_5NO]^n$ complexes. In both plots, from left to right: $[Fe(CN)_5NO]^{2-}$ (down); $[Ru(EDTA)NO]^-$ (up); *trans*- $[Ru(NH_3)_4NO(pz)]^{3+}$; *cis*- $[Ru(bpy)_2ClNO]^{2+}$; *cis*- $[Ru(bpy)_2(NO_2)NO]^{2+}$; *trans*- $[NCRu(py)_4CNRu(py)_4NO]^{3+}$; *cis*- $[Ru(bpy)(trpy)NO]^{3+}$; *cis*- $[Ru(AcN)(bpy)_2NO]^{3+}$; $[Ru(bpz)(trpy)NO]^{3+}$ [120].

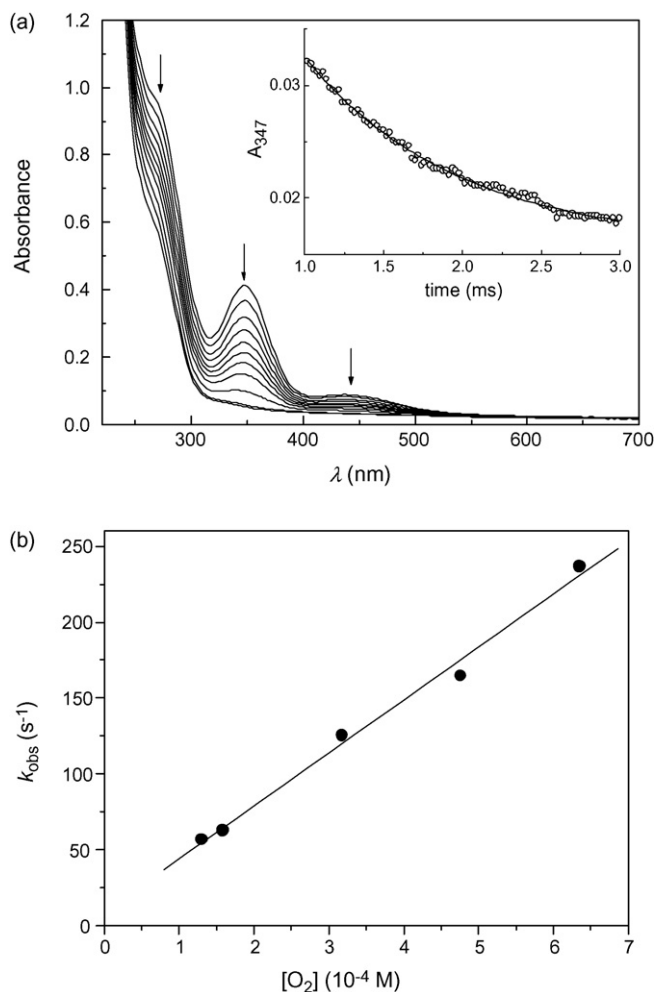
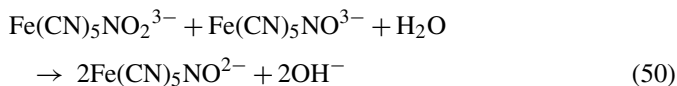


Fig. 14. Reaction of O₂ with the [Fe(CN)₅NO•]³⁻ ion. Successive UV-vis spectra for 10⁻⁴ M [Fe(CN)₅NO•]³⁻ reacting with aliquots of a 2.6 × 10⁻⁴ M [O₂]; pH 10, I = 0.1 M; excess cyanide, 5 × 10⁻⁴ M; T = 25 °C. Inset: stopped-flow trace for the decay of [Fe(CN)₅NO•]³⁻, at 347 nm. (b) Plot of k_{obs} against [O₂] [121].

as a peroxynitrite anion bound to Fe(III), as shown in Fig. 15, according to DFT computations.

In some related studies (see below for Mb^{II}NO) [122], an isomerization of the peroxynitrite adduct has been proposed [122a], subsequent to a reaction similar to (48), in order to explain the formation of NO₃⁻ as a final product. Instead, we propose the fast bimolecular formation of Fe(CN)₅NO₂³⁻, Eq. (49), which may further react as in Eq. (50):



Both reactions (49) and (50) probably involve several steps. The oxidation equivalents remain bound to the metal all along the reaction, leading to the experimentally found 4:1 global stoichiometry, without other detectable by-products.

Assuming steady state conditions for Fe(CN)₅N(O)O₂³⁻ we get $-\text{d}[\text{Fe(CN)}_5\text{NO}^{3-}]/\text{dt} = 4k_{\text{ad}}k_{49}[\text{O}_2][\text{Fe(CN)}_5\text{NO}^{3-}]^2/(k_{-\text{ad}} + k_{49}[\text{Fe(CN)}_5\text{NO}^{3-}])$. With $k_{49}[\text{Fe(CN)}_5\text{NO}^{3-}] > k_{-\text{ad}}$, this expression reduces to the observed first order rate law in each reactant, with $k_{47} = k_{\text{ad}}$.

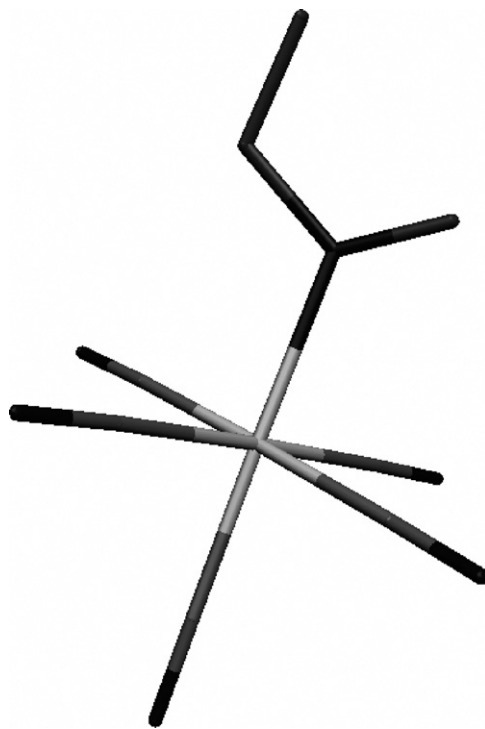


Fig. 15. DFT optimized geometry of the Fe(III)-peroxynitrite adduct formed in the initial step of the reaction of [Fe(CN)₅NO•]³⁻ with O₂ [121].

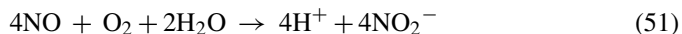
Second order rate laws have also been found for the Ru(bpy)(tpm)NO²⁺ and Ru(NH₃)₅NO²⁺ complexes reacting with O₂ [24g,123]. As the spin density distribution along the different {MNO}⁷ moieties remains essentially invariable [48], it is reasonable to expect similar reactivity patterns for the NO-complexes. The Fe(CN)₅NO³⁻ and Ru(NH₃)₅NO²⁺ complexes (affording E_{NO⁺/NO} values near to -0.10 V) react with very similar addition rate constants. However, the Ru(bpy)(tpm)NO²⁺ ion (with E_{NO⁺/NO} = 0.55 V) showed a much lower value of k_{ad}, by five orders of magnitude. If a tentative plot is build up with ln k_{ad} against E_{NO⁺/NO} for the above three complexes, a linear trend can be appreciated, with a *negative slope* of 18.4 ± 0.9 V⁻¹. Even although this correlation ought to be confirmed by measuring the autoxidation reactions of other nitrosyl-complexes, particularly those expected to behave with intermediate values of k_{ad} and E_{NO⁺/NO}, the result appears as remarkable. The value of the slope is in close agreement with the theoretically predicted Marcus-type behavior previously considered for bimolecular reactions occurring with associative character, 19.4 V⁻¹ [104]. Not unexpectedly, the plot appears as very similar to the one showed in Fig. 11 for the *electrophilic* addition reactions of ML₅(NO⁺) complexes with OH⁻ as a nucleophile, although with a *positive slope*.

It can be concluded that six-coordination is a necessary condition to achieve autooxidation of bound NO-complexes. We stated above on the rate decrease for reaction (47) with decreasing pHs, suggesting the *unreactivity* of Fe(CN)₄NO²⁻, cf. Eq. (5). Also, the picket-fence compound Fe(TpivPP)NO reacts with O₂ in nonaqueous medium *only* in the presence of pyridine, to give Fe(TpivPP)(NO₂)(py) [124]. A product with bound

NO_2^- is also obtained in the autoxidation of the non-heme $\text{Fe}(\text{PaPy}_3)\text{NO}^+$ complex in acetonitrile solution [24b]. In both cases, the two-electron processes (with a 2:1 $\text{Fe}:\text{O}_2$ stoichiometry) formally involve a one-electron oxidation of NO^\bullet to NO_2^- and a conversion of $\text{Fe}(\text{II})$ to $\text{Fe}(\text{III})$.

The slow decay of some $\text{Fe}^{\text{II}}(\text{Por})\text{NO}$ in aerated media are poorly understood. Compounds with $\text{Por} = \text{TPP}$, TTP , OEP , form NO_3^- and $[\text{Fe}^{\text{III}}(\text{Por})]_2\text{O}$ oxo dimers [125]. Rate determining NO -dissociations have been proposed for the autoxidations of $\text{Mb}^{\text{II}}\text{NO}$ and $\text{Hb}^{\text{II}}\text{NO}$ [125b,c]. Some mechanistic ambiguities arise because of the competitive rates of NO -dissociation and of the autoxidation reaction itself [22].

Indeed, that the redox potentials of the $\text{MNO}^+/\text{MNO}^\bullet$ couples could quantitatively predict the NO -autoxidation reactivities appears as quite significant. More work on additional, well characterized NO -complexes is desirable in order to extend the mechanistic analysis and eventually validate the predictive approach. It must be recognized that one of the routes for the decay of free NO in biologically relevant solutions is through the reaction described by Eq. (51):



Reaction (51) is termolecular, with $k = 2.88 \times 10^6 \text{ M}^{-2} \text{ s}^{-1}$ [108,126]. Thus, NO is expected to survive a long time under the dilute NO concentrations in the bodily fluids, unless immune response conditions are generated [22c]. The previous discussion shows that NO^\bullet -coordination compounds could readily react with O_2 in order to provide a fast route to NO^\bullet -consumption. However, the complexes like $\text{Fe}(\text{CN})_5\text{NO}_3^-$ could hardly compete with other main sinks for NO reactivity, namely the very fast processes involving the reactions of free NO with sGC or with HbO_2 [7,9].

6. Reactivity of bound NO^-/HNO complexes: protonation, metal-dissociation and reactions toward electrophiles or nucleophiles

Different methods for preparing HNO -complexes have been described in Section 2. More recently, the formal coupling of an H-atom with the NO -ligand has been observed in complexes containing *trans*-hydride. The $\text{MHCl}(\text{CO})(\text{NO})(\text{P}^i\text{Pr}_3)_2$ complexes ($\text{M} = \text{Ru}$, Os) lead to the nitroxyl-derivatives, $\text{MHCl}(\text{CO})(\text{HNO})(\text{P}^i\text{Pr}_3)_2$ through a H-atom transfer reaction, also generating $\text{MCl}(\text{CO})(\text{NO})(\text{P}^i\text{Pr}_3)_2$ as an additional product [79].

Protonation of bound NO^- is a viable route to HNO -complexes. In fact, the NO^- species are expected to be strongly nucleophilic, and to abstract rapidly the protons from an adequate source, viz. water. The recently reported pK_a values for free $^1\text{HNO}/^3\text{NO}^-$ and $^1\text{HNO}/^1\text{NO}^-$ are 11.4 and 23, respectively [91,127]. However, we know nothing about the pK_a values for bound $^1\text{HNO}/^1\text{NO}^-$ in aqueous solutions. These should be at least ≥ 10 , on the basis of the unchanged electronic and NMR spectra of $\text{Mb}^{\text{II}}\text{HNO}$ up to this pH [69]. For the $\text{Ru}(\text{'pyS}_4\text{'})\text{HNO}$ complex, HNO has been replaced by DNO , and its decomposition has been monitored in CD_3OD . The recovery of the

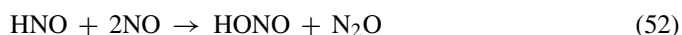
signal at 19.56 ppm for HNO in the course of 12 h suggests that a slow H^+/D^+ exchange with traces of H_2O in the solution has been occurred. Interestingly, the latter HNO -complex reacts with one-electron oxidants to give, step by step, NO^\bullet and NO^+ -complexes (Fig. 4), and also affords a full two-electron oxidation when treated with Bronsted acids like HBr . The latter reaction may be considered a reverse process compared to the synthetic procedure, cf. Eq. (9) [26a].

In contrast with the above described HNO -complexes, the solubility in aqueous solution of $\text{Mb}^{\text{II}}\text{HNO}$ appears as remarkable [69], as also can be said on the reported inertness toward the release of HNO (hour's time scale). This result has also been observed for $\text{Fe}(\text{cyclam-ac})\text{NO}^0$ in AcN [24c], and for the $\text{MHCl}(\text{CO})(\text{HNO})(\text{P}^i\text{Pr}_3)_2$ complexes described above [79]. The inertness of bound HNO toward dissociation (although not toward the reaction with excess redox-active substrates) is consistent with the previous postulation of it being a sufficiently long-lived intermediate in the reaction of MeHNNHMe with SNP , Eq. (44) [110], or in the disproportionation reaction of NH_2OH catalyzed by pentacyanoferrates, leading to bound NO^+ as the final oxidized product [128]. HNO has been also proposed as an intermediate in the oxidation of NH_2OH to NO_2^- mediated by HAO [14].

All the reported HNO -complexes appear as air sensitive, but the products and mechanisms have not been studied in detail. In principle, one would expect a decrease in the nucleophilic reactivity of bound HNO , compared to NO^- complexes. The $[\text{CoL}_4\text{NO}]$ complexes (formally $\text{Co}^{\text{III}}\text{NO}^-$, with L =diverse tetradentate dianions) reacted with O_2 in nonaqueous media, *only* in the presence of nitrogen- and phosphorus bases (B) to yield the corresponding nitrocompounds, $\text{CoL}_4(\text{NO}_2)\text{B}$. The rates of these autoxidation reactions were strongly dependent on the nature of the *trans*-ligand to NO^- in the Co^{III} complexes, and this was interpreted as influencing the nucleophilicity of the $\{\text{CoNO}\}^8$ moieties [65b]. A series of $\text{IrCl}(\text{CO})(\text{NO})(\text{PPh}_3)_2\text{X}$ complexes (also formally $\text{Ir}^{\text{III}}\text{NO}^-$, with $\text{X} = \text{I}^-$, Br^- , Cl^- , NCS^- , etc.) are also attacked by O_2 , giving in this case NO_3^- as product [65c]. Other complexes may form mixtures of NO_2^- and NO_3^- [129]. Given the results with the autoxidation reactions of the NO^\bullet -complexes (Section 5), showing a generalized predictive behavior through the LFER plots, systematic kinetic investigations with NO^-/HNO complexes are in order, as far as more of them become well characterized in aqueous solutions.

The electrophilic behavior of bound HNO is also biologically relevant, given the known reactivity of free HNO toward the thiolates, rendering NH_2OH and disulfides as products [130].

Additional reactivity studies show that bound HNO (as in the above mentioned hydride-nitrosyl Ru - and Os -complexes), react under excess NO conditions [131] in the same way as reported for free HNO [132], Eq. (52):



7. Conclusions and outlook

A significant progress has been achieved in the recent years in the synthesis and characterization (either in the solid state

or in solution) of complexes containing formally any of the three redox forms of bound nitrosyl: NO^+ , NO^\bullet and NO^-/HNO . The structural and spectroscopic properties (mainly IR, EPR, UV–vis, but also others as Mossbauer, resonance Raman, magnetic susceptibility, etc.), together with theoretical calculations, allow to obtain adequate descriptions of the electronic structure of the {MNO} moieties, although one must still be careful in the interpretation of these results (i.e., in assigning limiting oxidation states to the metal and NO ligand), due to the delocalized nature of the electronic density.

In spite of the above comment, more well characterized nitrosyl-complexes in aqueous solutions would be desired for the NO^\bullet and HNO ligands. In this context, dissociation processes, mutual *trans*-labilization effects effected by NO, NO^- or HNO, dinitrosyl formation reactions, redox-interconversions of the three redox forms (including disproportionations), and different types of reactivity of the bound nitrosyl-species toward substrates (namely O_2 , excess NO or HNO, nitrogen hydrides, thiolates, etc.) are only a sample of reactivity issues that need to be clarified in order to mimic the relevant biochemical processes associated with the physiological roles of NO.

Significant advances have been made in the electrophilic reactivity studies of NO^+ -complexes. Kinetic measurements and mechanistic considerations, together with DFT calculations, allow the prediction of electrophilic abilities for a vast amount of different {MNO}⁶ moieties in classical coordination compounds, by only considering the redox potentials of the corresponding MNO^+/MNO couples. This approach showed to be valid for OH^- and cysteine, and is seemingly valid for other nucleophiles as well, such as the nitrogen hydrides and nitrite. For the porphyrins and hemoproteins, this could also be the case, although the mechanistic ambiguities (including the lack of measured redox potentials in many cases) still pose a question on the possibility of considering these systems under a common framework. The studies with porphyrins and hemoproteins are receiving a great input of new results, dealing with the basic formation-dissociation reactions of the NO-complexes and the ensuing reductive nitrosylation processes that are observed under excess NO-conditions. Crucial questions relate to the influence of the heme-structure, charge effects, nature of the coligands in the axial positions, etc. The more recent kinetic studies reveal a complex picture in which the coordination of NO becomes associated with drastic changes in the redox nature of the ligand and in the spin state of the metal center.

Emerging work on the nucleophilic abilities of the {MNO}⁷ moieties implied the use of O_2 as the electrophilic reactant. Detailed kinetic and mechanistic studies of the autoxidation reactions of MNO complexes are remarkably very scarce. The new results with a few of them suggest that a dependence of the addition rate constants on the redox potentials is operative for classical nitrosyl-complexes. DFT-methods showed to be useful in characterizing peroxynitrite intermediates, which may evolve with formation of nitrite or nitrate, depending on conditions. The reactivity picture of bound HNO toward O_2 is still unraveled.

Summing up, the scene is ready for significant improvements in the diversified scenario comprising the different biorelevant NO-reactivity issues.

Acknowledgments

We thank the University of Buenos Aires and the funding agencies ANPCYT and CONICET, for providing support. FR and MV were doctoral fellows, and LDS and JAO are members of the research staff of CONICET.

References

- [1] (a) G.B. Richter-Addo, P. Legdzins, *Metal Nitrosyls*, Oxford University Press, New York, 1992;
(b) J.N. Armor (Ed.), *Environmental Catalysis*, ACS Symp. Ser., 1993, p. 552.
- [2] (a) J.L.E. Ignarro, *Nitric Oxide, Biology and Pathobiology*, Academic Press, San Diego, CA, 2000;
(b) M. Feelisch, J.S. Stamler (Eds.), *Methods in Nitric Oxide Research*, Wiley, New York, 1996.
- [3] J.A. Olabe, L.D. Slep, in: J.A. Me Cleverty, T.J. Meyer (Eds.), *Comprehensive Coordination Chemistry II, from Biology to Nanotechnology*, vol. 1, Elsevier, Oxford, 2004, p. 603.
- [4] (a) I.M. Wasser, S. de Vries, P. Moënne-Loccoz, I. Schröder, K.D. Karlin, *Chem. Rev.* 102 (2002) 1201;
(b) D.J. Richardson, N.J. Watmough, *Curr. Opin. Chem. Biol.* 3 (1999) 207;
(c) B.A. Averill, *Chem. Rev.* 96 (1996) 2951.
- [5] (a) M.A. Tayeh, M.A. Marletta, *J. Biol. Chem.* 264 (1989) 19654;
(b) H.M. Abu-Soud, K. Ichimori, H. Nakazawa, D.J. Stuehr, *Biochemistry* 40 (2001) 6876;
(c) D.J. Stuehr, S. Pou, G.M. Rosen, *J. Biol. Chem.* 276 (2001) 14533, and references therein.
- [6] R. Radi, *Chem. Res. Toxicol.* 9 (1996) 828.
- [7] (a) A.E. Yu, S. Hu, T.G. Spiro, J.N. Burstyn, *J. Am. Chem. Soc.* 116 (1994) 4117;
(b) J.N. Burstyn, A.E. Yu, E.A. Dierks, B.K. Hawkins, J.H. Dawson, *Biochemistry* 34 (1995) 5896;
(c) S. Kim, G. Delnum, M.T. Gardner, M.A. Marletta, G.T. Babcock, *J. Am. Chem. Soc.* 118 (1996) 8769, and references therein.
- [8] (a) Y. Minamiyama, S. Takemura, S. Imaoka, Y. Funae, Y. Tanimoto, M.J. Inoue, *J. Pharmacol. Exp. Ther.* 282 (1997) 1479;
(b) M. Odaka, K. Fujii, M. Hoshino, T. Noguchi, M. Tsujimura, S. Nagashima, M. Yohda, T. Nagamune, Y. Inoue, I. Endo, *J. Am. Chem. Soc.* 119 (1997) 3785;
(c) M. Tsujimura, N. Dohmae, M. Odaka, M. Chijimatsu, K. Takio, M. Yohda, M. Hoshino, S. Nagashima, I. Endo, *J. Biol. Chem.* 272 (1997) 29454;
(d) M.W.J. Cleeter, J.M. Cooper, V.M. Darley-Usmar, S. Moncada, A.H.V. Scapira, *FEBS Lett.* 345 (1994) 50;
(e) T. Noguchi, M. Hoshino, M. Tsujimura, M. Odaka, Y. Inoue, I. Endo, *Biochemistry* 35 (1996) 16777;
(f) G.C. Brown, *Eur. J. Biochem.* 232 (1995) 188;
(g) B. D'Autréaux, O. Horner, J.L. Oddou, C. Jeandey, S. Gambarelli, C. Berthomieu, J.M. Latour, I. Michaud-Soret, *J. Am. Chem. Soc.* 126 (2004) 6005.
- [9] (a) S. Herold, T. Matsui, Y.J. Watanabe, *J. Am. Chem. Soc.* 123 (2001) 4085;
(b) M.P. Doyle, J.W. Hoekstra, *J. Inorg. Biochem.* 14 (1991) 351.
- [10] P.G. Wang, M. Xian, X. Tang, X. Wu, Z. Wen, T. Cai, A.J. Janczuk, *Chem. Rev.* 102 (2002) 1091.
- [11] J.S. Stamler, D.J. Singel, J. Loscalzo, *Science* 258 (1992) 1898.
- [12] (a) M.C. Silvestrini, M.G. Tordi, G. Musci, M.J. Brunori, *J. Biol. Chem.* 265 (1990) 11783;
(b) J.M. Vega, J. Cardenas, M. Losada, *Methods Enzymol.* 69 (1980) 255;
(c) O. Einsle, A. Messerschmidt, R. Huber, P.M.H. Kroneck, F.J. Neese, *J. Am. Chem. Soc.* 124 (2002) 11737.
- [13] (a) E.A.E. Garber, S. Wehrli, T.C. Hollocher, *J. Biol. Chem.* 258 (1983) 3587;

- (b) Y. Shiro, M. Fujii, S.I. Iizuka, K. Adachi, K. Tsukamoto, H. Nakahara, *J. Biol. Chem.* 270 (1995) 1617;
(c) Y. Shiro, M. Fujii, Y.I. Isogai, S.I. Adachi, T. Iizuka, E. Obayashi, R. Makino, K. Nakahara, H. Shoun, *Biochemistry* 34 (1995) 9052;
(d) K. Nakahara, T. Tanimoto, K. Hatano, K. Usuda, H. Shoun, *J. Biol. Chem.* 268 (1993) 8350.
- [14] (a) M.P. Hendrich, M. Logan, K.K. Andersson, D.M. Arriero, J.D. Lipscomb, A.B. Hooper, *J. Am. Chem. Soc.* 116 (1994) 11961;
(b) M.Z. Cabail, J. Kostera, A.A. Pacheco, *Inorg. Chem.* 44 (2005) 225.
- [15] (a) S. Adak, Q. Wang, D.J. Stuehr, *J. Biol. Chem.* 275 (2000) 33554;
(b) K.M. Rusche, M.M. Spiering, M.A. Marletta, *Biochemistry* 37 (1998) 15503.
- [16] J.M. Fukuto, P. Gulati, *Biochem. Pharmacol.* 47 (1994) 922.
- [17] (a) S.A. Lipton, D.J. Singel, J.S. Stamler, *Ann. N.Y. Acad. Sci.* 738 (1994) 382;
(b) D.A. Wink, M. Feelisch, J.M. Fukuto, D. Chistodoulou, D. Jour'd'heil, M.B. Grisham, Y. Vodovotz, J.A. Cook, M. Krishna, W.G. DeGraff, S.M. Kim, J. Gamson, J.B. Mitchell, *Arch. Biochem. Biophys.* 351 (1998) 66.
- [18] H.T. Nagasawa, F.N. Shirota, E.G. DeMaster, *Biomed. Chem.* (2000) 73.
- [19] (a) K.M. Miranda, N. Paolocci, T. Katori, D.D. Thomas, M.D. Bartberger, M.G. Espey, D.A. Kass, M. Feelisch, J.M. Fukuto, D.A. Wink, *Proc. Natl. Acad. Sci. U.S.A.* 100 (2003) 9196;
(b) D.A. Wink, K.M. Miranda, T. Katori, D. Mancardi, D. Thomas, L. Ridnour, M.G. Espey, M. Feelisch, C. Colton, J.M. Fukuto, D.A. Kass, N. Paolocci, *Am. J. Physiol.* 285 (2003) H2264.
- [20] (a) K.M. Miranda, *Coord. Chem. Rev.* 249 (2005) 433;
(b) P.J. Farmer, F.J. Sulc, *J. Inorg. Biochem.* 99 (2005) 166.
- [21] (a) J.H. Enemark, R.D. Feltham, *Coord. Chem. Rev.* 13 (1974) 339;
(b) R.D. Feltham, J.H. Enemark, *Topics Inorg. Organomet. Stereochem.* 12 (1981) 155;
(c) B.L. Westcott, J.H. Enemark, in: E.I. Solomon, A.B.P. Lever (Eds.), *Inorganic Electronic Structure and Spectroscopy*, vol. II, Wiley, New York, 1999, p. 403.
- [22] (a) P.C. Ford, L. Laverman, *Coord. Chem. Rev.* 249 (2005) 391;
(b) P.C. Ford, L.A. Laverman, I.M. Lorkovic, *Adv. Inorg. Chem.* 54 (2003) 203;
(c) P.C. Ford, I.M. Lorkovic, *Chem. Rev.* 102 (2002) 993.
- [23] (a) F. Bottomley, in: P.S. Braterman (Ed.), *Reactions of Coordinated Ligands*, vol. 2, Plenum Publishing Corp, New York, 1989;
(b) J.A. Olabe, *Adv. Inorg. Chem.* 55 (2004) 61.
- [24] (a) D. Sellmann, N. Blum, F.W. Heinemann, B.A. Hess, *Chem. Eur. J.* 7 (2001) 1874;
(b) A.K. Patra, J.M. Rowland, D.S. Marlin, E. Bill, M.M. Olmstead, P.K. Mascharak, *Inorg. Chem.* 42 (2003) 6812;
(c) R. García Serres, C.A. Grapperhaus, E. Bothe, E. Bill, T. Weyhermüller, F. Neese, K. Wieghardt, *J. Am. Chem. Soc.* 126 (2004) 5138;
(d) M.K. Ellison, C.E. Schultz, W.R. Scheidt, *Inorg. Chem.* 38 (1999) 100;
(e) M.D. Carducci, M.R. Pressprich, P.J. Coppens, *J. Am. Chem. Soc.* 119 (1997) 2669;
(f) J.A. Olabe, L.A. Gentil, G.E. Rigotti, A. Navaza, *Inorg. Chem.* 23 (1984) 4297;
(g) M. Videla, J.S. Jacinto, R. Baggio, M.T. Garland, P. Singh, W. Kaim, L.D. Slep, J.A. Olabe, *Inorg. Chem.* 45 (2006) 8608;
(h) H. Hadadzadeh, M.C. DeRosa, G.P.A. Yap, A.R. Rezvani, R.J. Crutchley, *Inorg. Chem.* 41 (2002) 6521;
(i) F. Bottomley, *J. Chem. Soc., Dalton Trans.* (1974) 1600;
(j) S. Borges, C.U. Davanzo, E.E. Castellano, J.Z. Schpector, S.C. Silva, D.W. Franco, *Inorg. Chem.* 37 (1998) 2670;
(k) D.R. Lang, J.A. Davis, L.G.F. Lopes, A.A. Ferro, L.C.G. Vasconcellos, D.W. Franco, E. Tfouni, A. Wieraszko, M.J. Clarke, *Inorg. Chem.* 39 (2000) 2294;
(l) T. Kimura, T. Sakurai, M. Shima, T. Togano, M. Mukaida, T. Nomura, *Inorg. Chim. Acta* 69 (1983) 135;
(m) T. Togano, H. Kuroda, M. Nagao, Y. Maekawa, H. Nishimura, F.S. Howell, M. Mukaida, *Inorg. Chim. Acta* 196 (1992) 57;
(n) S. Sarkar, B. Sarkar, N. Chanda, S. Kar, S.M. Mobin, J. Fiedler, W. Kaim, G.K. Lahiri, *Inorg. Chem.* 44 (2005) 6092;
(n) A.K. Patra, M.J. Rose, K.A. Murphy, M.M. Olmstead, P.K. Mascharak, *Inorg. Chem.* 43 (2004) 4487;
(o) P.G. Zanichelli, A.M. Miotto, H.F.G. Estrela, F. Rocha Soares, D.N. Grassi-Kassisse, R.C. Spadari-Bratfisch, E.E. Castellano, F. Roncaroli, A.R. Parise, J.A. Olabe, A.R.M.S. de Brito, D.W. Franco, *J. Inorg. Biochem.* 98 (2004) 1921;
(p) J.T. Veal, D.J. Hodgson, *Acta Crystallogr.* 28B (1972) 3525;
(q) L.M. Baraldo, M.S. Bessega, G.E. Rigotti, J.A. Olabe, *Inorg. Chem.* 33 (1994) 5890;
(r) P. Singh, B. Sarkar, M. Sieger, M. Niemeyer, J. Fiedler, S. Zalis, W. Kaim, *Inorg. Chem.* 45 (2006) 4602;
(s) F. Bottomley, S.G. Clarkson, S.B. Tong, *J. Chem. Soc., Dalton Trans.* (1974) 2344.
- [25] (a) J. Pitarch López, F.W. Heinemann, R. Prakash, B.A. Hess, O. Horner, C. Jeandey, J.J. Oddou, J.M. Latour, A. Grohmann, *Chem. Eur. J.* 8 (2002) 5709;
(b) H. Nasri, M.K. Ellison, S. Chen, B.H. Huynh, W.R. Scheidt, *J. Am. Chem. Soc.* 119 (1997) 6274;
(c) G.R. Wyllie, C.E. Schulz, W.R. Scheidt, *Inorg. Chem.* 42 (2003) 5722;
(d) C. Hauser, T. Glaser, E. Bill, T. Weyhermüller, K. Wieghardt, *J. Am. Chem. Soc.* 122 (2000) 4352;
(e) M. Li, D. Bonnet, E. Bill, F. Neese, T. Weyhermüller, N. Blum, D. Sellmann, K. Wieghardt, *Inorg. Chem.* 41 (2002) 3444;
(f) K. Pohl, K. Wieghardt, B. Nuber, J.J. Weiss, *J. Chem. Soc., Dalton Trans.* (1987) 187.
- [26] (a) D. Sellmann, T. Gottschalk-Gaudig, D. Haussinger, F.W. Heinemann, B.A. Hess, *Chem. Eur. J.* 7 (2001) 2099;
(b) R.D. Wilson, J.A. Ibers, *Inorg. Chem.* 18 (1979) 336;
(c) R. Melenkivitz, G.L. Hillhouse, *Chem. Commun.* (2002) 660.
- [27] F. Roncaroli, M.E. Ruggiero, D.W. Franco, G.L. Estiu, J.A. Olabe, *Inorg. Chem.* 41 (2002) 5760.
- [28] (a) R.W. Callahan, T.J. Meyer, *Inorg. Chem.* 16 (1977) 574;
(b) D.W. Pipes, T.J. Meyer, *Inorg. Chem.* 23 (1984) 2466.
- [29] M.H. Barley, K.J. Takeuchi, T.J. Meyer, *J. Am. Chem. Soc.* 108 (1986) 5876.
- [30] (a) E.I. Solomon, A.B.P. Lever (Eds.), *Inorganic Electronic Structure and Spectroscopy*, vols. I and II, Wiley, New York, 1999;
(b) C.A. Brown, M.A. Pavlovsky, T.E. Westre, Y. Zhang, B. Hedman, K.O. Hodgson, E.I. Solomon, *J. Am. Chem. Soc.* 117 (1995) 715;
(c) T.E. Westre, A. Di Cicco, A. Filippini, C.R. Natoli, B. Hedman, E.I. Solomon, K.O. Hodgson, *J. Am. Chem. Soc.* 116 (1994) 6757.
- [31] D.M. Mingos, *Inorg. Chem.* 12 (1973) 1209.
- [32] Z. Assefa, D.M. Stanbury, *J. Am. Chem. Soc.* 119 (1997) 521.
- [33] P. Gans, A. Sabatini, L. Sacconi, *Inorg. Chem.* 5 (1966) 1877.
- [34] M. Sieger, B. Sarkar, S. Zalis, J. Fiedler, N. Escola, F. Doctorovich, J.A. Olabe, W. Kaim, *Dalton Trans.* (2004) 1797.
- [35] F.J. Bottomley, *J. Chem. Soc., Dalton Trans.* (1975) 2538.
- [36] P. Chen, T.J. Meyer, *Chem. Rev.* 98 (1998) 1439.
- [37] (a) W.R. Scheidt, Y.J. Lee, K.J. Hatano, *J. Am. Chem. Soc.* 106 (1984) 3191;
(b) G.B. Richter-Addo, R.A. Wheeler, C.A. Hixson, L. Chen, M.A. Khan, M.K. Ellison, C.E. Schulz, W.R. Scheidt, *J. Am. Chem. Soc.* 123 (2001) 6314.
- [38] J. Li, J. Noodleman, D.A. Case, in: E.I. Solomon, A.B.P. Lever (Eds.), *Inorganic Electronic Structure and Spectroscopy*, vol. I, Wiley, New York, 1999.
- [39] (a) P.T. Manoharan, H.B. Gray, *J. Am. Chem. Soc.* 87 (1965) 3340;
(b) R. Fenske, R.L. DeKock, *Inorg. Chem.* 11 (1972) 437.
- [40] S.N. Greene, N.G. Richards, *J. Inorg. Chem.* 43 (2004) 7030.
- [41] S.I. Gorelsky, S. da Silva, A.B.P. Lever, D.W. Franco, *Inorg. Chim. Acta* 300–302 (2000) 698.
- [42] (a) N. Chanda, S.M. Mobin, V.G. Puranik, A. Datta, M. Niemeyer, G.K. Lahiri, *Inorg. Chem.* 43 (2004) 1056;
(b) B. Mondal, H. Paul, V.G. Puranik, G.K. Lahiri, *J. Chem. Soc., Dalton Trans.* (2001) 481;
(c) N. Chanda, D. Paul, S. Kar, S.M. Mobin, A. Datta, V.G. Puranik, K.K. Rao, G.K. Lahiri, *Inorg. Chem.* 44 (2005) 3499;

- (d) R.K. Afshar, A.K. Patra, M.M. Olmstead, P.K. Mascharak, *Inorg. Chem.* 43 (2004) 5736;
- (f) B.R. Cameron, M.C. Darles, H. Yee, M. Olsen, S. Fricker, R.T. Skerlj, G.J. Bridger, N.A. Davies, M.T. Wilson, D.J. Rose, J. Zubieta, *Inorg. Chem.* 42 (2003) 1868;
- (g) R.K. Afshar, A.K. Patra, E. Bill, M.M. Olmstead, P.K. Mascharak, *Inorg. Chem.* 45 (2006) 3774;
- (h) N. Xu, J. Lee, D.R. Powell, G.B. Richter-Addo, *Inorg. Chim. Acta* 358 (2005) 2855;
- (i) M.K. Ellison, W.R. Scheidt, *J. Am. Chem. Soc.* 121 (1999) 5210;
- (j) V.R. de Souza, A.M. da Costa Ferreira, H.E. Toma, *Dalton Trans.* (2003) 458;
- (k) R.C.L. Zampieri, G. Von Poelsitz, A.A. Batista, O.R. Nascimento, J. Ellena, E.E. Castellano, *J. Inorg. Biochem.* 92 (2002) 82;
- (l) L.F. Szczepura, J.G. Muller, C.A. Bessel, R.F. See, T.S. Janik, M.R. Churchill, K.J. Takeuchi, *Inorg. Chem.* 31 (1992) 859;
- (m) D. Ooyama, Y. Miura, Y. Kanazawa, F.S. Howell, N. Nagao, M. Mukaida, H. Nagao, K. Tanaka, *Inorg. Chim. Acta* 237 (1995) 47;
- (n) B.J. Coe, M. Chery, R.L. Beddoes, H. Hope, P.S. White, *Chem. Dalton Trans.* (1996) 3917;
- (n) B. Serli, E. Zangrando, E. Iengo, E. Alessio, *Inorg. Chim. Acta* 339 (2002) 265;
- (o) A.A. Batista, S.L. Queiroz, P.C. Healy, R.W. Buckley, S.E. Boyd, S.J. Berners-Price, E.E. Castellano, J. Ellena, *Can. J. Chem.* 79 (2001) 1030;
- (p) K. Karidi, A. Garoufis, A. Tsipis, N. Hadjiliadis, H. den Dulk, J. Reddijk, *Dalton Trans.* (2005) 1176;
- (q) Y. Chen, F.T. Lin, R.E. Shepherd, *Inorg. Chem.* 38 (1999) 973;
- (r) L.G.F. Lopes, E.H.S. Sousa, J.C.V. Miranda, C.P. Oliveira, I.M.M. Carvalho, A.A. Batista, J. Ellena, E.E. Castellano, O.R. Nascimento, I.S. Moreira, *J. Chem. Soc., Dalton Trans.* (2002) 1903;
- (s) A.K.M. Holanda, D.L. Pontes, I.C.N. Diógenes, I.S. Moreira, L.G.F. Lopes, *Trans. Met. Chem.* 29 (2004) 430;
- (t) F.O.N. Silva, S.X.B. Araujo, A.K.M. Holanda, E. Meyer, F.A.M. Sales, I.C.N. Diógenes, I.M.M. Carvalho, I.S. Moreira, L.G.F. Lopes, *Eur. J. Inorg. Chem.* (2006) 2020;
- (u) L.G.F. Lopes, E.E. Castellano, A.G. Ferreira, C.U. Davanzo, M.J. Clarke, D.W. Franco, *Inorg. Chim. Acta* 358 (2005) 2883;
- (v) L.G.F. Lopes, A. Wieraszko, Y. El-Sherif, M.J. Clarke, *Inorg. Chim. Acta* 312 (2001) 15.
- [43] F.A. Walker, *J. Inorg. Biochem.* 99 (2005) 216.
- [44] F. Roncaroli, J.A. Olabe, R. van Eldik, *Inorg. Chem.* 42 (2003) 4179.
- [45] R.G. Hayes, M.K. Ellison, W.R. Scheidt, *Inorg. Chem.* 39 (2000) 3665.
- [46] (a) J.C. Salerno, in: J. Lancaster (Ed.), *Nitric Oxide, Principles and Actions*, Academic Press, New York, 1996 (Chapter 2);
- (b) H. Kon, *Biochim. Biophys. Acta* 379 (1975) 103.
- [47] V.K.K. Praneeth, F. Neese, N. Lehnert, *Inorg. Chem.* 44 (2005) 2570.
- [48] S. Frantz, B. Sarkar, M. Sieger, W. Kaim, F. Roncaroli, J.A. Olabe, S. Zalis, *Eur. J. Inorg. Chem.* (2004) 2902.
- [49] (a) J.D.W. van Voorst, P.J. Hemmerich, *J. Chem. Phys.* 45 (1966) 3914;
- (b) M. Wanner, T. Scheiring, W. Kaim, L.D. Slep, L.M. Baraldo, J.A. Olabe, S. Zalis, E.J. Baerends, *Inorg. Chem.* 40 (2001) 5704.
- [50] B.R. McGarvey, A.A. Ferro, E. Tfouni, C.W.B. Bezerra, I. Bagatin, D.W. Franco, *Inorg. Chem.* 39 (2000) 3577.
- [51] (a) D.M. Arciero, J.D. Lipscomb, B.H. Huynh, T.A. Kent, E.J. Munck, *Eur. J. Biol. Chem.* 258 (1983) 14981;
- (b) J.M. Nocek, D.M. Kurtz Jr., J.T. Sage, Y.M. Xia, P. Debrunner, A.K. Shiemke, T.M. Sanders Loehr, *Biochemistry* 27 (1988) 1014;
- (c) J.H. Rodríguez, Y.M. Xia, P.J. Debrunner, *J. Am. Chem. Soc.* 121 (1999) 7846;
- (d) E. Bill, F.H. Bernhardt, A.X. Trautwein, H. Winkler, *Eur. J. Biochem.* 147 (1985) 177;
- (e) C.J. Haskin, N. Ravi, J.B. Lynch, E. Münck, L. Que Jr., *Biochemistry* 34 (1995) 11090;
- (f) V.J. Chen, A.M. Orville, M.R. Harpel, C.A. Frolik, K. Sureros, E. Münck, J.D. Lipscomb, *J. Biol. Chem.* 264 (1989) 21677;
- (g) A.M. Orville, V.J. Chen, A. Kriauciunas, M.R. Harpel, B.G. Fox, E. Miinck, J.D. Lipscomb, *Biochemistry* 31 (1992) 4602.
- [52] A. Wanat, T. Schnepfensieper, G. Stochel, R. van Eldik, E. Bill, K. Wieghardt, *Inorg. Chem.* 41 (2002) 4.
- [53] M.G. Sauer, F. de Souza Oliveira, R. Galvao de Lima, A. de Lima Cacciarri, E. Tfouni, R. Santana da Silva, *Inorg. Chem. Commun.* 8 (2005) 347.
- [54] W.R. Scheidt, M.K. Ellison, *Acc. Chem. Res.* 32 (1999) 350.
- [55] T.G. Traylor, V.J. Sharma, *Biochemistry* 31 (1992) 2847.
- [56] R.P. Cheney, M.G. Simic, M.Z. Hoffman, I.A. Taub, K.D. Asmus, *Inorg. Chem.* 16 (1977) 2187.
- [57] (a) J. Schmidt, H. Kühn, W.L. Dorn, J. Kopf, *Inorg. Nucl. Chem. Lett.* 10 (1974) 55;
- (b) R. Nast, J.Z. Schmidt, *Z. Anorg. Allg. Chem.* 421 (1976) 15;
- (c) C. Glidewell, I.L. Johnson, *Inorg. Chim. Acta* 132 (1987) 145;
- (d) J.D. Schwane, M.T. Ashby, *J. Am. Chem. Soc.* 124 (2002) 6822.
- [58] (a) J.C. Toledo, B. dos Santos Lima Neto, D.W. Franco, *Coord. Chem. Rev.* 249 (2005) 419;
- (b) J.C. Toledo, H.S. Hilva, M. Scarpellini, V. Mori, A.J. Camargo, M. Bertotti, D.W. Franco, *Eur. J. Inorg. Chem.* (2004) 2879;
- (c) L.F.F. Lopes, A. Wieraszko, Y. El-Sherif, M.J. Clarke, *Inorg. Chim. Acta* 312 (2001) 15.
- [59] A.G. De Candia, J.P. Marcolongo, L.D. Slep, *Polyhedron*, in press.
- [60] M. Gonzalez Lebrero, D.A. Scherlis, G.L. Estiu, J.A. Olabe, D.A. Estrin, *Inorg. Chem.* 40 (2001) 4127.
- [61] H.E. Toma, J.M. Malin, *Inorg. Chem.* 12 (1973) 2080.
- [62] (a) D.J. Hodgson, J.A. Ibers, *Inorg. Chem.* 7 (1968) 2345;
- (b) D.J. Hodgson, J.A. Ibers, *Inorg. Chem.* 8 (1969) 1282;
- (c) D.A. Snyder, D.L. Weaver, *Inorg. Chem.* 9 (1970) 2760;
- (d) P.L. Johnson, J.H. Enemark, R.D. Feltham, K. Bizot Swedo, *Inorg. Chem.* 15 (1976) 2989;
- (e) B.A. Kelly, A.J. Welch, P. Woodward, *J. Chem. Soc., Dalton Trans.* (1977) 2237.
- [63] (a) W.R. Scheidt, J.L. Hoard, *J. Am. Chem. Soc.* 95 (1973) 8281;
- (b) M.K. Ellison, W.R. Scheidt, *Inorg. Chem.* 37 (1998) 382;
- (c) G.B. Richter-Addo, S.J. Hodge, G.B. Yi, M.A. Khan, T. Ma, E. Van Caemelbecke, N. Guo, K.M. Kadish, *Inorg. Chem.* 36 (1997) 2696.
- [64] M. Wolak, A. Zahl, T. Schnepfensieper, G. Stochel, R. van Eldik, *J. Am. Chem. Soc.* 123 (2001) 9780.
- [65] (a) F.T. Bonner, J. Akhtar, *Inorg. Chem.* 20 (1981) 3155;
- (b) S.G. Clarkson, F. Basolo, *Inorg. Chem.* 12 (1973) 1528;
- (c) M. Kubota, D.A. Phillips, *J. Am. Chem. Soc.* 97 (1975) 5637.
- [66] W.R. Roper, K.R. Grundy, C.R. Reed, *J. Chem. Soc., Chem. Commun.* (1970) 1501.
- [67] The assignment of HNO as a member of the {MNO}⁸ group relates to the expected facile protonation of the highly nucleophilic NO⁻. In fact, HNO pertains to the family of angular NOR ligands (R = thiolate, benzyl, etc.). Nitrosothiolate (NOSR) ligands result from the nucleophilic addition of SR⁻ to M^{II}NO⁺ (see Section 4.4), and H⁻ has proved to be an efficient nucleophile-reductant for synthesizing HNO complexes starting from the NO⁺-derivatives. All these reactions imply the formal conversion of {MNO}⁶ into {MNO}⁸.
- [68] (a) J. Lee, G.B. Richter-Addo, *J. Inorg. Biochem.* 98 (2004) 1247;
- (b) J.S. Southern, G.L. Hillhouse, A.L. Rheingold, *J. Am. Chem. Soc.* 119 (1997) 12406;
- (c) R. Melenkevitz, J.S. Southern, G.L. Hillhouse, T.E. Concolino, L.M. Liable-Sands, A.L. Rheingold, *J. Am. Chem. Soc.* 124 (2002) 12068;
- (d) J.S. Southern, M.T. Green, G.L. Hillhouse, I.A. Guzei, A.L. Rheingold, *Inorg. Chem.* 40 (2001) 6039.
- [69] (a) R. Lin, P.J. Farmer, *J. Am. Chem. Soc.* 122 (2000) 2393;
- (b) M. Bayachou, R. Lin, W. Cho, P.J. Farmer, *J. Am. Chem. Soc.* 120 (1998) 9888;
- (c) C.E. Immoos, F. Sulc, P.J. Farmer, K. Czarnecki, D. Bocian, A. Levina, J.B. Aitken, R. Armstrong, P.A. Lay, *J. Am. Chem. Soc.* 127 (2005) 814;
- (d) F. Sulc, E. Fleischer, M.D. Farmer, G.N. La Mar, *J. Biol. Inorg. Chem.* 8 (2003) 348;
- (e) D.P. Linder, K.R. Rodgers, *Inorg. Chem.* 44 (2005) 8259.
- [70] (a) J. Masek, E. Maslova, *Coll. Czech. Chem. Commun.* 39 (1974) 2141;
- (b) A. Montenegro, S.E. Bari, J.A. Olabe, in preparation.
- [71] J.H. Ridd, *Adv. Phys. Org. Chem.* 16 (1979) 1.

- [72] J.H. Swinehart, *Coord. Chem. Rev.* 2 (1967) 385.
- [73] E. Tfouni, M. Krieger, B.R. McGarvey, D.W. Franco, *Coord. Chem. Rev.* 236 (2003) 57.
- [74] (a) P.C. Ford, S. Weckler, *Coord. Chem. Rev.* 249 (2005) 1382;
(b) M. Videla, S.E. Braslavsky, J.A. Olabe, *Photochem. Photobiol. Sci.* 4 (2005) 75;
(c) S.K. Wolfe, J.H. Swinehart, *Inorg. Chem.* 14 (1975) 1049;
(d) R. Prakash, A.U. Czaja, F.W. Heinemann, D.J. Sellmann, *J. Am. Chem. Soc.* 127 (2005) 13758;
(e) M.G. Sauaia, F. de Souza Oliveira, A.C. Tedesco, R. Santana da Silva, *Inorg. Chim. Acta* 355 (2003) 191;
(f) F. de Souza Oliveira, V. Togniolo, A.C. Tedesco, R. Santana da Silva, *Inorg. Chem. Commun.* 7 (2004) 160.
- [75] C.W.B. Bezerra, S.C. Silva, M.T.P. Gambardella, R.H.A. Santos, E. Tfouni, D.W. Franco, *Inorg. Chem.* 38 (1999) 5660.
- [76] (a) T. Schnepf, S. Finkler, A. Czap, R. van Eldik, M. Heus, P. Nieuwenhuizen, C. Wresemann, W. Abma, *Eur. J. Inorg. Chem.* (2001) 491;
(b) T. Schnepf, S. Finkler, A. Czap, R. van Eldik, M. Heus, P. Nieuwenhuizen, C. Wresemann, W. Abma, *Eur. J. Inorg. Chem.* (2001) 2317;
(c) T. Schnepf, S. Finkler, A. Czap, R. van Eldik, *Inorg. Chem.* 41 (2002) 2565.
- [77] T. Schnepf, S. Finkler, A. Czap, R. van Eldik, *Angew. Chem. Int. Ed.* 40 (2001) 1678.
- [78] (a) D.H. Macartney, *Rev. Inorg. Chem.* 9 (1988) 101;
(b) H.E. Toma, N.M. Moroi, N.Y.M. Iha, *An. Acad. Brasil. Cienc.* 54 (1982) 315;
(c) J. Legros, *J. Chim. Phys. Phys. Chim. Biol.* 61 (1964) 909;
(d) H.E. Toma, J.M. Malin, E. Giesbrecht, *Inorg. Chem.* 12 (1973) 2084;
(e) H.E. Toma, A.A. Batista, H.B. Gray, *J. Am. Chem. Soc.* 104 (1982) 7509.
- [79] A.V. Marchenko, A.N. Vedernikov, D.F. Dye, M. Pink, J.M. Zaleski, K. Caulton, *Inorg. Chem.* 43 (2004) 351.
- [80] H.E. Toma, J.M. Malin, *Inorg. Chem.* 12 (1973) 1039.
- [81] A.R. Butler, L.L. Megson, *Chem. Rev.* 102 (2002) 1155.
- [82] K. Szacilowski, A. Wanat, A. Barbieri, E. Wasiliewska, M. Witko, G. Stochel, *G. Stasicka, New J. Chem.* 26 (2002) 1495.
- [83] F. Roncaroli, R. van Eldik, J.A. Olabe, *Inorg. Chem.* 44 (2005) 2781.
- [84] (a) J.C. Patterson, I.M. Lorkovic, P.C. Ford, *Inorg. Chem.* 42 (2003) 4902;
(b) J. Conradie, T. Wondimagegn, A.J. Ghosh, *J. Am. Chem. Soc.* 125 (2003) 4968.
- [85] (a) F.T. Tsai, S.J. Chiou, M.C. Tsai, m.M.L. Tsai, H.W. Huang, M.H. Chiang, W.F. Liaw, *Inorg. Chem.* 44 (2005) 5872;
(b) C.M. Lee, C.H. Chen, H.W. Chen, J.L. Hsu, G.H. Lee, W.F. Liaw, *Inorg. Chem.* 44 (2005) 6670.
- [86] N. Reginato, C.T.C. McCrory, D. Pervitsky, L. Li, *J. Am. Chem. Soc.* 121 (1999) 10217.
- [87] F. Roncaroli, J.A. Olabe, R. van Eldik, *Inorg. Chem.* 41 (2002) 5417.
- [88] (a) S.D. Pell, J.N. Armor, *J. Am. Chem. Soc.* 95 (1973) 7625;
(b) A. Czap, R. van Eldik, *Dalton Trans.* (2003) 665.
- [89] N.A. Davies, M.T. Wilson, E. Slade, S.P. Fricker, B.A. Murrer, N.A. Powell, G.R. Henderson, *Chem. Commun.* (1997) 47.
- [90] L.E. Laverman, A. Wanat, J. Oszejka, G. Stochel, P.C. Ford, R. van Eldik, *J. Am. Chem. Soc.* 123 (2001) 285.
- [91] V. Shafirovich, S.V. Lyman, *Proc. Natl. Acad. Sci. U.S.A.* 99 (2002) 7340.
- [92] D.S. Bohle, C.H. Hung, *J. Am. Chem. Soc.* 117 (1995) 9584.
- [93] A. Ikazaki, M. Nakamura, *Inorg. Chem.* 41 (2002) 6225.
- [94] M. Hoshino, K. Ozawa, H. Seki, P.C. Ford, *J. Am. Chem. Soc.* 115 (1993) 9568.
- [95] (a) M. Wolak, R. van Eldik, *J. Am. Chem. Soc.* 127 (2005) 13312;
(b) J.E. Jee, S. Eigler, F. Hampel, N. Jux, M. Wolak, A. Zahl, G. Stochel, R. van Eldik, *Inorg. Chem.* 44 (2005) 7717.
- [96] F. Sulc, C.E. Immoos, D. Pervitsky, P.J. Farmer, *J. Am. Chem. Soc.* 126 (2004) 1096.
- [97] M.P. Doyle, S.N. Mahapatro, R.D. Broene, J.K. Guy, *J. Am. Chem. Soc.* 110 (1988) 593.
- [98] (a) D.A. Bazylinski, T.C. Hollocher, *J. Am. Chem. Soc.* 107 (1985) 7982;
(b) M.P. Doyle, S.N. Mahapatro, *J. Am. Chem. Soc.* 106 (1984) 3678;
(c) M.A. Sharpe, C.E. Cooper, *Biochem. J.* 332 (1998) 9.
- [99] S.E. Bari, M.A. Marti, V.T. Amorebieta, D.A. Estrin, F. Doctorovich, *J. Am. Chem. Soc.* 125 (2003) 15272.
- [100] M.A. Marti, S.E. Bari, D.A. Estrin, F. Doctorovich, *J. Am. Chem. Soc.* 127 (2005) 4680.
- [101] C.H. Kim, T.C. Hollocher, *J. Biol. Chem.* 259 (1984) 2092.
- [102] (a) J.H. Swinehart, P.A. Rock, *Inorg. Chem.* 5 (1966) 573;
(b) J. Masek, H. Wendt, *Inorg. Chim. Acta* 3 (1969) 455.
- [103] R.G. Wilkins, *Kinetics and Mechanism of Reactions of Transition Metal Complexes*, 2nd ed., VCH Publishers Inc., New York, 1991.
- [104] (a) R.A. Marcus, *J. Phys. Chem.* 72 (1968) 891;
(b) R.A. Marcus, *Angew. Chem. Int. Ed. Engl.* 32 (1993) 1111.
- [105] (a) M. Hoshino, M. Maeda, R. Konishi, H. Seki, P.C. Ford, *J. Am. Chem. Soc.* 118 (1996) 5702;
(b) M. Hoshino, L. Laverman, P.C. Ford, *Coord. Chem. Rev.* 187 (1999) 75;
(c) P.C. Ford, B.O. Fernandez, M.D. Lim, *Chem. Rev.* 105 (2005) 2439.
- [106] (a) B.O. Fernandez, I.M. Lorkovic, P.C. Ford, *Inorg. Chem.* 42 (2003) 2;
(b) B.O. Fernandez, P.C. Ford, *J. Am. Chem. Soc.* 125 (2003) 10510;
(c) B.O. Fernandez, I.M. Lorkovic, P.C. Ford, *Inorg. Chem.* 43 (2004) 5393.
- [107] J.E. Jee, R. van Eldik, *Inorg. Chem.* 45 (2006) 6523.
- [108] P.C. Ford, D.A. Wink, D.M. Stanbury, *FEBS Lett.* 326 (1993) 1.
- [109] K. Cosby, K.S. Partovi, J.H. Crawford, R.P. Patel, C.D. Reiter, S. Martyr, B.K. Yang, M.A. Wacławski, G. Zalos, X. Xu, K.T. Huang, H. Shields, D.B. Kim-Shapiro, A.N. Schechter, R.O. Cannon III, M.T. Gladwin, *Nat. Med.* 9 (2003) 1498.
- [110] M.M. Gutierrez, V.T. Amorebieta, G.L. Estiu, J.A. Olabe, *J. Am. Chem. Soc.* 124 (2002) 10307.
- [111] S.K. Wolfe, C. Andrade, J.H. Swinehart, *Inorg. Chem.* 13 (1974) 2567.
- [112] (a) N.E. Katz, M.A. Blesa, J.A. Olabe, P.J. Aymonino, *J. Inorg. Nucl. Chem.* 42 (1980) 581;
(b) I. Maciejowska, Z. Stasicka, G. Stochel, R. van Eldik, *J. Chem. Soc., Dalton Trans.* (1999) 3643.
- [113] J.A. Olabe, G.L. Estiu, *Inorg. Chem.* 42 (2003) 4873.
- [114] (a) F. Bottomley, J.R. Crawford, *J. Am. Chem. Soc.* 94 (1972) 9092;
(b) P.G. Douglas, R.D. Feltham, H.G. Metzger, *J. Am. Chem. Soc.* 93 (1971) 84.
- [115] R. Prakash, A.W. Götz, F.W. Heinemann, A. Görling, D. Sellmann, *Inorg. Chem.* 45 (2006) 4661.
- [116] (a) J.R. Perrott, G. Stedman, N. Uysal, *J. Chem. Soc., Dalton Trans.* (1976) 2058;
(b) J.R. Perrott, G. Stedman, N. Uysal, *J. Chem. Soc., Perkin Trans.* (1977) 274.
- [117] K. Szacilowski, G. Stochel, Z. Stasicka, H. Kisch, *New J. Chem.* 21 (1997) 893.
- [118] L.L. Perissinotti, D.A. Estrin, G. Leitun, F. Doctorovich, *J. Am. Chem. Soc.* 128 (2006) 2512.
- [119] M.D. Johnson, R.G. Wilkins, *Inorg. Chem.* 23 (1984) 231.
- [120] F. Roncaroli, J.A. Olabe, *Inorg. Chem.* 14 (2005) 4719.
- [121] M. Videla, F. Roncaroli, L.D. Slep, J.A. Olabe, *J. Am. Chem. Soc.* 129 (2007) 278.
- [122] (a) E.V. Arnold, D.S. Bohle, *Methods Enzymol.* 269 (1996) 41;
(b) J.K.S. Moller, L.H. Skibsted, *Chem. Eur. J.* 10 (2004) 2291;
(c) S. Herold, G. Röck, *Biochemistry* 44 (2005) 6223.
- [123] J.N. Armor, M.Z. Hoffman, *Inorg. Chem.* 23 (1975) 231.
- [124] L. Cheng, D.R. Powell, M.A. Khan, G.B. Richter-Addo, *Chem. Commun.* (2000) 2301.
- [125] M.G. Finnegan, A.G. Lappin, W.R. Scheidt, *Inorg. Chem.* 29 (1990) 181.
- [126] S. Goldstein, G.J. Czapski, *J. Am. Chem. Soc.* 117 (1995) 12078.
- [127] M.D. Bartberger, W. Liu, E. Ford, K.M. Miranda, C. Switzer, J.M. Fukuto, P.J. Farmer, D.A. Wink, K.N. Houk, *Proc. Natl. Acad. Sci. U.S.A.* 99 (2002) 10958.
- [128] G. Alluisetti, A.E. Almaraz, V.T. Amorebieta, F. Doctorovich, J.A. Olabe, *J. Am. Chem. Soc.* 126 (2004) 13432.
- [129] (a) W.C. Troglor, L.G. Marzilli, *Inorg. Chem.* 13 (1974) 1008;
(b) K.R. Laing, W.R. Roper, *Chem. Commun.* (1968) 1568;

- (c) K.R. Grundy, K.R. Laing, W.R. Roper, *Chem. Commun.* (1970) 1500.
- [130] P.S.Y. Wong, J. Hyun, J.M. Fukuto, F.N. Shirota, E.G. DeMaster, D.W. Shoeman, H.T. Nagasawa, *Biochemistry* 37 (1998) 18129.
- [131] A.V. Marchenko, A.N. Vedernikov, D.F. Dye, M. Pink, J.M. Zaleski, K.G. Caulton, *Inorg. Chem.* 41 (2002) 4087.
- [132] (a) M. Graetzel, S. Taniguchi, A. Henglein, *Berichte Bunsen-Gesellschaft Bot. Acta* 74 (1970) 1003;
(b) V. Shafirovich, S.V. Lymar, *J. Am. Chem. Soc.* 125 (2003) 6547.